Standard Feeder and Load Model Synthesis Using Voltage and Current Measurements

by

Sameer Nekkalapu

A Thesis Presented in Partial Fulfillment
of the Requirements for the Degree
Master of Science

Approved October 2018 by the
Graduate Supervisory Committee:

Vijay Vittal, Chair
John Undrill
Raja Ayyanar

ARIZONA STATE UNIVERSITY

December 2018

Abstract

Until late 1970's the primary focus in power system modeling has been largely directed towards power system generation and transmission. Over the years, the importance of load modeling grew and having an accurate representation of load played an important role in the planning and operation studies. With an emphasis on tackling the topic of load modeling, this thesis presents the following intermediary steps in developing accurate load models:

1. Synthesis of a three-phase standard feeder and load model using the measured voltages and currents, for events such as faults and feeder pickup cases, obtained at the head of the feeder.
2. Investigated the impact of the synthesized standard feeder and load model on the sub-transmission system for a feeder pick-up case.

In the first phase of this project, a standard feeder and load model had been synthesized by capturing the current transients when three-phase voltage measurements (obtained from a local electric utility) are played-in as input to the synthesized model. The comparison between the measured currents and the simulated currents obtained using an electromagnetic transient analysis software (PSCAD) are made at the head of the designed feeder. The synthesized load model has a load composition which includes impedance loads, single-phase induction motor loads and three-phase induction motor loads. The parameters of the motor models are adjusted to obtain a good correspondence between measured three-phase currents and simulated current responses at the head of the feeder when subjected to events under which measurements were obtained on the feeder. These events include faults which occurred upstream of the feeder at a higher voltage level and a feeder pickup event that occurred downstream from the head of the feeder. Two different load compositions have been obtained for this feeder and load model depending on the types of

load present in the surrounding area (residential or industrial/commercial).

The second phase of this project examines the impact of the feeder pick-up event on the 69 kV sub-transmission system using the obtained standard feeder and load model. Using the 69 kV network data obtained from a local utility, a sub-transmission network has been built in PSCAD. The main difference between the first and second phase of this project is that no measurements are played-in to the model in the latter case. Instead, the feeder pick-up event at a particular substation is simulated using the reduced equivalent of the 69 kV sub-transmission circuit together with the synthesized three-phase models of the feeder and the loads obtained in the first phase of the project. Using this analysis, it is observed that a good correspondence between the PSCAD simulated values of both three-phase voltages and currents with their corresponding measured responses at the substation is achieved.

Acknowledgments

I would like to first and foremost express my sincerest gratitude to my advisor, Dr. Vijay Vittal, whose encouragement, guidance and support have motivated me to make significant progress on the research and complete my thesis. I also attribute the success of my master's degree to Dr. John Undrill for his extensive input on both my research topic and the practical issues associated with the phenomenon. I also want to express my gratitude to Dr. Raja Ayyanar for his time and consideration in being a member of my graduate supervisory committee.

I would also like to thank Mr. Brian Keel, Mr. Ken Brown and Mr. Phil Augustin from the Salt River Project company for providing us the data that helped facilitate this work.

I especially want to thank my parents Mr. Ravindra Kumar Nekkalapu and Mrs. Madhavi Nekkalapu for their support during my higher education. A special mention to my grandparents Mr. Mohan Rao Kondrupati and Mrs. Samrajyam Kondrupati, who motivated me during my master's to strive for excellence. I am also grateful to my uncle and aunt, Mr. Srinivas Nalajala and Mrs. Renuka Nalajala, who shared their wisdom to help me make my stay in the USA more productive and comfortable. I also would like to thank my roommates and friends who encouraged me during some tough times of my master's.

Table of Contents

Page

LIST OF TABLES

Table Page

LIST OF FIGURES

Figure Page

Figure Page

Figure Page

Figure Page

1 INTRODUCTION

1.1 Project Goals and Overview

The primary objective of this study is to obtain a distribution feeder and load model with a fixed set of model dynamic parameters and load composition to study the effects of events such as faults and feeder pick-up events at the distribution and sub-transmission levels of a local utility near Phoenix. The standard feeder and load model is comprised of single-phase induction motors, three-phase induction motors, impedance loads, distribution line segments and distribution transformers. It should also be noted that the following project objectives have been achieved in this work:

- **Case1:** A fault induced delayed voltage recovery (FIDVR) event, which is a 69 kV Phase A fault at a substation K, has been investigated in detail using the proposed feeder and load model by using the measured voltages and currents at the head of a 69/13.8 kV substation (substation A). This event occurred during summer conditions.

- **Case2:** The same model obtained in Case 1 has been used to investigate another fault event at the 69-kV voltage level on phase A, which occurred during the winter season. The only change made in this model compared to the model used in summer case is that the load composition of the model in Case1 is scaled appropriately (by exactly a factor of 0.4) to match the pre-fault and post-fault measured steady state current values in this case. Similarly, the measurements of voltages and currents at the same 69/13.8 kV substation A (as used in summer case) has been used for this case.

- **Case3:** A feeder pick-up case, at another 69/13.8 kV substation (substation B), has been investigated using the same feeder and load model used in Case1 and Case2 except for the variation in the ratio of single-phase to three-phase induction motor load composition. This

different ratio of motor load composition is accounted for by considering the types of load present in substation B area. From discussions with the local utility engineers, it has been determined that the load present on the substation B feeder is predominantly industrial/commercial type. For this reason, more three-phase induction motors loads compared to single-phase induction motor loads have been considered for this case. This event also occurred during summer conditions.

- **Case4:** A sub-transmission model (containing two 230 kV Thévenin sources: bus1 and bus2 as shown in Fig. 38) has been assembled to investigate the effects of substation B feeder pick-up event on the 69 kV and 230 kV buses of the system.

In the cases mentioned above, Case1, Case2 and Case3 have been analyzed by comparing the simulated current responses obtained in PSCAD to the measured current responses. In these cases, the measured voltages for all three-phases are played-in to the developed standard model in PSCAD to obtain the simulated current responses. Accurate simulated currents are obtained in all these cases by considering the following conditions:

- Using identical motor and feeder parameters in all the three cases Case1, Case2, Case3
- Scaling the load composition used in Case 1 by a factor of 0.4 to obtain the load composition for the Case 2.
- Using a total motor loads composition of 90% and a lighting load impedance composition of 10% respectively, for all cases.
- The ratio of single-phase motor load to three-phase motor load is taken to be 4 for the substation A summer and winter cases.
- The ratio of three-phase motor load to single-phase motor load is taken to be 4 for

Case3.

- For all three cases (Case1, Case 2, Case 3) considered, the single-phase motor load composition in each segment of the feeder is taken be in the ratio of 1:1.4:1.4
- For all the cases, the three-phase motor load composition and lighting load composition in each segment of the feeder is taken be 1:1:1

However, in Case4, no measured responses have been played into the model, but both the simulated voltage and current responses have been obtained to study the system response. For Case4, the sub-transmission model in the neighborhood of substation B has been developed in both PSCAD and Open DSS tools to analyze the time domain response and to obtain the power flow solution of the system respectively. This sub-transmission model contains two constant AC Thévenin sources at bus1 and bus2 230 kV substations. This equivalent representation was obtained from the local utility using the ASPEN protection software tool.

1.2 Background of this Research and Literature Review

Load modeling has long been considered to be a difficult problem to solve because of the unavailability of the parameters of the loads and its variability according to location and time. Until late 1970's, the loads were modeled as constant current loads to represent active power 'P' part of the loads and as constant impedance loads to represent the reactive power 'Q' part of the loads. These types of loads are considered to be ZIP type loads. However, many works which came later [1], [2], [3], [4] included rotating load machinery dynamics (Induction motors) into the load models which made a significant impact on the simulation results when compared to using all the loads as either constant current (for P) and constant impedance (for Q) loads. This new type of ZIP + Induction motors load has been widely used due to its simple structure. In [5], a complex load model (CLOD), has been investigated which had two induction motor types included (two types

with two different torque speed and current speed curves to represent small and large three phase motors), discharge lightning loads, constant MVA loads. However, these types of models are unable to model fault induced delayed voltage recovery (FIDVR) events. The FIDVR events are basically slow voltage recovery events for low voltage faults. It was observed that this slow voltage recovery has been caused due to the low inertia of the single-phase induction motors (SPIM) [6]. Due to their low inertia, the SPIM's are assumed to be stalling which causes them to draw even more reactive power in the stalled condition. This leads to the voltage being recovered very slowly. To accurately capture this low voltage recovery phenomenon, a WECC composite load model 'cmpldw' has been developed [7]. The composite load model included SPIM's as part of their load composition along with large motors with high inertia, small motors with low inertia, small low inertia motors with a quick trip, static ZIP load, electronic loads. However, most of the simulation tools such as PSLF, PSSE where many of the simulations for transmission planning are conducted, contain only positive sequence models. Therefore, a performance-based model for the SPIM's has been developed after rigorous testing on these single-phase motors [8], [9], [10].

It is understood that having a proper set of parameters for the load model is very important to represent the load accurately in planning and operation studies. Having a set of conservative default parameters for the load which are not accurate might lead to either over-estimation of the system load parameters or under-estimation of the system load parameters depending on the operating condition of the system. Therefore, the main challenge in using these composite load models lies in obtaining an accurate set of parameters that replicates the measured responses of the system (for various disturbance events) by accurate simulated responses. There are many approaches available in the literature to estimate the parameters of the load models. Typically, parameter estimation is done by using one of the four approaches: analytical approach

[11], optimization-based approach [12], stochastic approach [13], measurement-based approach [14], [15], [16]. The analytical approach is used to derive the load parameters using field tests such as a step test, which might be sensitive to measurement errors. An optimization approach is used to obtain a set of best parameters which minimizes the error function between the measured response and the simulated response of the system. Traditional gradient search algorithms such as Gauss Newton, Levenberg- Marquardt are typically used for these optimization approaches [17]. It is important that the initial values of the parameters considered shouldn't be too far from the actual values because the optimization solution might diverge or might give a local optimal minimal solution instead of a global minimal solution. A measurement-based approach uses the field measurement data obtained from various digital fault recorders or phasor measurement units (PMUs) placed at the distribution level, to obtain the load model parameters. It should be noted that the PMUs provide a very good understanding of the system behavior at the transmission level but do not provide complete information at the distribution level. For this reason, the data obtained from the digital faults, whose sampling rate of the measured data is very high compared to the PMUs, is more useful for the transient analysis of the load models. In [18], the procedure to model the load using load survey and load curves has been discussed in detail.

In this work, a measurement-based approach has been considered to determine a standard set of parameters for the feeder and load components which gives an accurate simulated current response at the head of the feeder (when compared to the measured current response) when measured voltage responses, from various events such as a fault at 69 kV substation during summer and winter conditions (Case 1 and Case 2), a feeder pick up event (Case 3), are played-in to the considered feeder and load model. From the fault events considered for this analysis, Case 1 is the FIDVR event which can be replicated by simulation only if the dynamic characteristics of the

SPIM stalling is correctly modeled. From [19], it was observed that the air-conditioner motors stalling depends on the point on the voltage waveform. For this reason, the performance based SPIM models considered in the literature that are used in the positive-sequence based software tools, whose simulation time step is about a quarter cycle, might not be sufficient to capture the transient characteristics in these kinds of events. Therefore, a point on wave (POW) based SPIM [20] has been considered in this work to represent single phase induction motors. A three-phase electromagnetic transient analysis simulator such as PSCAD has been used in this work to include the POW based SPIM model.

Apart from the parameters of the feeder and load model, the type of load composition considered for a feeder model is also critically important in obtaining an accurate feeder and load model. From the geographical information gathered from the local utility engineers, it was known that the loads near substation A for Case 1 and Case 2 are predominantly residential and the loads near substation B for Case 3 are predominantly industrial and commercial loads. Using this information and the measurements data for the events considered in Case 1, Case 2 and Case 3 are used to obtain the parameters and the load composition of the standard feeder and load model, whose procedure has been discussed in detail in the following chapters.

1.3 Organization of Thesis

The thesis report is organized into six chapters.

The first chapter presents the objectives of this work, background of the research conducted in the thesis and also presents a discussion about the previous and existing techniques, available in the literature, that are used in load modeling.

Chapter 2 mainly deals with different types of loads and the feeder components used to

obtain the final standard feeder and load model.

Chapter 3 provides the procedure implemented to obtain the parameters and the load composition of the feeder and load model using the measurements of voltages and currents from a 69-kV bus fault event in both summer and winter conditions.

Chapter 4 presents the documentation on the findings of the impact of transformer saturation on the current inrush characteristic during a feeder pick up event and also the load composition of the standard feeder and load model in industrial/commercial areas.

Chapter 5 details the validation of the standard feeder and load model obtained from Chapter 3 and Chapter 4 by studying the impact of the previously considered feeder pick up event on the sub-transmission system.

The conclusions from this work has been provided in the Chapter 6 of this report. Possible future works based on the obtained standard feeder and load model has also been discussed in this chapter.

2 FEEDER AND LOAD MODEL COMPONENTS DESIGN

2.1 Introduction

Composite load models consisting of load components such as motor loads, static loads, electronic loads are being widely used to conduct transient stability studies to meet NERC transmission planning (TPL) standards requiring the load models to accurately capture the dynamic characteristics of the load behavior at peak load levels in the system [21].

In order to obtain a clear understanding of the load composition in the local utility system, a close consultation was held with its engineers. This discussion resulted in the following determination for the three cases which were analyzed. Two of the cases dealt with disturbances for which measurements at substation A were obtained and one case for which measurements at the substation B were obtained. The feeders at the substation A primarily supplied residential areas and the feeders at the substation B primarily supplied commercial and industrial loads. This information provided the basis to design the load model composition depending on the substation at which measurements were obtained. It should also be noted that the main objective of this work is to obtain a consistent set of parameters for a standard load model irrespective of the type of loads supplied by the feeders. However, varying the load composition by adjusting the percentage of different types of loads components depending on the nature of the load supplied is critical in capturing the transient behavior of the feeder and load model.

This step of load model development has been discussed in more detail in chapters 3, 4, 5. The following loads and feeder components, along with the right combination for load composition, have been incorporated in to the model to recreate the fault and feeder pick-up events at substation A and substation B respectively:

1. Single-phase induction motor loads.

2. Three-phase induction motor loads.

3. Impedance loads.

4. Distribution line segments

5. Distribution transformers

Fig. 1, depicts how the above components are represented in the proposed feeder and load model within PSCAD which has been used in this project.

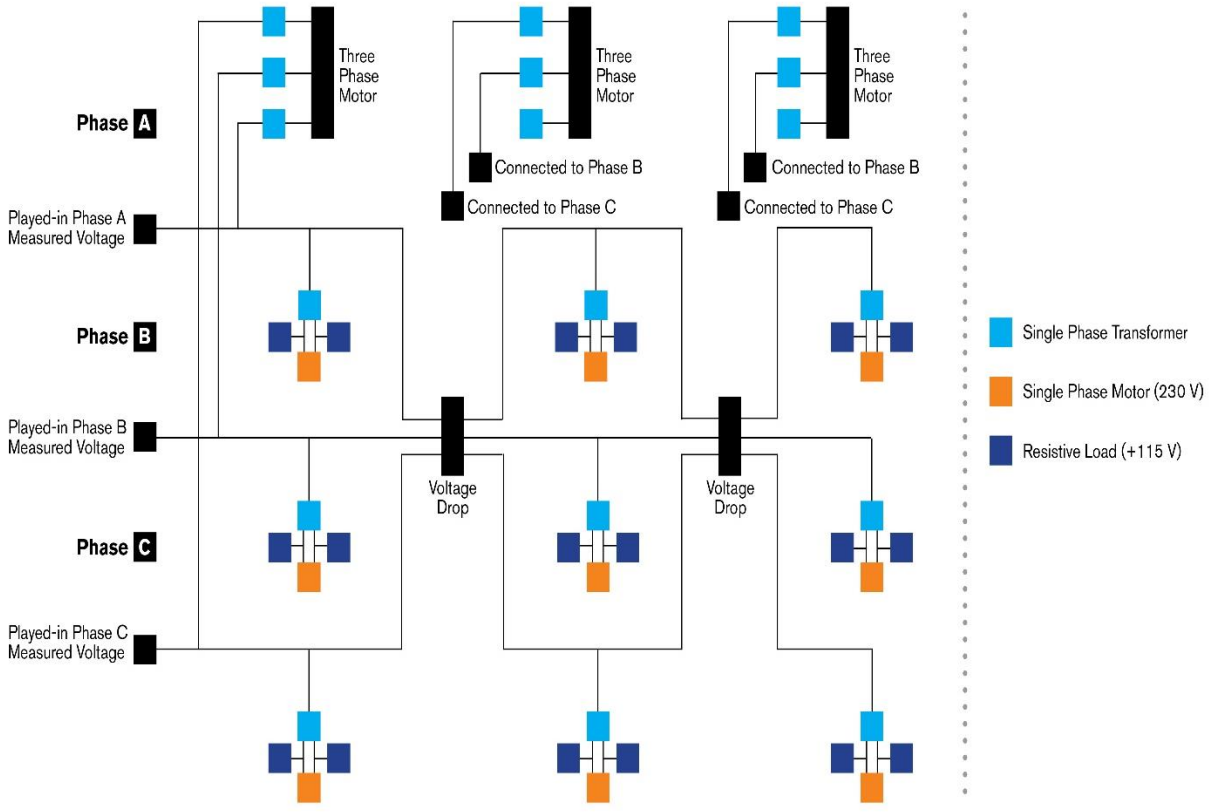

Fig. 1 Feeder and load model used in Case1, Case2 and Case3

2.2 Overhead Lines

The loads in the feeder model developed are represented as aggregated loads. For example, to represent 100 single-phase induction motors (SPIMs) at a particular location on the feeder, a

single aggregated motor rated at 450 kVA is deployed (The rating of each SPIM is of 4.5 kVA rating).

The feeder model is assumed to have a total of less than 5% voltage drop across its length, in accordance with the recommendation provided by National Electrical Code (NEC) [22]. From Fig. 1, it can be clearly seen that the proposed feeder is divided into three parts of equal length. It should also be noted that in this model the distribution lines are represented as overhead lines. In the PSCAD model, this line is represented using a short length coupled pi-section. The line data for this pi model is provided in terms of positive, negative and zero sequence data. For this reason, from [23], the line parameters of a typical overhead distribution line considered are:

Positive Seq Resistance (r1) = Negative Seq Resistance (r2) = 0.3 ohm/mile

Positive Seq Inductive Reactance (x1) = Negative Seq Inductive Reactance (x2) = 0.64 ohm/mile

Positive Seq Capacitive Reactance (Xc1) = Negative Seq Capacitive Reactance (Xc2) = 0.01 Mohm*mile

Zero Seq Resistance (r0) = 0.7980 ohm/mile

Zero Seq Inductive Reactance (x0) = 2.04 ohm/mile

Zero Seq Capacitive Reactance (Xc0) = 0.01 Mohm*mile

The length of the feeder (in miles) is adjusted so as to achieve a total voltage drop of 4% from the head of the feeder to the end of the feeder. To satisfy this condition, a total feeder length of 1.2 miles has been assumed in Case1 and Case 2 whereas a length of 1.6 miles has been assumed in Case3 and Case4.

2.3 Three-phase Induction Motors

The three-phase induction motor model considered is the squirrel cage type because of its ubiquitous presence in most of the motors present in practical distribution feeders. For this model, in PSCAD/EMTDC, torque control mode is used to operate the three-phase induction motors. These are motors which are typically rated at 460 V line-line RMS. Table 1 provides the data for the standard parameters considered for this model.

Table 1 Three-phase Induction Motor Parameters

Number	Parameter	Values
1.	Voltage Rating (line-line RMS)	460 V
2.	H (Inertia Constant)	0.3 s
3.	Stator Resistance	0.013 pu
4.	Inner Rotor Resistance	0.009 pu
5.	Outer Rotor Resistance	0.15 pu
6.	Stator Leakage Inductance	0.067 pu
7.	Inner Rotor Leakage Inductance	0.17 pu
8.	Outer Rotor Leakage Inductance	0.225 pu
9.	Magnetizing Inductance	3.8 pu
10.	Initial Load Percentage Pickup	65%
11.	Type of Mechanical Load	D =1
12.	Power Factor	0.88

This motor model is available in the PSCAD library. The mechanical torque, in pu, of this motor is modeled using the following equation:

$$T_{mechanical} = k * \omega$$

Where, k is the initial load percentage pickup factor (0.65 in this case)

ω is the speed of the motor in pu

2.4 Single -phase Induction Motors

One of the most important type of load that needs to be considered in the residential areas

are the single-phase air conditioner compressor motors. It should be noted that this model is not available in the PSCAD library. For this reason, a user-defined single-phase induction motor (SPIM) model developed in [20] has been used for this work. This motor model is a transient model of air-conditioner compressor single-phase motor. From Fig. 2, it can be clearly seen that the load torque of the single-phase induction motor is represented in the form of a triangular wave which includes both speed dependent load torque and angle dependent load torque.

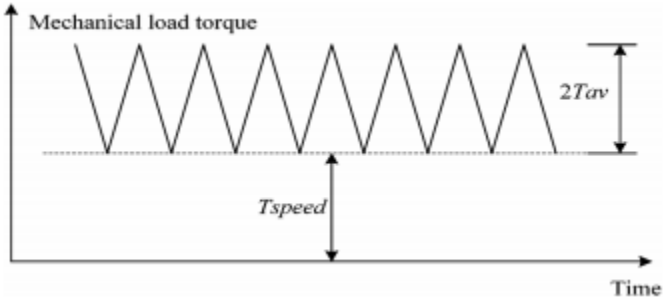

Fig. 2 Load torque profile for SPIM

Table 2 Single-phase Motor Parameters

Number	Parameter	Values
1.	Voltage Rating (line-line RMS)	230 V
2.	Rotor Diameter	0.07 m
3.	Stator Resistance	0.3 ohm
4.	Main to auxiliary winding turns	1.4
5.	Rotor Resistance	0.5 ohm
6.	Stator Leakage reactance	0.6 ohm
7.	Rotor Leakage reactance	0.4 ohm
8.	Speed dependent load torque	7.1 N-m
9.	Angle dependent load torque	5.1 N-m
10.	Magnetizing reactance	30 ohm

The terminal resistance of a single SPIM is considered to be 5 μohm. This terminal resistance represents the line resistance between the distribution transformer and the SPIM. Similarly, the run capacitor of a single SPIM is assumed to be 80 μF. It should be noted that in this

model, if the SPIM is scaled by a factor 'x' to represent the aggregated load, then the terminal resistance and the run capacitor should be scaled by the same factor 'x' to represent their equivalent values for the aggregated SPIM load.

From Table 2, it can be observed that rotor diameter is very small (7 cm) which characterizes the typical low inertia of single-phase induction motors used to represent A/C compressor motors. This low inertia plays an important role in the stalling characteristics of these single-phase induction motors in fault induced delayed voltage recovery (FIDVR) events.

2.5 Distribution Transformers

The modeling of the distribution transformers has been discussed in great detail in Chapter 4 to investigate the effects of transformer saturation on feeder pick-up currents transients.

2.6 Load Composition

The load composition of the feeder plays an important role in determining the response of the system to a disturbance. For this reason, efforts have been made in this work to determine a proper load composition of the designed feeder and load model depending on the type of location the feeder is located. After conducting sensitivity analysis using the parameters of the feeder and load components (Sections 2.2, 2.3, 2.4, 2.5) the following conclusions have been drawn about the load compositions of the proposed feeder and load models:

Table 3 Load Composition of feeder and load model according to their location

Geographical Location Type of the Feeder and Load Model	Single-phase Load Percentage	Three-phase Load Percentage	Impedance Load Percentage
Residential	72%	18%	10%
Industrial and Commercial	18%	72%	10%

From Table 3, it can be observed that the percentage of single-phase load and three-phase load is varied according to the type of load served by the feeder. This information can be determined by performing a load survey. In this project, this information was determined by a consultation with the local utility engineers. In Chapter 3, the feeder and load composition have been modeled for a residential area (substation A area) whereas in Chapter 4, the feeder and load composition have been modeled for an industrial and commercial area (substation B area) using the load compositions from Table 3. In Chapter 3 and Chapter 4 the load composition for the feeder and load models have been discussed in greater detail.

3 SUBSTATION A FEEDER MODEL

3.1 Case 1: Substation A Summer Event: Introduction

This section details the procedure for obtaining a novel feeder model to estimate appropriate (when compared to corresponding measured responses) current responses, for a FIDVR event, when measured three-phase voltages are played-in to the model. The details of this FIDVR event are given below:

Event type: Phase A line to ground fault at substation K on a 69-kV circuit breaker.

Event time of occurrence: 10:33 AM on 8th August 2016.

Available DFR measurements: Voltages, Currents point on wave data at substation A (13.8 kV – low voltage side of the substation)

For this feeder analysis, the available three-phase voltage measurements are played into a three- phase feeder model in PSCAD. The played-in voltages for this event are presented below in Fig. 3, Fig. 4, Fig. 5.

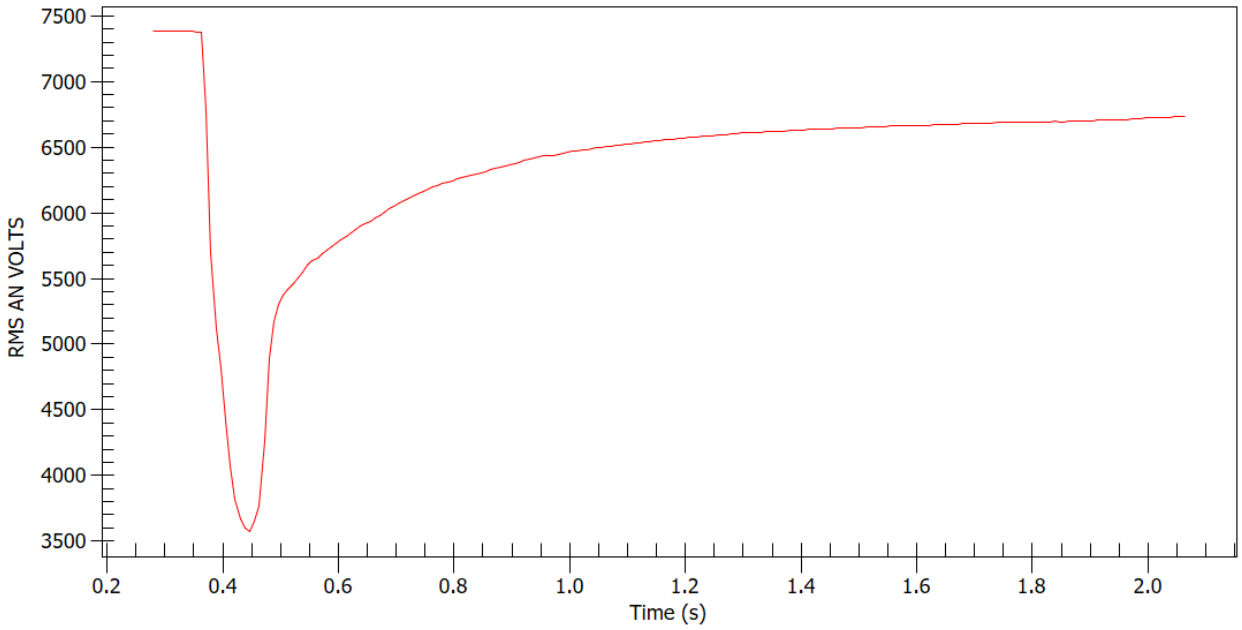

Fig. 3 Phase-A faulted RMS voltage profile

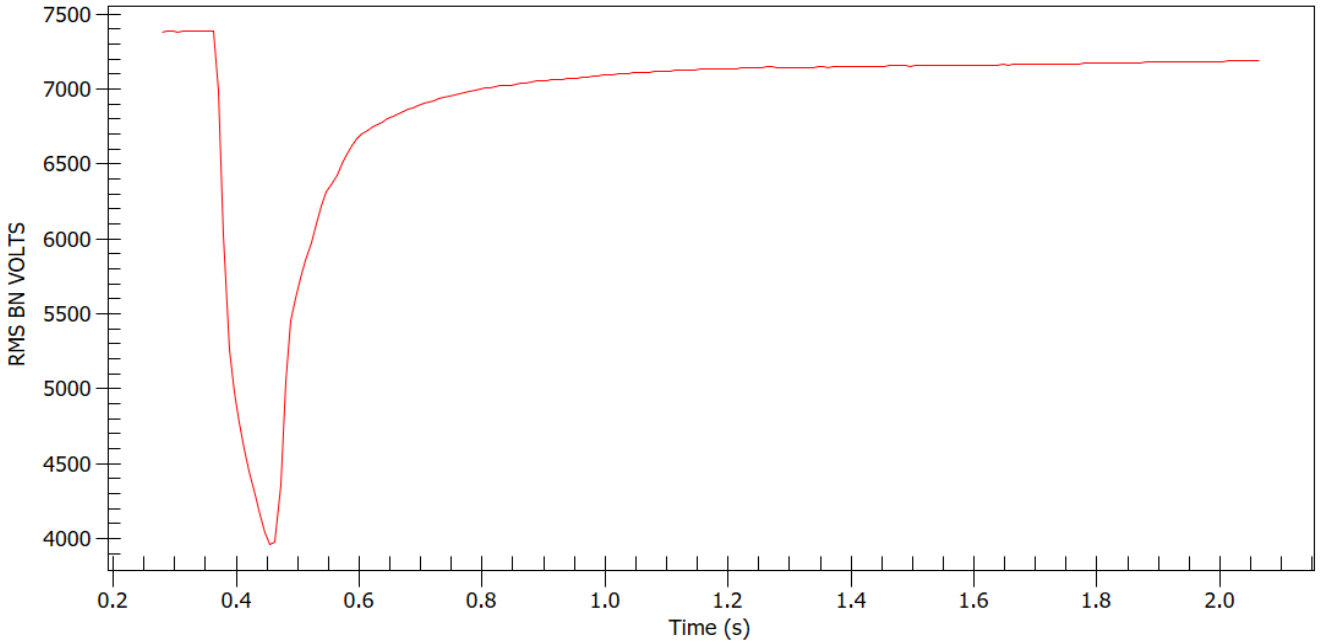

Fig. 4 Phase B non-faulted RMS voltage profile

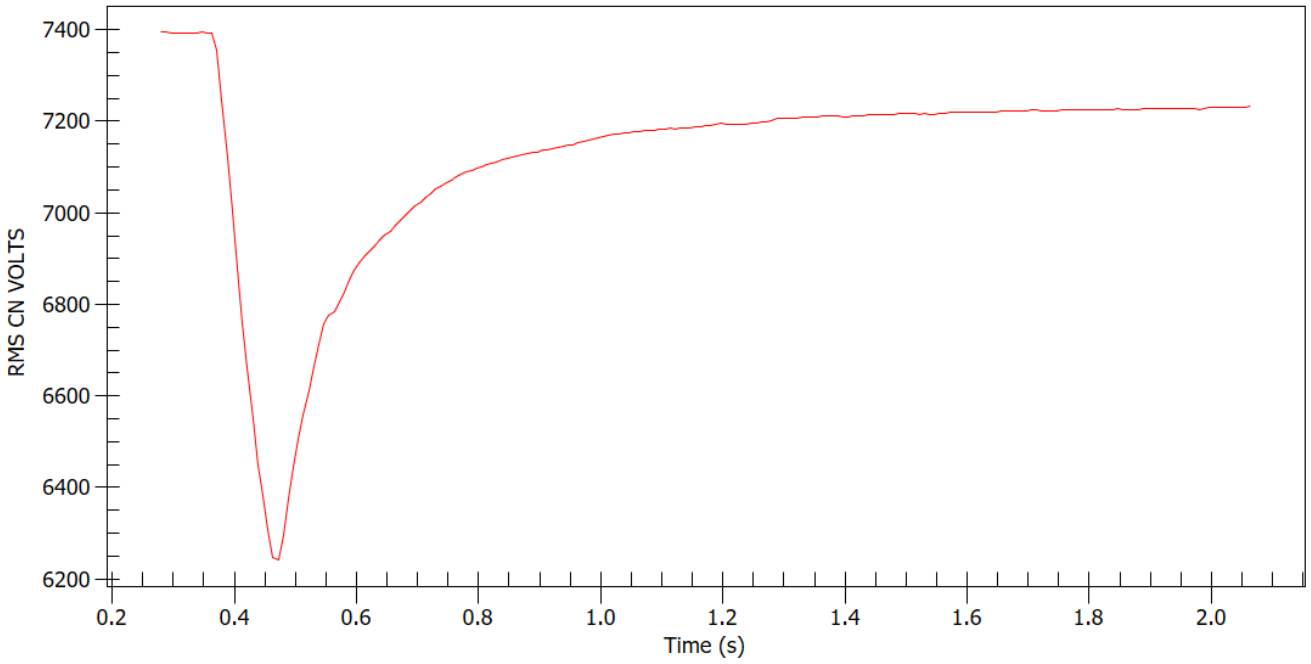

Fig. 5 Phase C non-faulted RMS voltage profile

Note1: It should be noted that the FIDVR event occurred just before 0.4 secs on time-axis in Fig. 3, Fig. 4, Fig. 5

Note2: Although only phase-A is faulted, phase-B voltage also seems to be affected due to the Delta-Star configuration of the transformers between the sub-transmission level and the distribution level

From Fig. 3, it can be clearly seen that the voltage plot characterizes a FIDVR event because the phase A voltage takes a long time to recover to the nominal state after the fault is cleared. In the literature [6], [20] many instances of single-phase induction motors stalling being the primary reason behind this type of FIDVR events, have been cited. This phenomenon is verified in Fig. 11.

3.2 Substation A Summer: Load composition

After consulting with the local utility engineers, it was determined that the substation A feeders are located in residential areas and primarily serve residential load. This information was used as a starting point to formulate the load model composition. The following loads have been incorporated in the model to synthesize an accurate load composition at substation A area:

1.Single-phase Induction Motor Loads.

2. Three-phase Induction Motor Loads.

3. Lighting Loads.

A large percentage of the load is assumed to be SPIM because residential areas usually have a large percentage of load which comprises of air conditioners, ceiling fans, refrigerators and

other appliances driven by SPIMs. A smaller portion of three-phase motor loads has been assumed to represent a few commercial buildings or offices with air conditioners driven by three-phase motors. An even smaller amount of lighting loads has also been represented in the model. The load compositions for this FIDVR case was determined after iterating using a simple trial and error process to obtain the best match between the simulated current obtained from PSCAD with the played-in measured voltage and the actual measured current is presented in Table 4.

Table 4 Load Composition for Substation A Summer Case Feeder Model

Type of load	Phase A	Phase B	Phase C
Lighting Load	0.594 MW	0.594 MW	0.594 MW
Single-Phase Load	4.56 MVA	4.56 MVA	4.56 MVA
Three-Phase Load (1/3 Total Load)	1.14 MVA	1.14 MVA	1.14 MVA

From Fig. 1, it can be observed that there are three segments along each phase of the feeder operating at different voltages because of two pi-coupled overhead distribution lines along the feeder. The load composition across these three segments are as shown in Table 5.

Table 5 Load Composition Across Three Segments of the Feeder Per Phase

Type of load	Segment 1	Segment 2	Segment 3
Lighting Load	0.2 MW	0.2 MW	0.2 MW
Single-Phase Load	1.2 MVA	1.68 MVA	1.68 MVA
Three-Phase Load	0.38 MVA	0.38 MVA	0.38 MVA

From Table 5, it can be observed that both lighting loads and three-phase loads are distributed equally along each segment of the feeder in each phase. Whereas, the single-phase loads are distributed in the ratio of 1:1.4:1.4 along the three segments of the feeder in each phase. The primary reason for choosing this ratio of SPIM loads across the three segments is to capture the FIDVR phenomenon observed in the measured voltages and is known to occur due to the stalling of SPIMS. It was conjectured, that since the voltage recovery was so slow, a large number of SPIMS might have stalled towards the tail end of the feeder. This is a reasonable assumption because the load near the substation (head of the feeder) is typically low when compared to the load farther from the substation (tail end of the feeder).

From Table 4, the following observations can be made:

$$\frac{\text{Total Single} - \text{phase Load}}{\text{Total Three} - \text{phase Load}} = \frac{13.68\ \text{MVA}}{3.42\ \text{MVA}} = 4$$

$$\frac{\text{Total Lighting Load}}{\text{Total Load}} = \frac{1.782\ \text{MW}}{18.882\ \text{MVA}} \sim 10\%$$

$$\frac{\text{Total Three} - \text{phase Load}}{\text{Total Load}} = \frac{3.42\ \text{MVA}}{18.882\ \text{MVA}} \sim 18\%$$

$$\frac{\text{Total Single} - \text{phase Load}}{\text{Total Load}} = \frac{13.68\ \text{MVA}}{18.82\ \text{MVA}} \sim 72\%$$

Therefore, motor load comprising of 90% of the total load has been considered in this model. It should be noted that the same percentage of motor loads (90%) and lighting loads (10%) as used in this case are used in both Case2 (substation A winter case), Case3 (substation B feeder pick-up case).

The ratio of single-phase load to three-phase load in this case is taken to be 4 as shown above. This follows the logic that the load near substation A is predominantly residential (this information is obtained from the local utility).

3.3 Case 1: Substation A Summer: Sensitivity Analysis

In previous sections it has been mentioned that the voltages depicted in Fig. 3, Fig. 4, Fig. 5 are played-in to this feeder and load model to capture accurate simulated current responses. For this reason, parameter sensitivity analysis has been done in this work. This analysis can be divided into two parts: Pre-fault analysis and post fault analysis. The feeder current profiles of all three-phases have been presented in Fig. 6, Fig. 7, Fig. 8. A vertical line has been shown in Fig. 6, Fig. 7, Fig. 8 to represent the instant of fault initiation in all the three-phases.

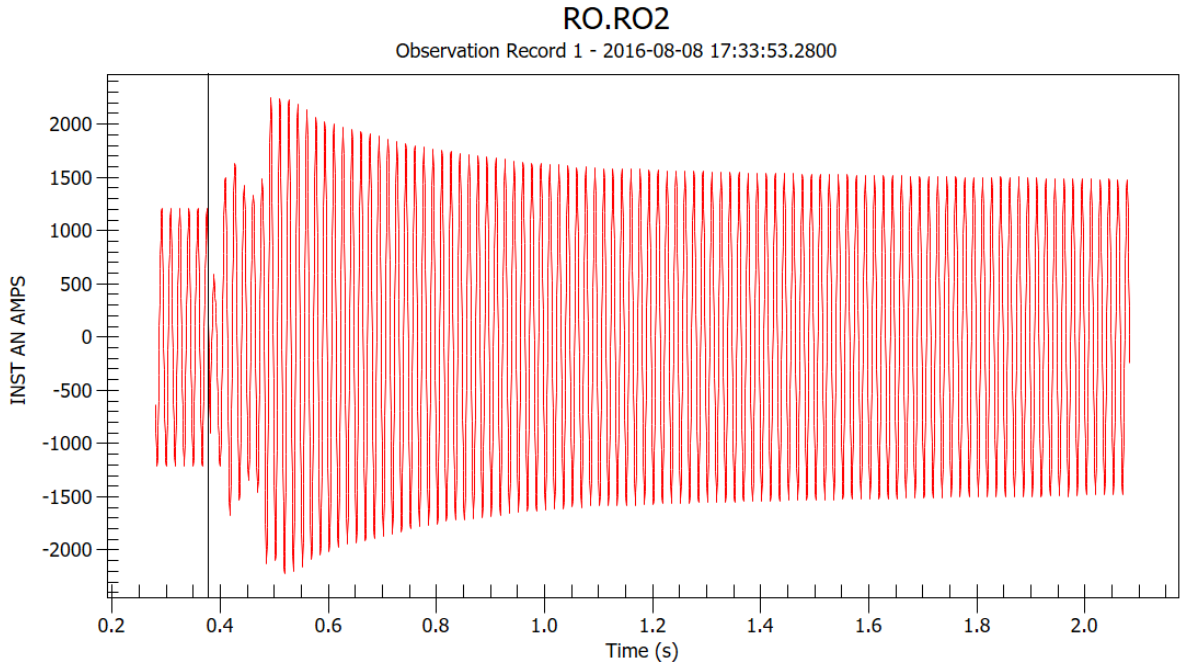

Fig. 6 Phase A Faulted Current at Substation A

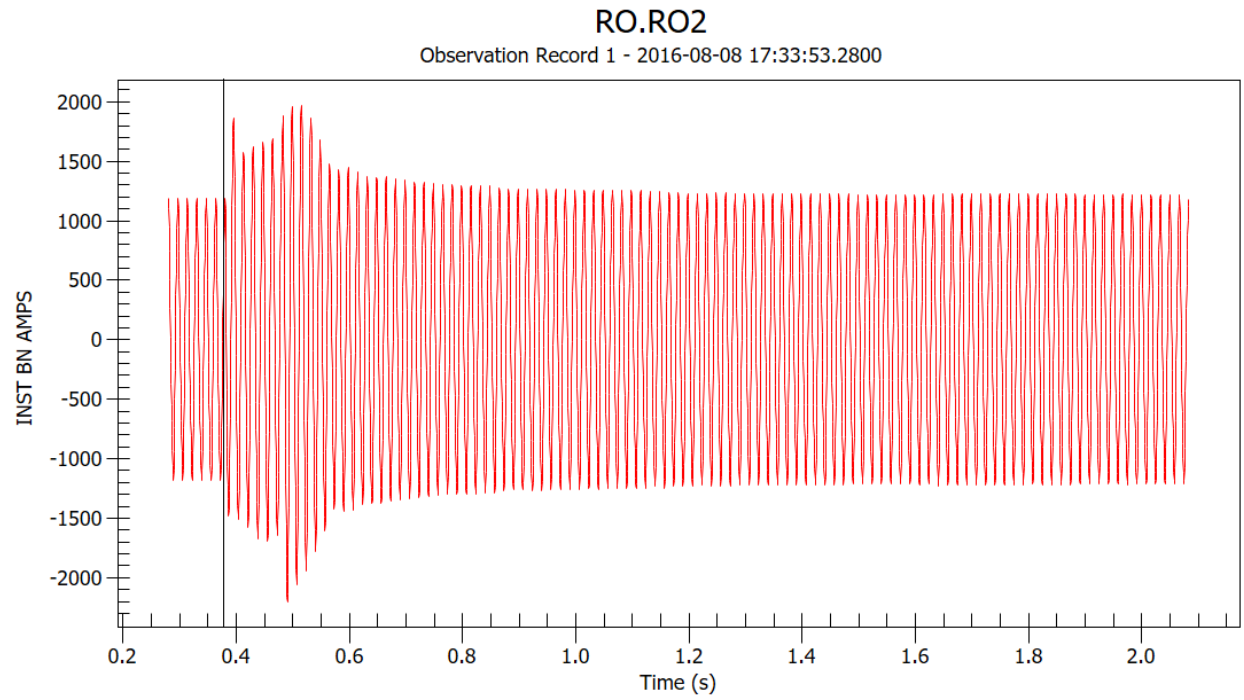

Fig. 7 Phase B Non-Faulted Current

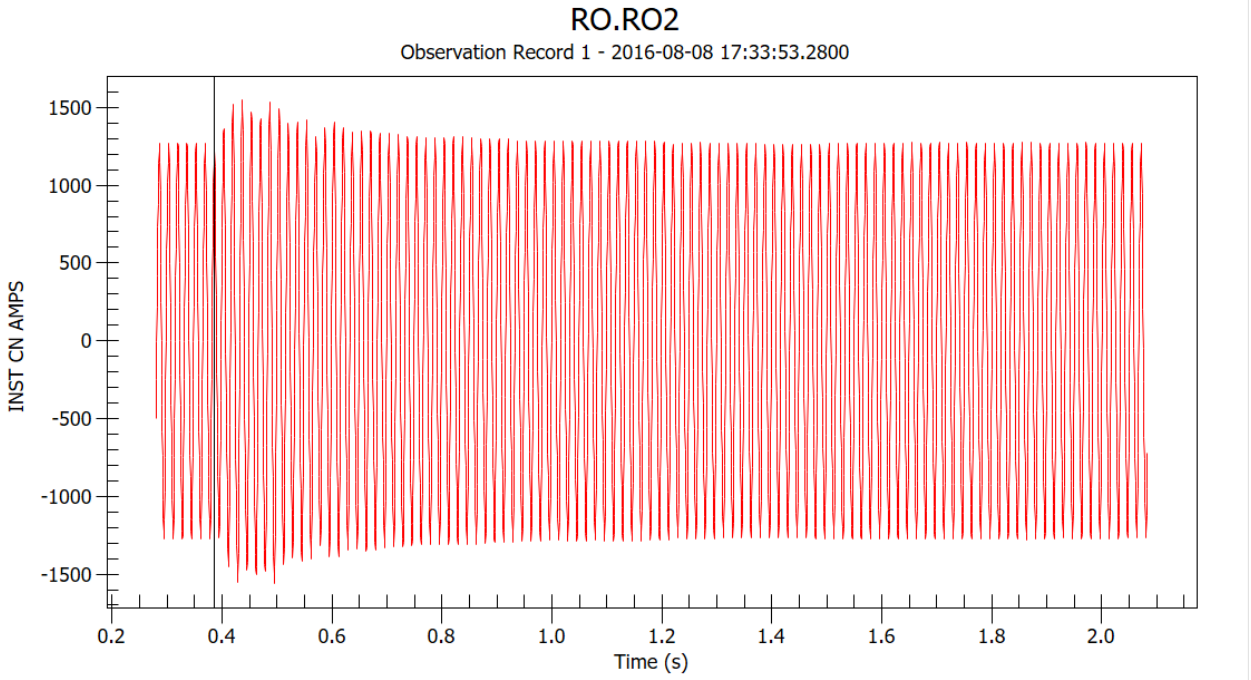

Fig. 8 Phase C Non-Faulted Current

From Fig. 6, it can be clearly observed that the post-fault current in Fig. 6 is higher than

the pre-fault current by around 300 Amps. This indicates stalling of motors, where the stalled motors draw locked rotor current until they are tripped due to internal protection. Since, in the available data obtained from Schneider ION 7650 and Schneider ION 8650A meters, the time span after the fault is cleared is only about 1 sec, the locked rotor current didn't die away in the observed time span. It should also be noted that this phenomenon is not observed in Fig. 7, Fig. 8. Hence, efforts have been concentrated on making motors stall (after the fault is applied) in only phase A of the feeder.

3.4 Substation A Summer: Pre-fault analysis, linear interpolation, linear extrapolation

Before analyzing this case, the pre-fault currents obtained from the simulation need to be matched with respective measured phase currents. To achieve this, the considered aggregate load should be scaled accurately to match the pre-fault current. Hence, the P (active power), Q (reactive power) values have been obtained from the feeder three-phase voltage and current measurements using Matlab Simulink's V-I to P-Q conversion circuit which involves the 'Power' block from the Simulink library.

Another important issue that needs to be addressed in this model is that from Fig. 3, Fig. 4, Fig. 5, it can be clearly observed that the voltage measurement data before the fault occurs (at time =0.1 sec) is available for only 0.1 secs. However, this time frame is insufficient to start the motors and to get them to operate at a steady state speed in the PSCAD model. For this reason, the first cycle of the available measured voltages has been **extrapolated linearly** backwards and is repeated for 1 sec in Matlab before playing the original measured voltages into the PSCAD model.

It should also be noted that the sampling frequency of the available measurements are in the order of 1921 Hz from Schneider ION 7650 and Schneider ION 8650A meters. However, the

sampling frequency of the time step in the PSCAD model is about 200 kHz. For this reason, **linear interpolation** for the extrapolated measurements has been done in Matlab to achieve the 200 kHz sampling frequency.

The procedure for matching the pre-fault measured currents to the simulated pre-fault current values is shown below:

Step1: Assume a load composition percentage for each load type (In this case, the following percentages are chosen: SPIM -72 %, Three-phase Motor -18 %, Lighting load – 10%)

Step2: Observe the amount of P, Q each SPIM and three-phase motor are drawing for the played-in measured voltages.

Step3: The P drawn by the lighting load can be calculated by V_{rms}^2 /r (at 115 V)

Step4: Using the pre-fault P value obtained from Simulink, the motor loads from Step2 need to be scaled to obtain the desired percentage of motors composition.

Step 5: Adjust the lighting load value 'r' (using the formula given in Step 3) to obtain the lighting load composition from Step1.

Step 6: Place a capacitor bank if necessary at the head of the feeder to make sure the pre-fault Q value obtained from Simulink model is equal to the pre-fault Q obtained in the PSCAD model for all three-phases.

Fig. 9, Fig. 10 shows the active power and reactive power at the head of the feeder which is obtained from PSCAD/EMTDC model.

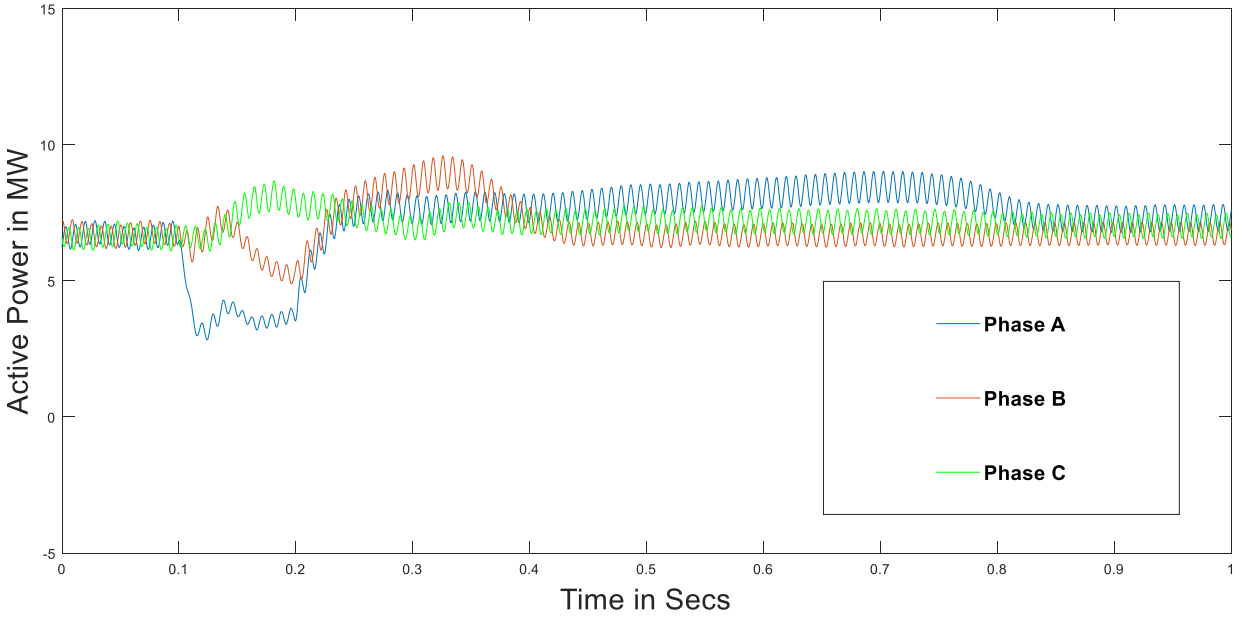

Fig. 9 Simulated active powers for three-phases at the head of the feeder

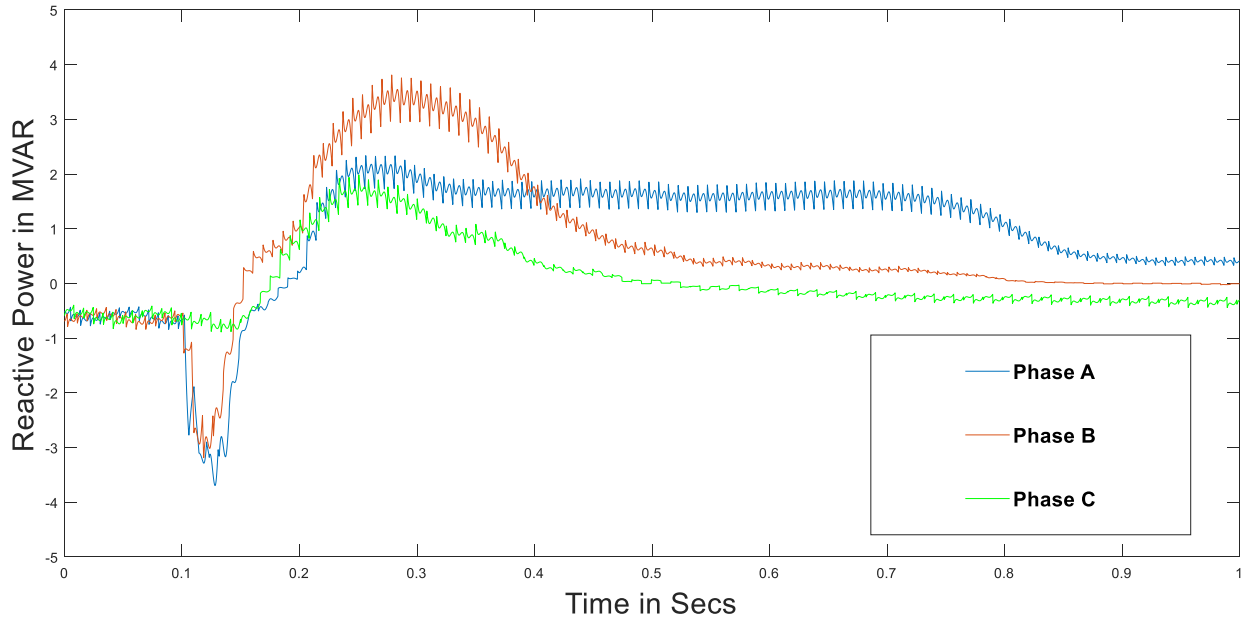

Fig. 10 Simulated reactive powers for three-phases at the head of the feeder

3.5 Substation A Summer: Post-fault analysis and parameter sensitivity

After obtaining the pre-fault currents, sensitivity analysis has been done to get a close match of the fault transients as seen from Fig. 6, Fig. 7, Fig. 8. In PSCAD simulations, it is observed from the plots of the speeds of the motors, that after a fault is applied, the SPIMs are the most affected by the fault whereas the three-phase motors are the least affected. This seems to be logical considering that the inertia of the SPIMs is very low whereas the three-phase motors have a higher inertia. This might also be due to the fact that only one phase is faulted. Hence, the two other phases are supporting the three-phase motors. For these reasons, the sensitivity analysis for this substation A case has been conducted only for SPIMS. As the post fault current in phase A is more than the pre-fault current, it is concluded from the sensitivity analysis (whose critical parameters are shown in the later part of this section) that the following three types of motor speeds need to be achieved in order to match the post fault current in phase A:

Figs. 11-13 depict the end-result of the sensitivity investigation. These figures show the speeds of the nine blocks of single-phase motors (see Fig. 1) from a single simulation conducted using the parameter values shown in Table 6.

(i) **Condition1:** Segment 1 SPIMs – Not stalled and less reacceleration time required to come back to nominal speed

(ii) **Condition2:** Segment 2 SPIMs – Not stalled and more reacceleration time required to come back to nominal speed

(iii) **Condition3:** Segment 3 SPIMs – Stalled and do not come back to the nominal speed

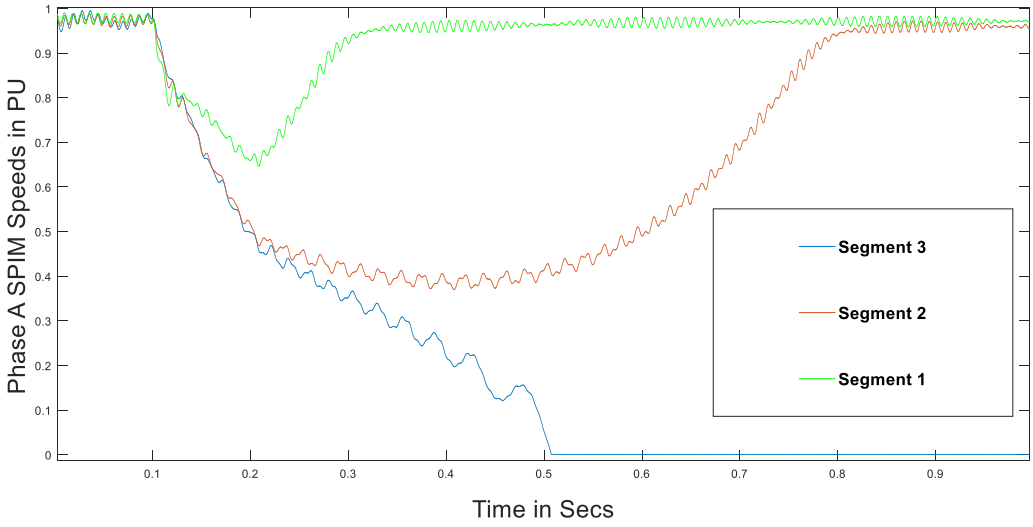

Fig. 11 SPIM speeds at three different segments across the feeder in phase A

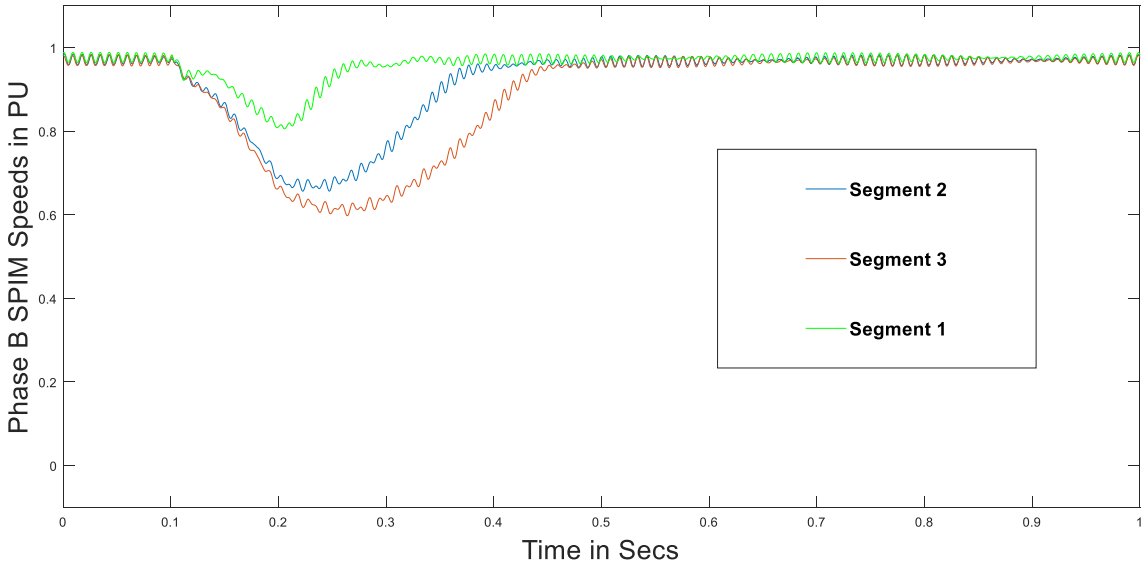

Fig. 12 SPIM speeds at three different segments across the feeder in phase B

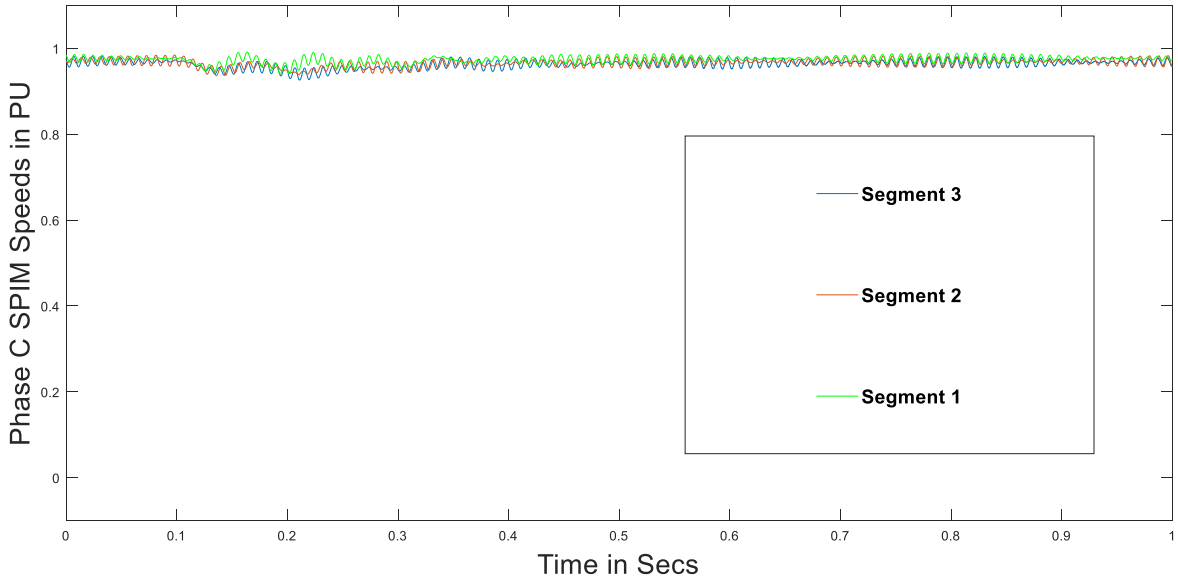

Fig. 13 SPIM speeds at three different segments across the feeder in phase C

From Fig. 12, it can be clearly observed that the speeds of the SPIMs are not as affected as observed in phase A from Fig. 11. This is to be expected because phase B is not the faulted phase. Although, the speeds of SPIMs in Fig. 13 (phase C) are even less affected due to the phase A fault. This is because as mentioned earlier in *Note2*, the voltage in phase B has a dip similar to phase A due to the Y-Delta transformers whereas voltage in phase C sees the least dip as it is not the faulted phase nor is affected by the Y-Delta transformers in the 69-kV network.

Critical Parameters:

The following four parameters of the SPIM are found from sensitivity analysis, to be the critical parameters in obtaining the speed curves shown in Fig. 11:

A. Number of Motors: After obtaining the total number of single-phase induction motors from the pre-fault analysis, they are distributed in such a way as to satisfy the desired speeds of SPIM mentioned above in phase A. It is known that during the fault, the voltage level in the system decreases. Due to this, the speeds of the SPIM motors reduce until the

fault is cleared. After the fault is cleared, the SPIMs require more reactive power to get back to the nominal speed. This indicates that more the number of motors in an aggregated motor, the more probable it is to stall (thereby all the individual motors stall) because the aggregated motor requires reactive power to reaccelerate to the nominal speed. Using this inference, it can be concluded that this parameter (number of motors) is very important in the sensitivity analysis. This parameter is especially useful in achieving Condition3 of the desired speeds of SPIM mentioned earlier.

B. Load Torque: In SPIMs, the load torque is modeled as a combination of speed dependent load torque (range of Tload from 7 N-m to 8 N-m has been considered) and angle dependent load torque (range of Tav from 5 N-m to 6 N-m has been considered). It can be clearly observed that more the load torque of the SPIM, the more time it takes for the SPIMs to reach the nominal speed after a fault is cleared.

C. Inertia of Motors: Apart from the load torque of SPIMs, the inertia of the motors itself also play an important role in determining at what time the SPIMs reach the nominal speed after a fault clearance. The inertia of the motor is closely related to its diameter. Therefore, using a base value of 6.5 cm from Table 2 the sensitivity analysis from 6 cm to 7.5 cm has been considered for different SPIM motors.

D. Rotor Resistance: The slip of an induction motor is directly affected by the rotor resistance. Since, slip is a function of the rotor speed this is another parameter which is considered important in the sensitivity analysis. This parameter is especially important in matching the current during the faulted condition (before the fault is cleared). In fact, even before conducting the sensitivity for the A, B, C parameters this parameter D needs to be adjusted to get a close match during the fault. It is concluded that a final value of rotor

resistance of 0.5 ohms is optimum for the best estimation of the currents.

Table 6 Final critical parameters values of SPIM obtained after implementing the sensitivity analysis mentioned above

Critical Parameter	Value
Number of SPIM per phase	300 (Segment1), 420 (Segment2), 420 (Segment3)
Load Torque of SPIM	Tload – 7.1 N-m and Tav – 5.1 N-m
Inertia of SPIM (represented by rotor diameter)	7 cm
Rotor Resistance	0.5 ohm

3.6 Substation A Summer: Results and discussion

The final simulated currents at the head of the feeder are as shown below in Fig. 14, Fig. 15, Fig. 16

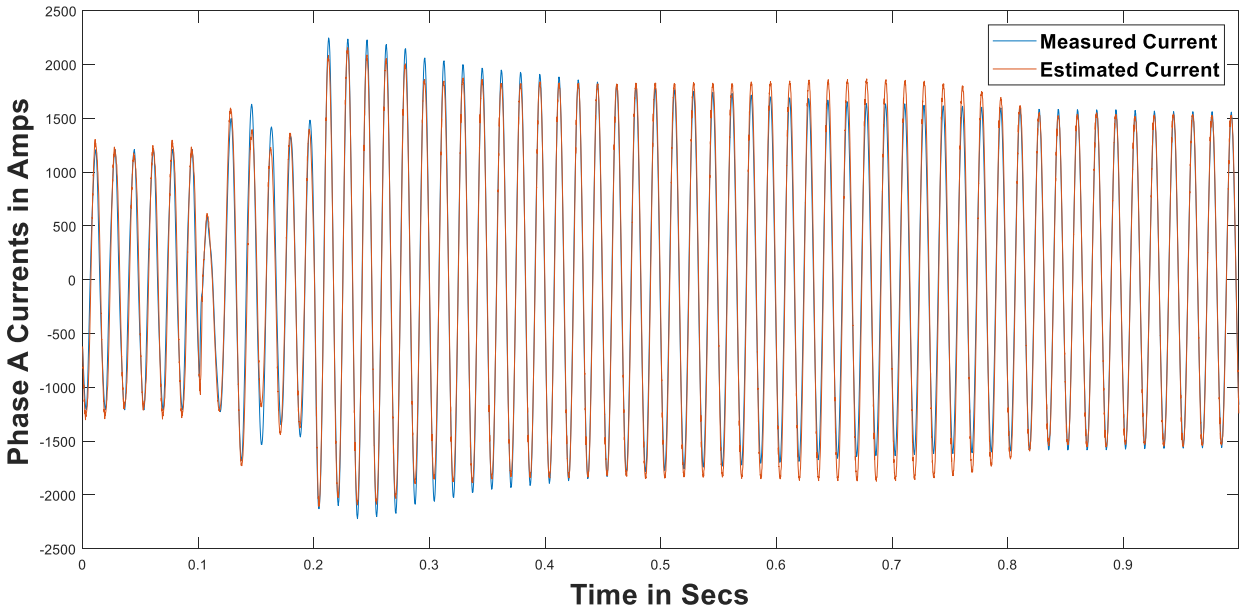

Fig. 14 Phase A current comparison for summer case

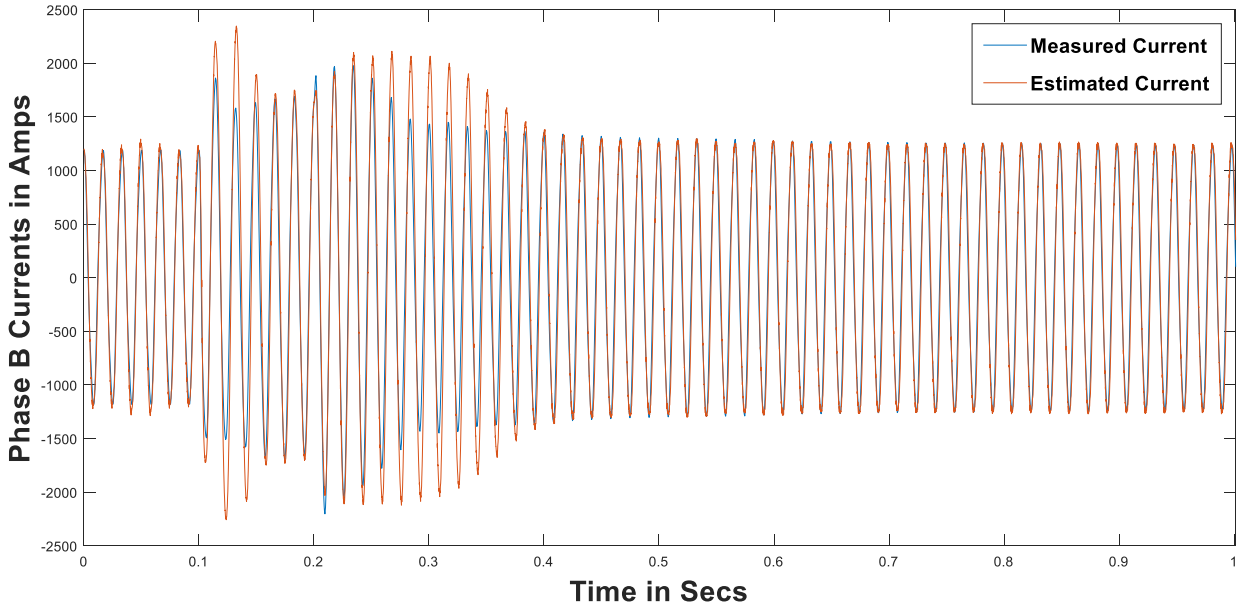

Fig. 15 Phase B current comparison for summer case

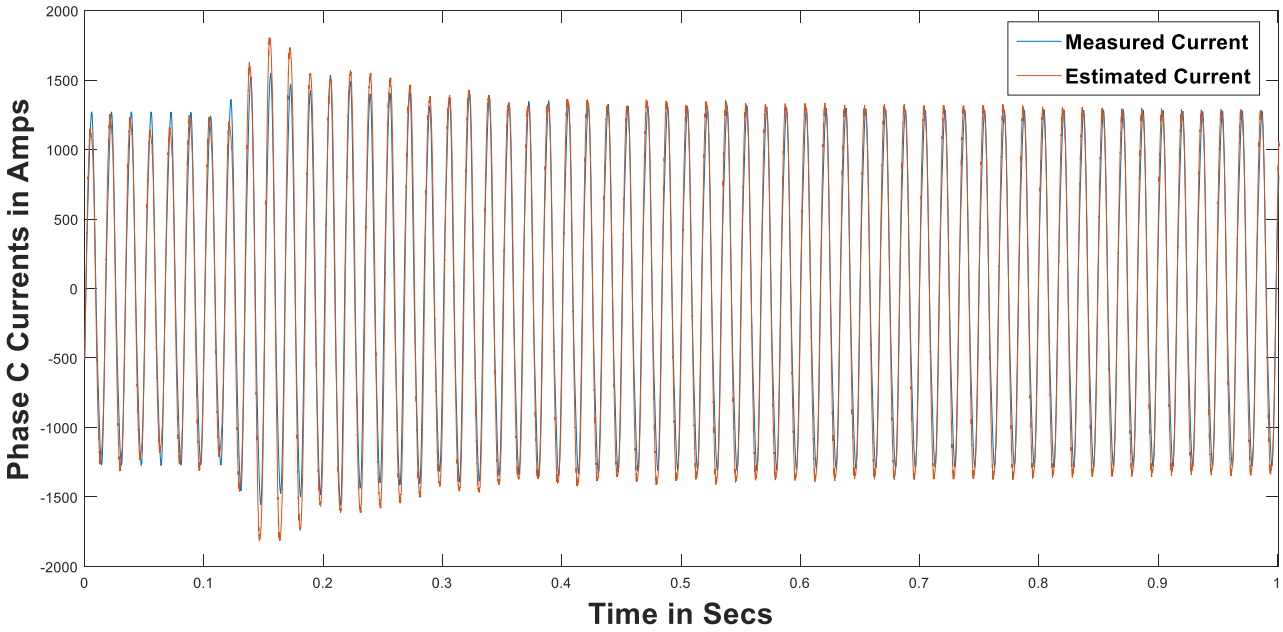

Fig. 16 Phase C current comparison for summer case

From Fig. 14, it can be clearly seen that for the faulted phase A current, a good match between the simulated current and measured current has been obtained. This is a clear indication that stalling occurred in the SPIM's of this phase due to this FIDVR event.

From Fig. 15, it can be observed that apart from the time period of 0.25 sec to 0.35 sec a very good match between the simulated current and measured current for phase B is obtained. From sensitivity analysis, it is observed that mismatch from 0.25 sec to 0.35 sec can be reduced by changing the inertia of SPIM's from chosen rotor diameter value of 7 cm to 8 cm. However, to keep the parameters for all the motors in all phases to be same the final result for rotor diameter of 7 cm is presented here.

From Fig. 16, it can be concluded that even for the least affected phase the simulated current obtained has a very good match with the measured current of phase C.

3.7 Case 2: Substation B Winter: Introduction

In this work, the same feeder and load model used in the substation A summer case has been used to verify the validity of the model during winter conditions.

Event Details:

Event type: Phase A line to ground fault at substation K 69 kV bus.

Event time of occurrence: 10:33 AM on 11th November 2016.

Available DFR measurements: Voltages, Currents point on wave data at substation A (13.8 kV – low voltage side of the substation)

Fig. 17, Fig. 18, Fig. 19 shows the measured voltages that are played into this model to obtain the simulated currents at the head of the feeder.

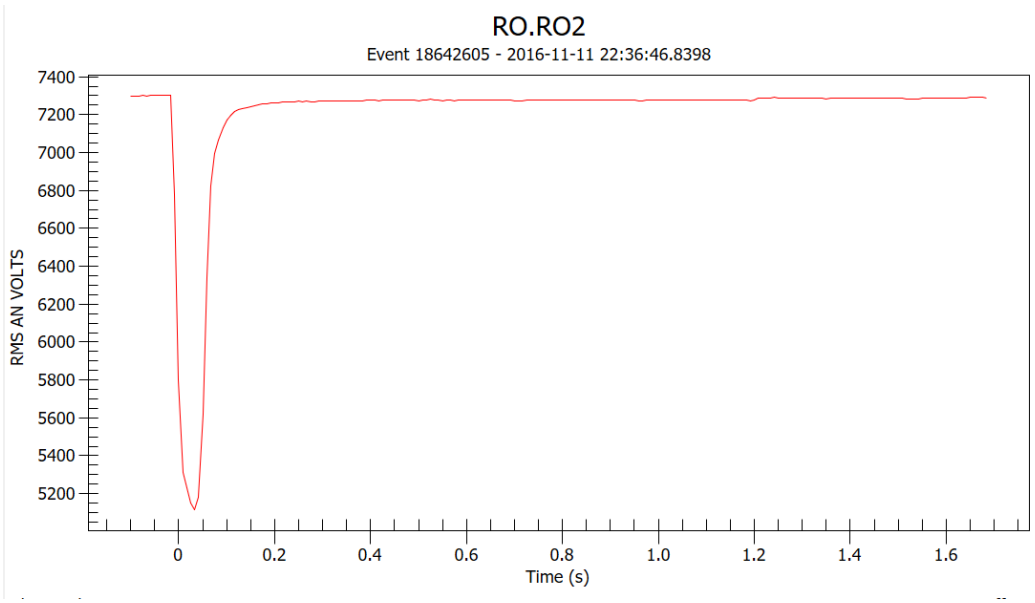

Fig. 17 Phase A faulted RMS voltage profile

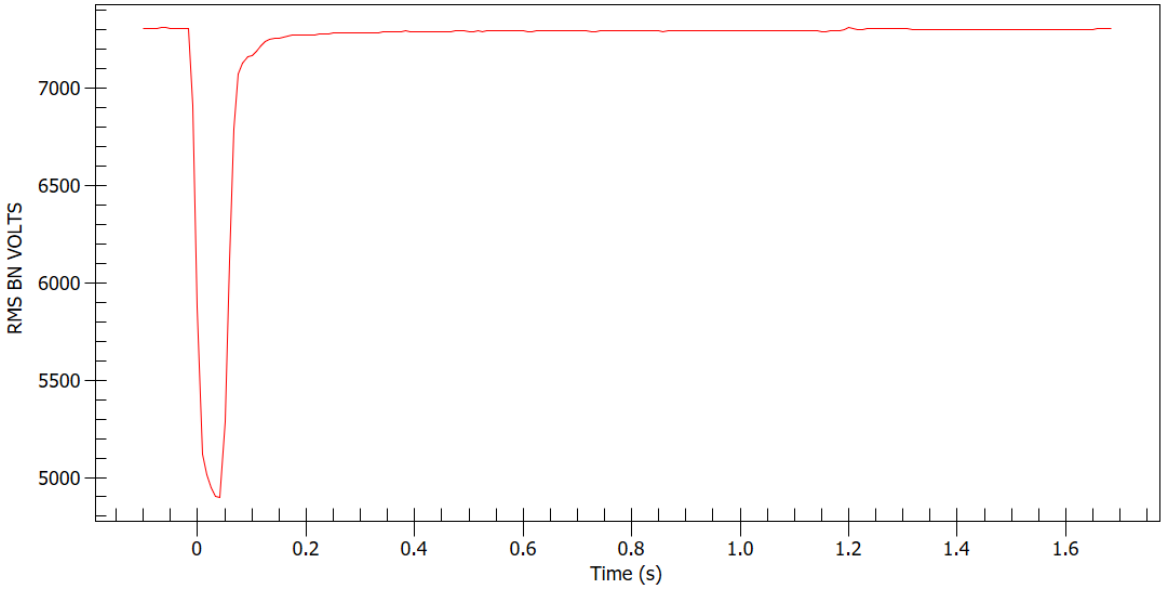

Fig. 18 Phase B non-faulted RMS voltage profile

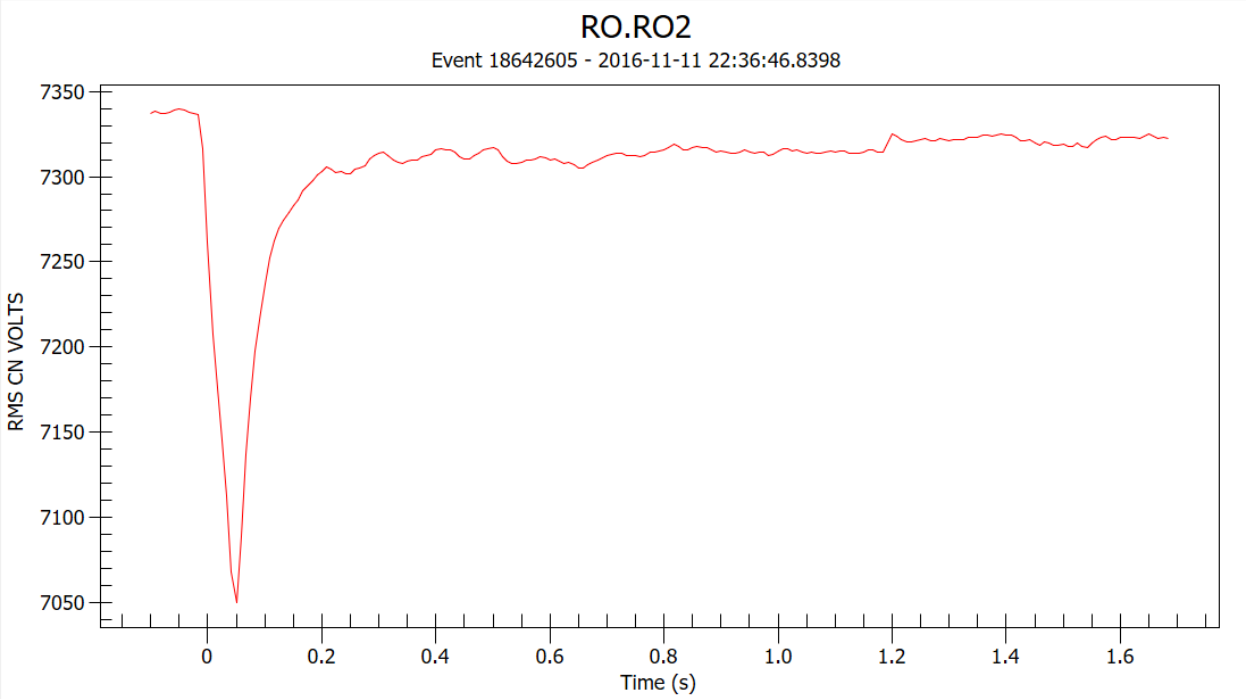

Fig. 19 Phase C non-faulted RMS voltage profile

From Fig. 17, Fig. 18, Fig. 19 it can be seen that all three voltages recover to the nominal voltage (after the fault is cleared) very quickly compared to the phase A voltage response of Case 1: Substation A Summer case. From this, we should expect that there would be no stalling of motors being involved in this case.

3.8 Substation A Winter: Load composition

The load composition from Table 3, Table 4 are scaled by exactly a factor of 0.4 to obtain the load composition for this winter case. This scaling is done to match the pre-fault current measured values from the obtained simulated responses. These scaled values are as shown in Table 7, Table 8.

Table 7 Load Composition for Substation A winter case feeder model

Type of load	Phase A	Phase B	Phase C
Impedance Load	0.2376 MW	0.2376 MW	0.2376 MW
Single-phase Load	1.14 MVA	1.14 MVA	1.14 MVA
Three-phase Load (1/3 Total Load)	0.285 MVA	0.285 MVA	0.285 MVA

Table 8 Load composition across three segments of the feeder per phase

Type of load	Segment 1	Segment 2	Segment 3
Impedance Load	0.05 MW	0.05 MW	0.05 MW
Single-phase Load	0.3 MVA	0.42 MVA	0.42 MVA
Three-phase Load	0.095 MVA	0.095 MVA	0.095 MVA

Although, the total load from the substation A summer case is scaled down by 0.4 the ratio between the single-phase motor load to three-phase motor load and the lighting load percentage composition is kept constant for these two cases.

3.9 Substation A Winter: Critical parameters and parametric sensitivity analysis

The same parameters for the feeder and load used in substation A summer model have been used for this case. Hence, sensitivity analysis is not required.

3.10 Substation A Winter: Results and discussions

The final simulated currents for the winter case at the head of the substation A feeder are as shown below in Fig. 20, Fig. 21, Fig. 22.

These results show that a very good correspondence has been achieved between simulated

and measured currents by using the same feeder and load model (only the total amount of load in summer conditions is scaled by a factor of 0.4 to obtain the total amount of load in winter conditions) from substation A summer case in winter conditions. These results also illustrate that this residential feeder and load model is able to capture the transient fault characteristics for both summer and winter conditions.

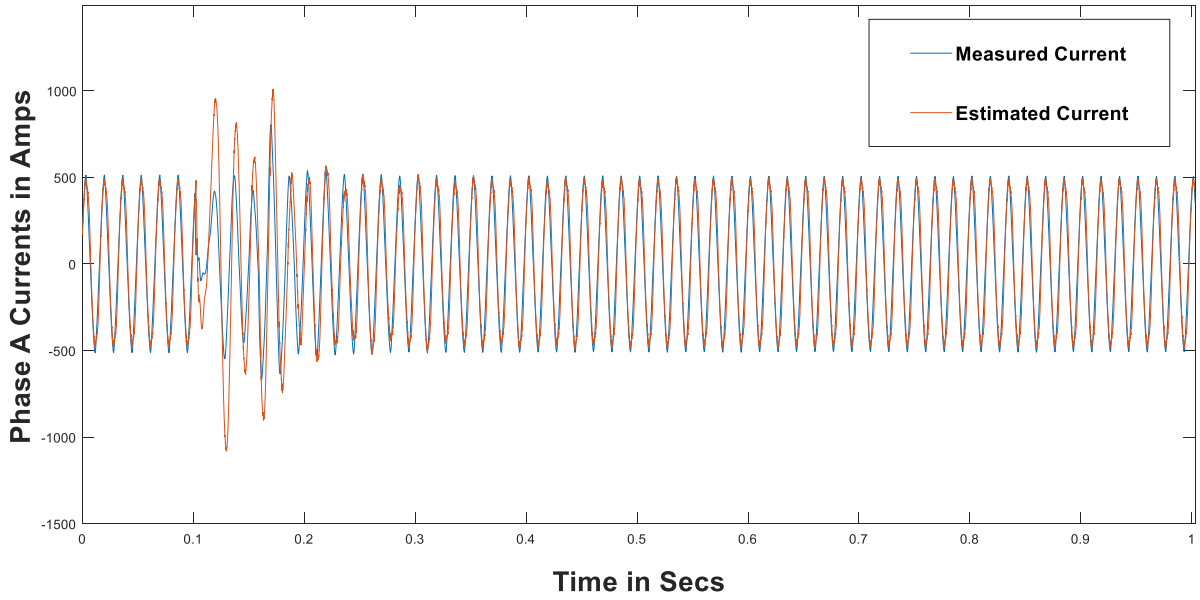

Fig. 20 Phase A current comparison for winter case

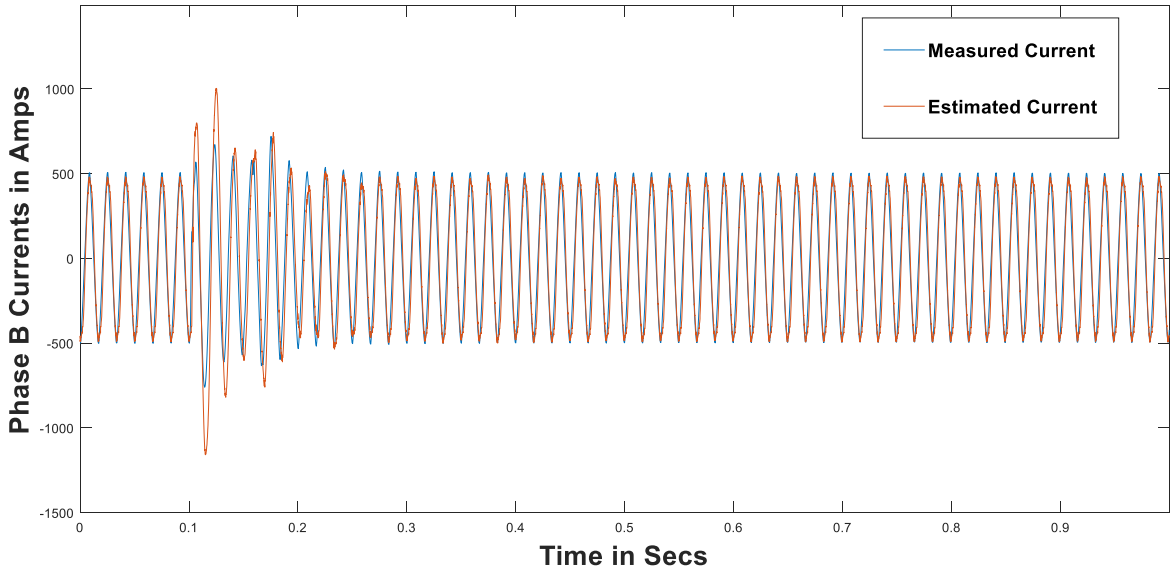

Fig. 21 Phase B current comparison for winter case

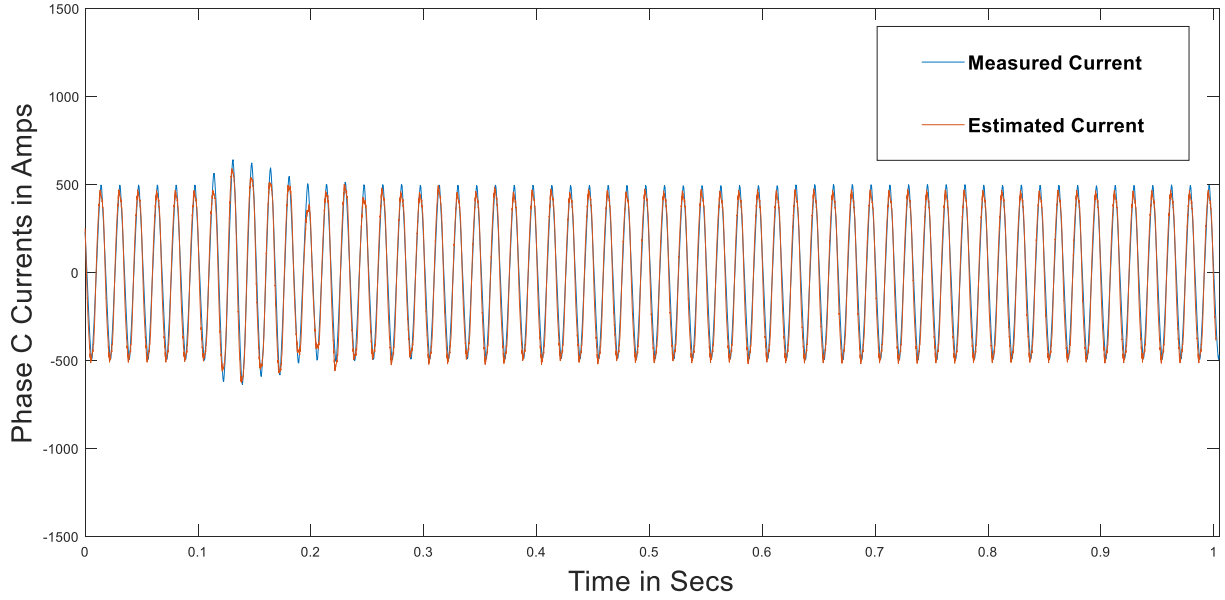

Fig. 22 Phase C current comparison for winter case

As expected, from Fig. 23, Fig. 24, Fig. 25 it can be clearly inferred that no stalling of SPIM is involved in this case.

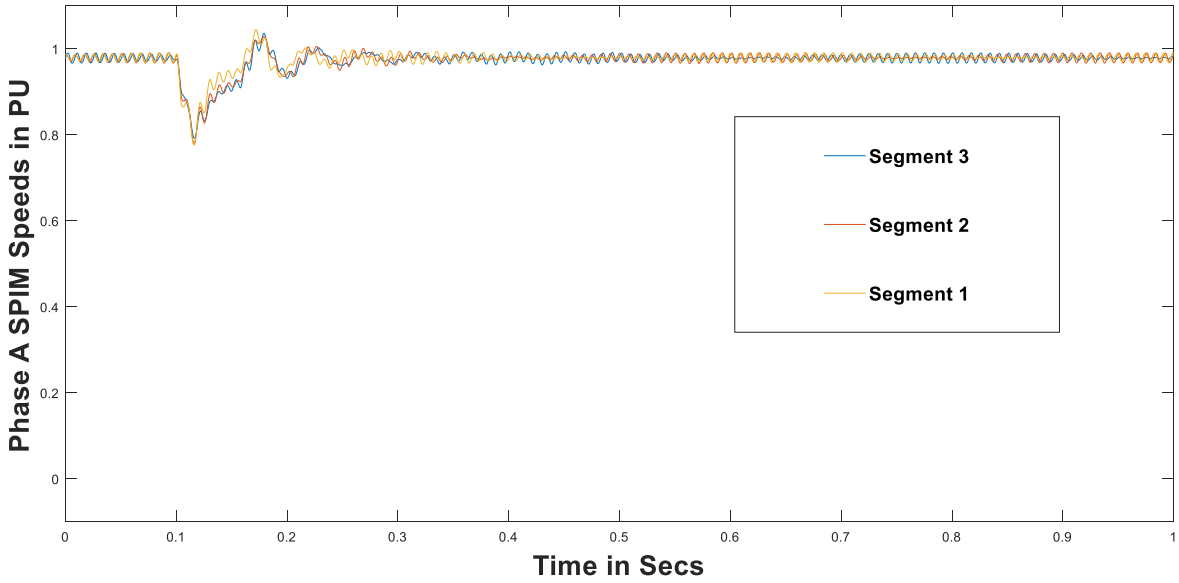

Fig. 23 SPIM speeds at three different segments across the feeder in phase A

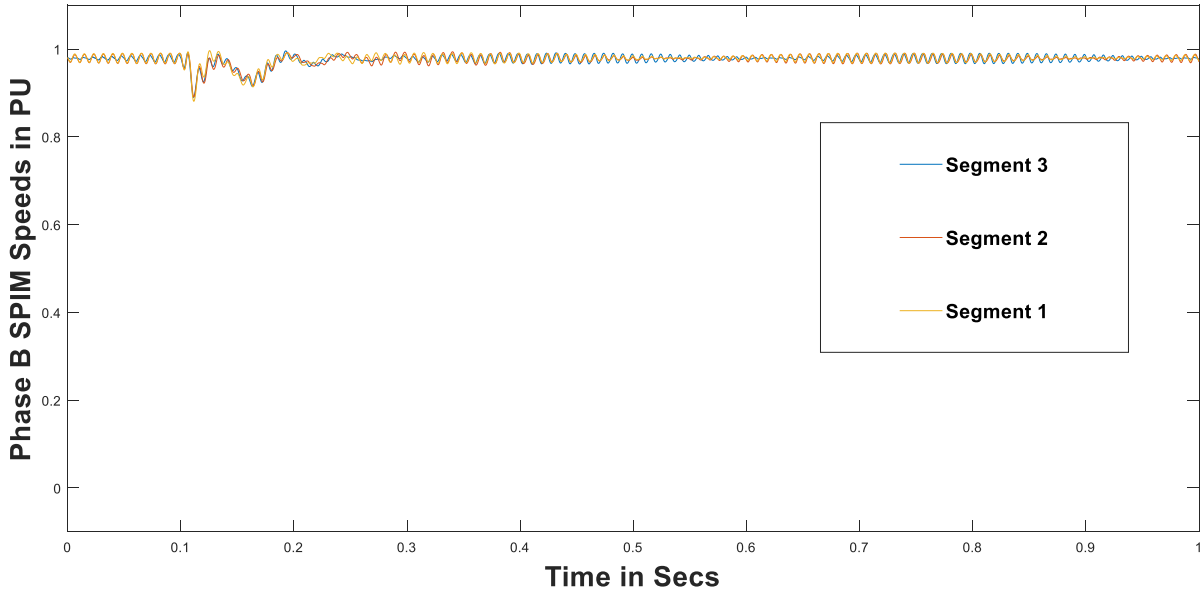

Fig. 24 SPIM speeds at three different segments across the feeder in phase B

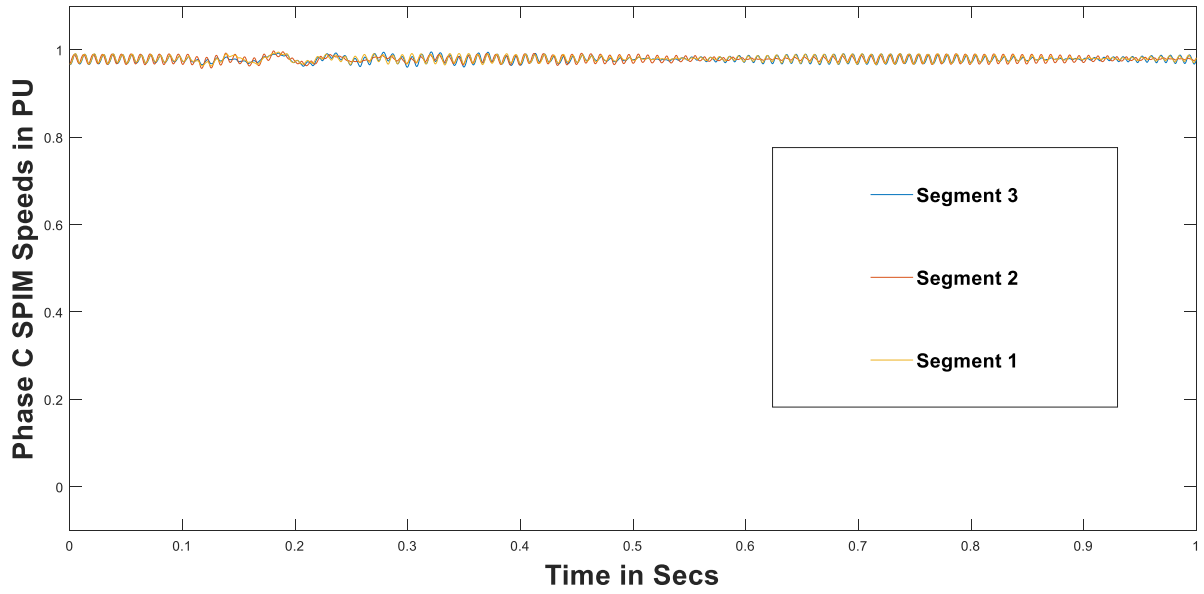

Fig. 25: SPIM speeds at three different segments across the feeder in phase C

4 SUBSTATION B FEEDER MODEL

4.1 Introduction

This section details the procedure for obtaining a novel feeder model to estimate accurate current responses, for a three-phase feeder pick-up event at the substation B, when measured three-phase voltages are played-in to the model. From the information provided by the local utility engineers, it was identified that the major load composition near substation B primarily consists of commercial buildings and industrial loads dominated by three-phase loads.

Event Details:

Event type: Three-phase feeder pick-up

Event time of occurrence: 8:59 PM on 29th July 2016.

Available DFR measurements: Voltages, Currents point on wave data at substation B (13.8 kV – low voltage side of the substation)

It should also be noted that a storm was present near the substation B area during this time due to which a three-phase feeder CA 152 is tripped to clear a fault that occurred along this feeder at 8:32 PM on 29th July 2016. However, the event considered in this Chapter is not related to the clearing of this fault. The event considered in this Chapter is the picking-up of the de-energized CA 152 feeder 27 minutes after of the clearing of this fault. Fig. 26 represents the single line diagram of the substation B and its downstream feeders. From Fig. 26, it should be noted that feeders CA 153, CA 154 are in service when CA 152 feeder is picked-up. The transient due to the closing of CA 152 feeder is the transient that we are trying to capture through the proposed standard model. In this model, feeders CA 153, CA 154 are represented as a single equivalent feeder to match the simulated pre-event currents with measured pre-event currents.

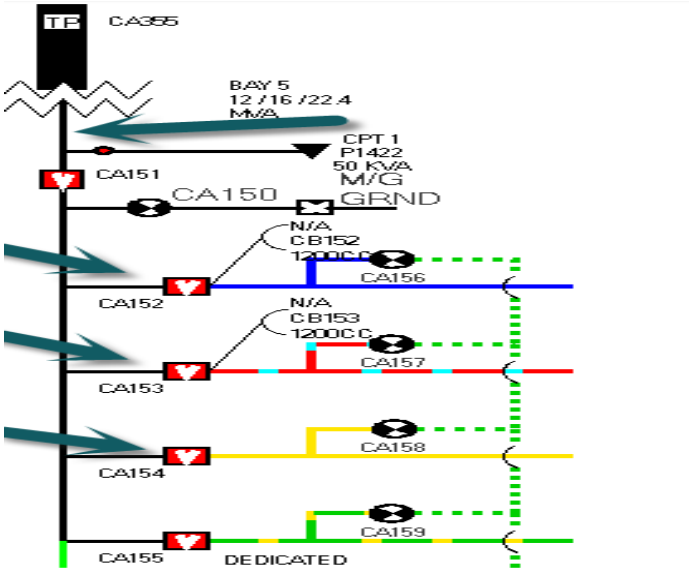

Fig. 26 Single line diagram of the substation B area

Similar to Case1, Case2, the three-phase voltages as shown in Fig. 27, Fig. 28, Fig. 29 are played-in to the substation B feeder model to obtain the simulated currents:

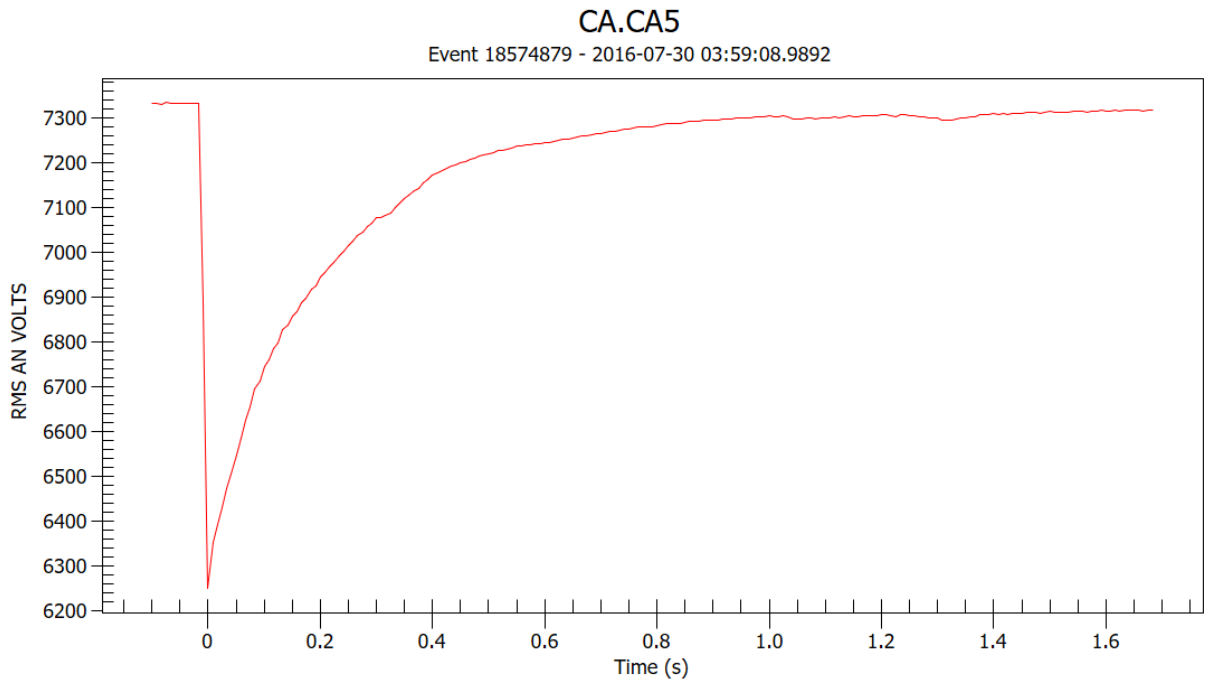

Fig. 27 Phase-A RMS voltage profile

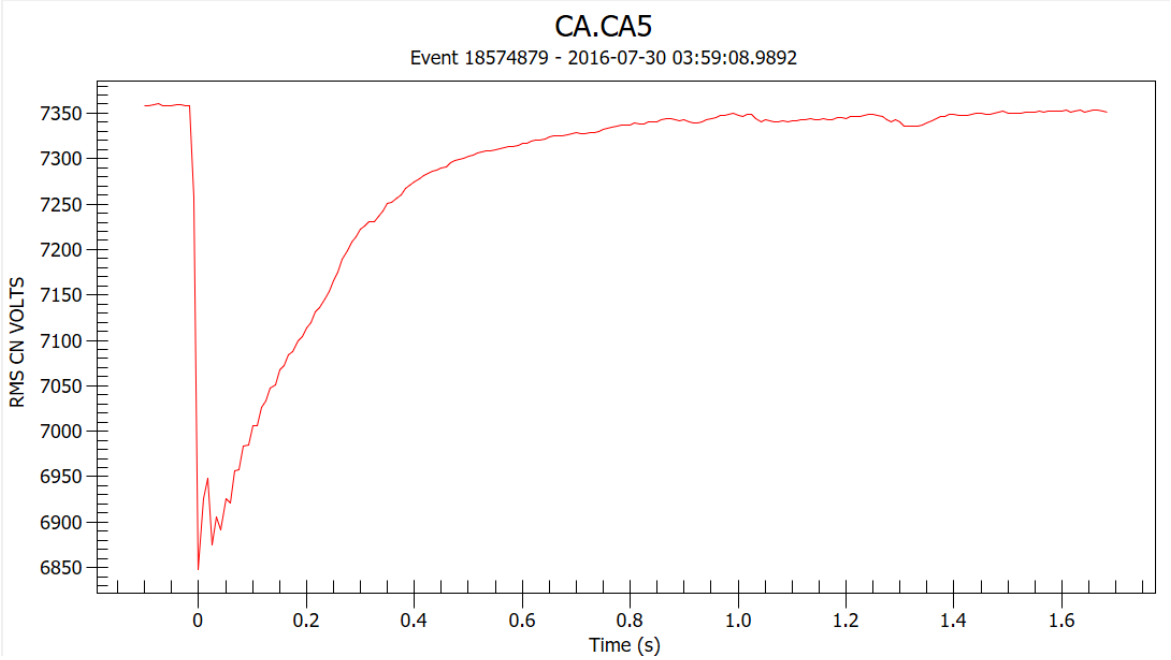

Fig. 28 Phase-B RMS voltage profile

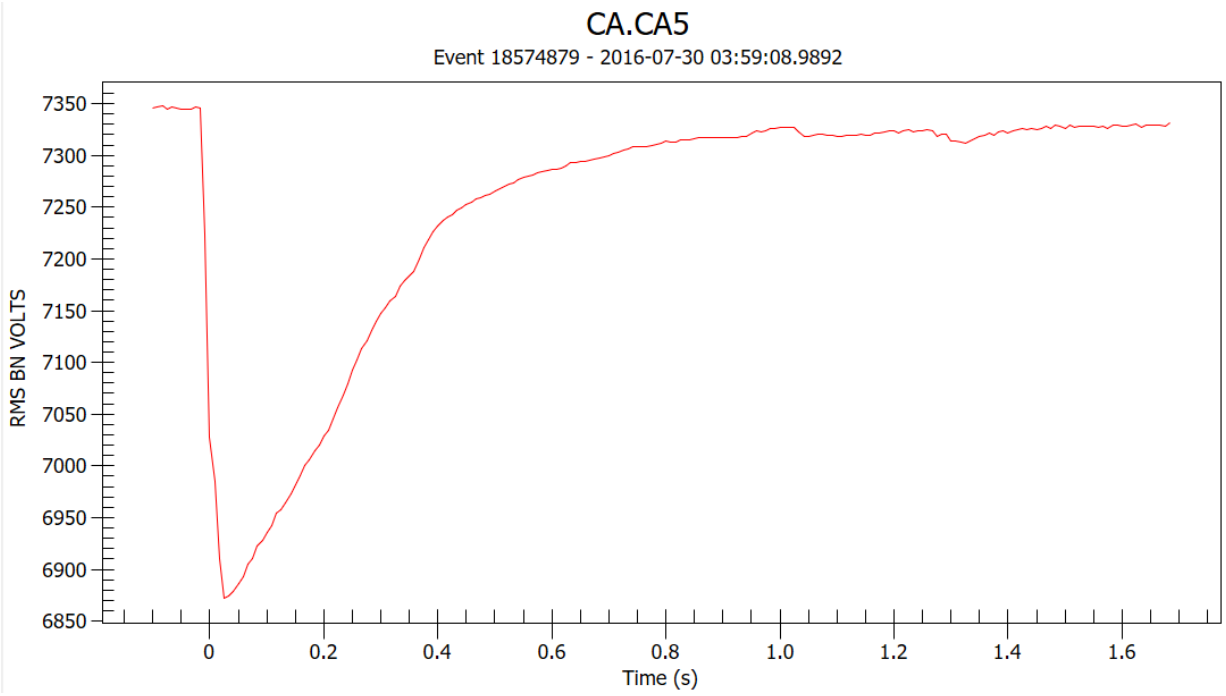

Fig. 29 Phase-C RMS voltage profile

Note3: Similar to Case1, Case2, the voltages played into this feeder model are instantaneous representations of Fig. 27, Fig. 28, Fig. 29

Similar to Case1, Case2, the primary objective of this chapter is to obtain an accurate estimate of the feeder currents measured at the head of the substation B feeder.

In Chapter 2, it was mentioned that the description of the distribution transformers used in the standard feeder and load model will be discussed in detail in this chapter. This rearrangement is done due to the heavy contribution of transformer saturation in obtaining the starting transient of the substation B feeder currents using the proposed substation B feeder and load model. From Fig. 30, it can be clearly seen that the inrush of the measured current is approximately 7 times higher in Phase A and 3 times higher in Phase B and Phase C during the transient when compared to the pre-event value. Therefore, efforts are made to model the distribution transformers properly to capture the saturation characteristics of the feeder currents.

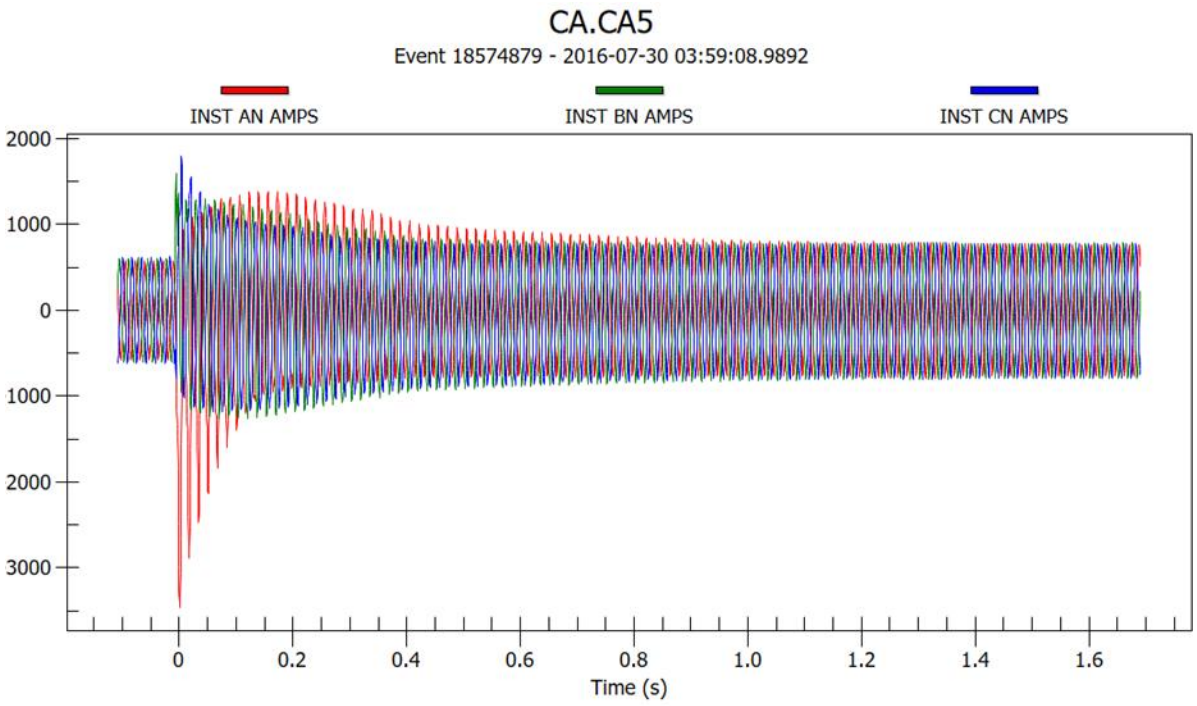

Fig. 30 Phase A, B, C measured currents at substation B

From Fig. 30, it should be noted that the total current from the substation B going into

feeders CA 153, CA 154 represents the total pre-event current and the total current from the substation B going into feeders CA 152, CA 153, CA 154 represents the total post-event current.

It should also be noted that the three-phase transformers, in this feeder and load model, are represented using three single-phase transformers (equivalent to Y-Y configuration in three-phase transformers). Table 9 shows the parameters used for these single-phase distributed transformers:

Table 9 Single-phase Distribution Transformers Parameters

MVA Rating	1 MVA
Leakage Reactance	0.02 pu
Air Core Reactance	0.02 pu
Inrush Decay Constant	0.25 sec
Magnetizing Current	2 %
Knee Voltage	1.17 pu
Saturation Enabled	Yes
Voltage Ratio (line to neutral RMS)	7.96 kV/ 265 V

4.2 Transformer Saturation and Critical Parameters

To represent transformer saturation in PSCAD [24], the following parameters need to be adjusted properly to obtain appropriate core saturation characteristic as shown in Fig. 31:

1. Air Core Reactance: The slope of the asymptotic line in Fig. 31, whose y-intercept is the knee point.
2. Magnetizing Current: This parameter determines how sharply the flux-current relationship of the transformer changes to non-linear in nature.
3. Knee Voltage: This parameter is helpful in determining the y-intercept of the asymptotic line.

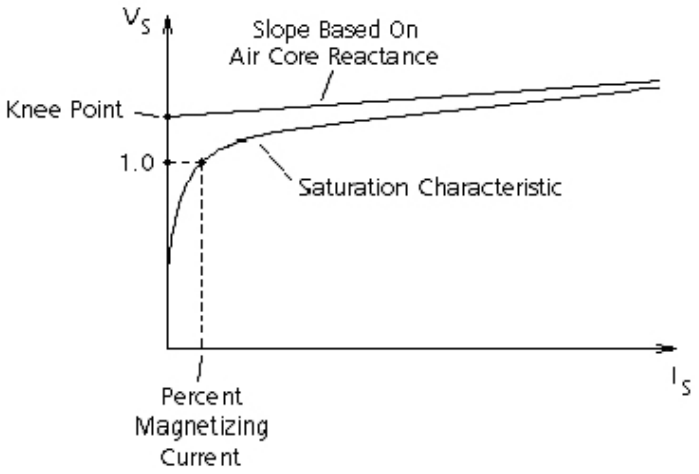

Fig. 31 Transformer knee curve characteristic from [24]

From [25], it can be seen that a typical magnetizing current value of a 1 MVA transformer is around 1 - 2 %. Additionally, to ensure the voltage regulation in the transformers is kept minimal, a low leakage impedance of a typical distribution transformer has been taken to be 2%.

Therefore, to determine the other transformer saturation parameters, a magnetizing current of 2% of the load current and a leakage impedance of 2 % has been chosen. Using these values, the other parameters of the transformer are estimated as follows:

The air core reactance of the transformer is assumed to be same value as that of leakage impedance. Therefore, using the chosen magnetizing current, air core reactance values, the knee voltage is chosen (1.17 pu) such that a decent approximation between the measured current and the estimated current has been obtained in the initial cycles of the pick-up transient.

It should also be noted that a primary resistance in series with the transformer has been added to control the saturation levels of the transformer. This resistance plays an important role to ensure that the saturation in the transformer dies out after the first few cycles of the transient. From Fig. 30, it can be clearly observed that a dc offset is present in the measured currents during the

transient whereas the dc offset is absent after the first few cycles in the measured current. Hence, **the optimum series primary resistance is found to be 0.5 ohm.**

Note4: This optimum primary resistance value of 0.5 ohm signifies the distance of the distribution transformers from each segment of the feeder model.

Another important factor in determining the current inrush transient characteristics is the switching instant on the point on wave of the voltage cycle on each phase. Fig. 32 shows the point of closing (by black markings) of the breaker along each phase. From Fig. 32, it can be observed that the point of closing for Phase A is the closest to the zero closing. This indicates that the saturation should be the highest in Phase A in all three-phases. This behavior is reflected in Fig. 30 where the inrush peak of Phase A current is 7 times the peak of the nominal current and has the highest dc component among all the three-phases.

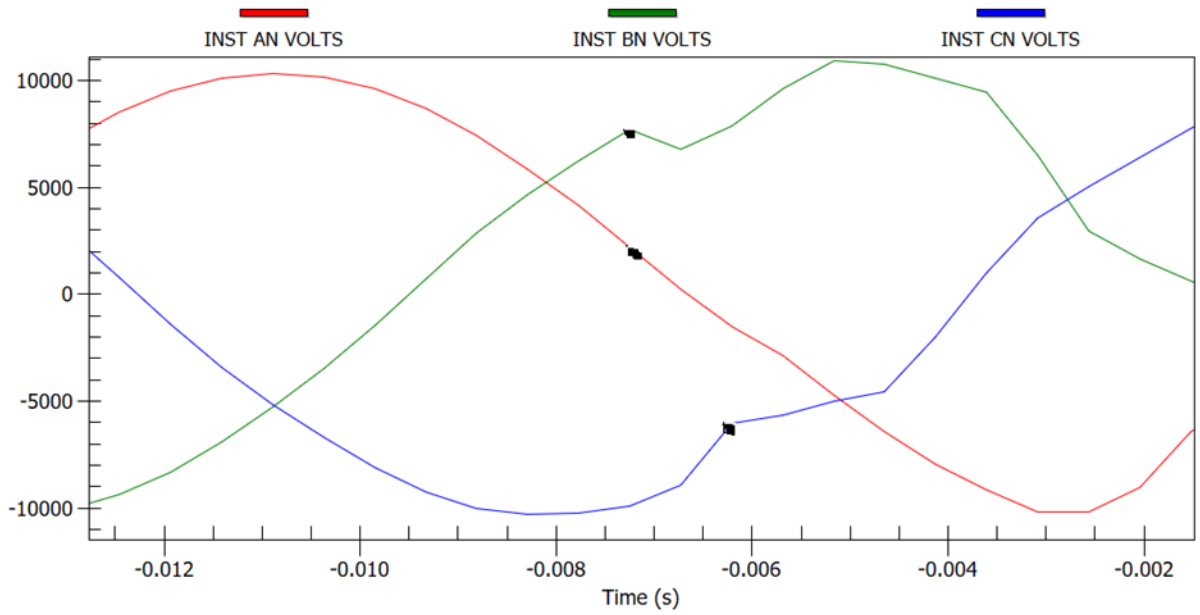

Fig. 32 Switching instances of three-phase played-in voltages

4.3 Substation B Area Load Composition

From the geographical information provided by the local utility near substation B, it is known that most of the loads located near substation B are of industrial/commercial type. For this reason, the load composition for this feeder model has been modified from the feeder model used in substation A summer and winter cases. This modification can be seen in Table 10 and Table 11:

Table 10 Load Composition for Substation B In-service Feeder

Type of load	Phase A	Phase B	Phase C
Impedance Load	0.283 MW	0.283 MW	0.283 MW
Single-phase Load	0.505 MVA	0.505 MVA	0.505 MVA
Three-phase Load (1/3 Total Load)	2.06 MVA	2.06 MVA	2.06 MVA

Table 11 Load Composition for Substation B Reclosed Feeder

Type of load	Phase A	Phase B	Phase C
Impedance Load	0.08 MW	0.08 MW	0.08 MW
Single-phase Load	0.144 MVA	0.144 MVA	0.144 MVA
Three-phase Load (1/3 Total Load)	0.588 MVA	0.588 MVA	0.588 MVA

From Table 10, Table 11 it can be clearly observed that the following proportions of loads has been used to match the pre-event measured P, Q values:

Three-phase Load = 72% of the total load

Single-phase Load = 18% of the total load

Resistive Load = 10% of the total load

$$\frac{\text{Total Single} - \text{phase Load}}{\text{Total Three} - \text{phase Load}} = 1/4$$

Note5: From the above load proportions, it can be observed that the ratio of single-phase load to three-phase load used in Chapter 3 has been used to represent the ratio of three-phase load to single-phase load in this substation B feeder model to reflect the dominating presence of industrial type loads near substation A.

It should also be noted that in the load compositions shown in Table 10, Table 11 the ratio of load composition across the three segments of the feeder is as shown below:

- Resistive Load – 1:1:1
- Three-phase Load – 1:1:1
- Single-phase Load – 1: 1.4: 1.4

The key point to be noted here is that the above proportions are the same as the proportions used to represent the load composition across the three segments of the substation A summer and winter case feeder and load models.

From Table 11 and from each load type distribution across the three segments of the substation B feeder, it can be inferred that the total load composition of the feeder across the three segments of the feeder is distributed in the ratio of 1: 1.07: 1.07. This total load distribution ratio is used to represent the load models in the Sub-transmission model in Chapter 5.

4.4 Results and Discussions

The simulated currents at the head of the substation B are compared with their corresponding measured currents as shown in Fig. 33, Fig. 34, Fig. 35:

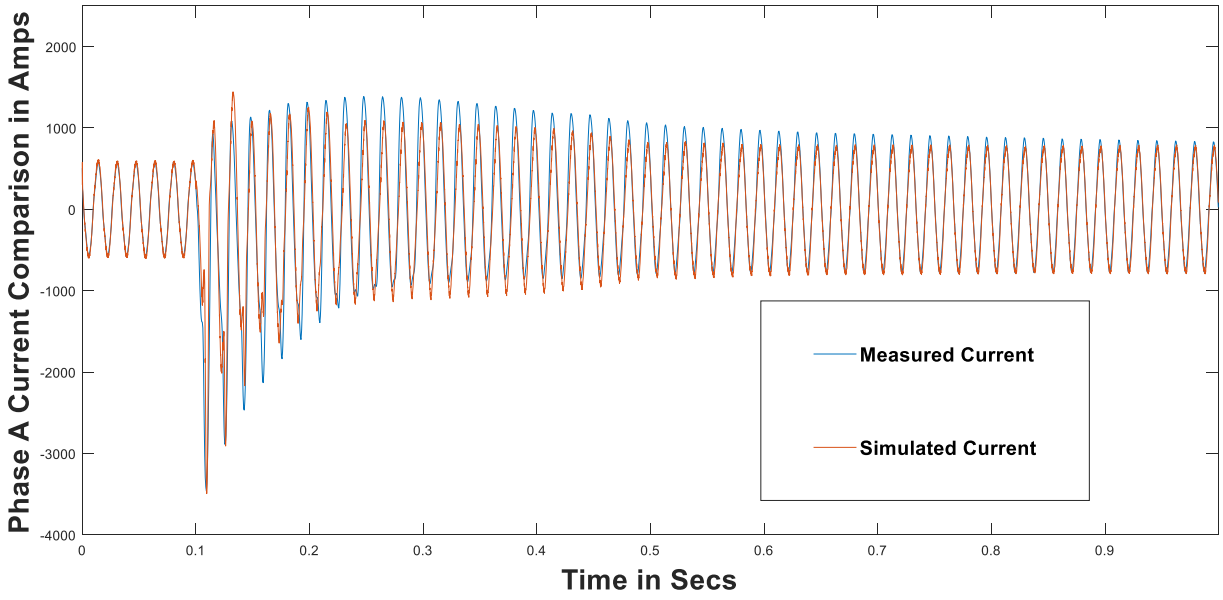

Fig. 33 Phase-A currents comparison

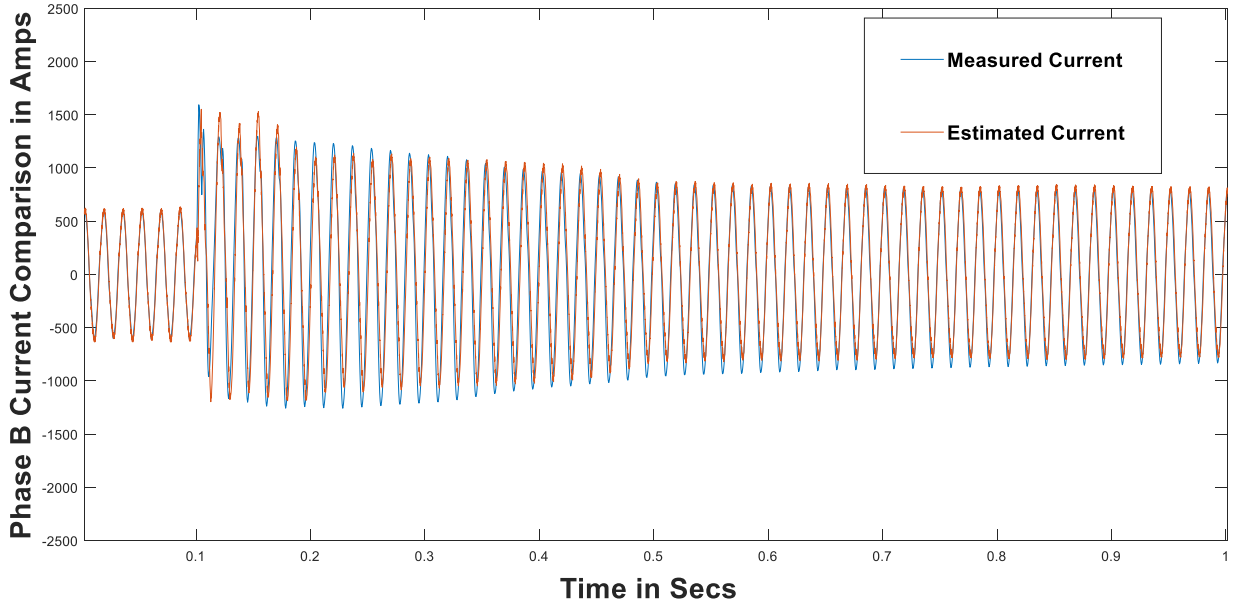

Fig. 34 Phase-B currents comparison

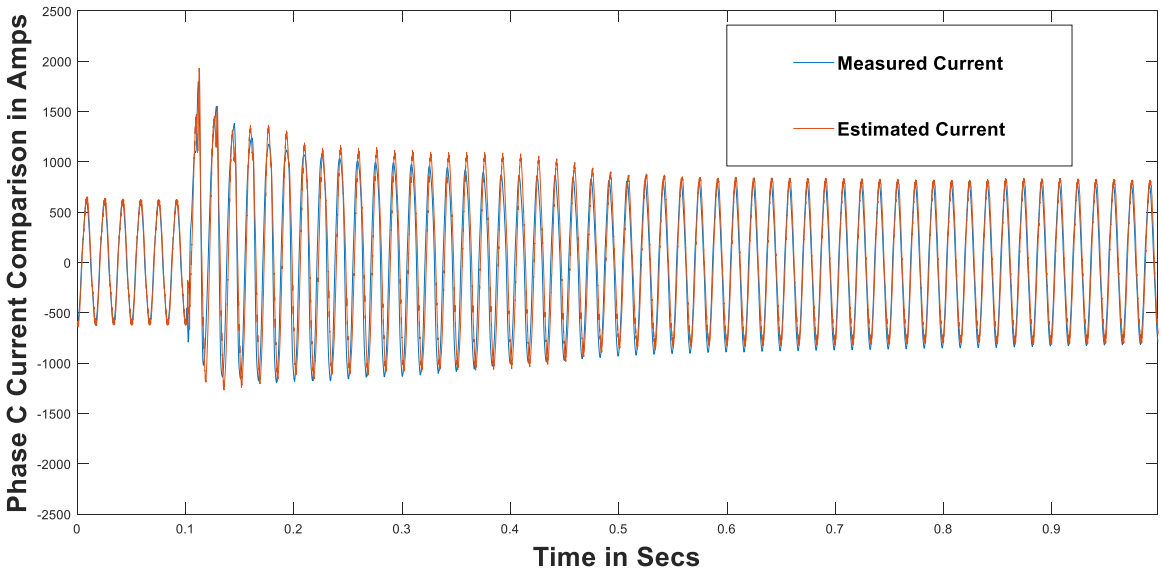

Fig. 35 Phase-C currents comparison

From Fig. 33, Fig. 34, Fig. 35 it can be observed that a good approximation of the starting inrush characteristic of the three-phases of the measured currents has been achieved from this substation B feeder and load model.

From Fig. 36, it can be clearly seen that at a high knee voltage (less saturation in the distribution transformer) the obtained estimated currents do not have a good correspondence with the measured currents in the first few cycles of the transient when compared to Fig. 32. However, at a low knee voltage 1.17 pu (chosen final value) there seems to be a better match with the measured current in the initial cycles of the transient.

From Fig. 37, it can be observed that by reducing the three-phase load by 1.08 MVA (from the total load in the feeder that is picked up as shown in Table 11) in the feeder that is picked up, the starting transient of the simulated currents is not affected and is very similar to the response obtained in Fig. 33. This indicates that for the first few cycles of the pick-up transient, the current

inrush characteristics doesn't depend on the type of load present in the feeder and is only dependent on the distribution transformer saturation characteristics.

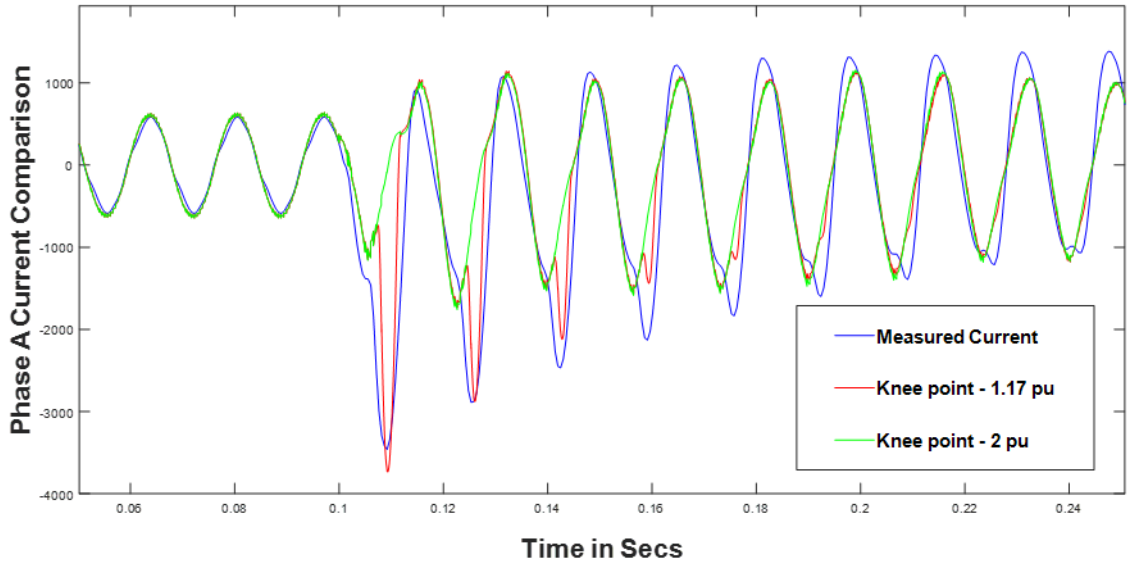

Fig. 36 Phase-A current comparison for different knee voltages

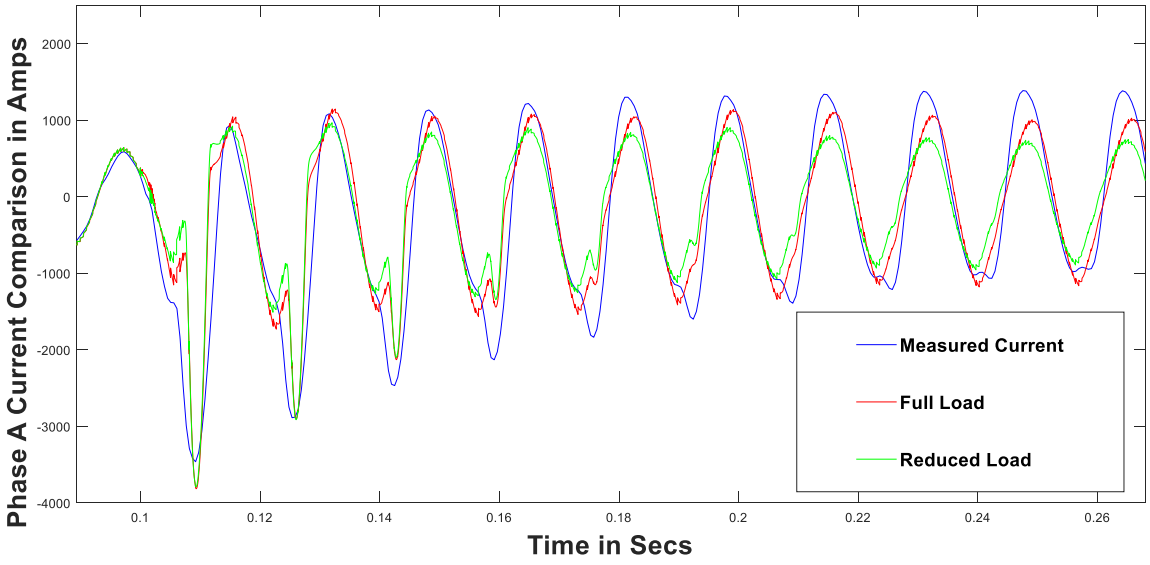

Fig. 37 Phase-A current comparison for different load conditions

5 SUB-TRANSMISSION MODEL

5.1 Introduction

In Chapters 2, 3, 4 a standard feeder and load model have been modeled. The proposed approach provides a good estimate of currents at the head of the feeder when three-phase voltages are played-in to the designed model in PSCAD software. In this chapter, a 69-kV sub-transmission system has been built near the substation B in PSCAD. The feeder pick-up event that occurred at substation B from Chapter 4, has been discussed in detail. The primary objective for conducting this analysis is to validate the proposed feeder and load model by comparing both the measured feeder voltages and feeder currents to the estimated feeder voltages and feeder currents. It should be noted that this method is different from the one used in Chapters 2,3,4 which involved playing-in the measured voltages to the proposed feeder and load model to estimate the currents at the head of the feeder.

This sub-transmission model, in PSCAD software, is developed using the short circuit data, line data, transformer data at the sub-transmission level near substation B (which has been provided by the local utility using ASPEN software). Fig. 38 presents the information about the one-line diagram of the 69-kV network near substation B including the 230 kV Thévenin sources at bus 1 and bus 2 as shown in Fig. 38. It should also be noted that a red arrow mark has been placed on Fig. 38 to show the 69- kV substation B bus (bus19) clearly.

5.2 Initial Conditions:

As mentioned earlier, there are two 230 kV Thévenin sources, bus 1 and bus 2, in the sub-transmission model. The former source is closer electrically to the substation B bus compared to the latter source. The loading conditions are unknown at other 69 kV buses in the system. Therefore, the 2016 summer case loading conditions (From the local utility planning case) has

been assumed in this model for the 69-kV buses other than substation B. The loading conditions at substation B has been assumed from Table 9, Table 10 from Chapter 4. Finally, to get the initial conditions for this model in PSCAD, a three-phase power flow program has been run using Open DSS using constant P, Q loads for the motor loads. From this power flow solution, the values of the Thévenin sources voltages behind the Thevenin impedances are obtained. The following initial conditions have been obtained using Open DSS (whose power flow script has been presented in the Appendix section of this report):

V_{bus1} = 1.0243 pu at an angle 29.9^0

V_{bus2} = 1.0246 pu at an angle 29.9^0

Note6: It should be noted that, although initially the power flow of this model is converging, there were some 69 kV buses in the system whose voltages are below 0.95 pu. For this reason, a shunt of 0.5 MVAR has been added to all the 13.8 kV buses (at distribution level) in the system to get the system voltages to near 1 pu (greater than 0.95 pu).

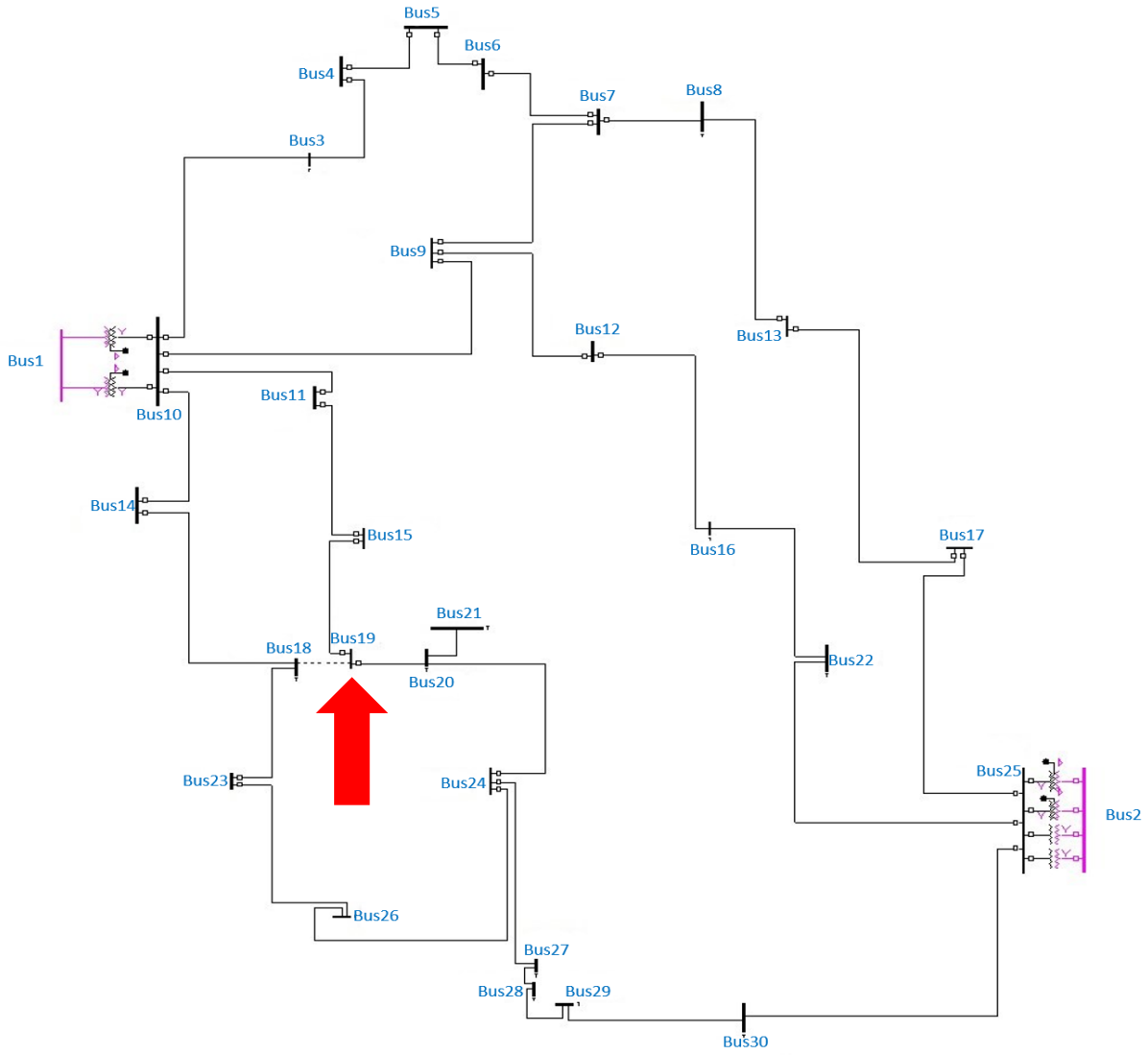

Fig. 38 69 kV Sub-transmission model

5.3 Assumptions

In the ASPEN data provided by the local utility, the data for the 69/13.8 kV transformers is not available. Therefore, the parameters provided in Table 12 have been assumed for these transformers:

Table 12 69/13.8 kV Transformers Parameters

Number	Parameter	Value
1.	Transformer Impedance	6%
2.	MVA Rating	10 MVA
3.	Windings Type	Y-Y

In PSCAD, the standard feeder and load model used to represent substation B feeders in Chapter 4 have been used to represent the load at the following buses in this system:

- Bus3
- Bus9
- Bus11
- Bus14
- Bus19 (upstream 69 kV bus of substation B)

However, an important point to be noted here is that unlike substation A and substation B feeder models, there is no voltage that is being played-in to this feeder model. Fig. 39 represents the feeder and load model used in PSCAD for the above buses.

At all the other 69 kV buses of this system, the loads placed in the standard substation B feeder model are replaced by constant P, Q loads as shown in Fig. 40

These constant P, Q load type assumptions are made to ensure that the PSCAD simulation run completes quickly (if the loads at all the 69 kV buses in the sub-transmission system are represented by standard feeder and load model consisting of motors then it was observed that the PSCAD simulation takes about 30 hours to complete whereas the proposed model in this chapter takes about 2 hours to complete the simulation). The standard substation B feeder and load model is assumed only at these four locations because they are the closest to both substation B bus and its nearest 230 kV Thevenin source (bus 1).

As mentioned earlier, the main difference between the sub-transmission load model and the standard load model used in substation A, substation B is that we just used two constant ac 230

kV sources (bus1, bus2) in the sub-transmission load model to obtain the simulated voltages, currents at the substation B which were then compared to their respective measured values. The following figure shows the feeder model representation used in the substation A & substation B cases where measured voltages are played-in to compare the three-phase simulated currents at the head of the feeder to their measured values.

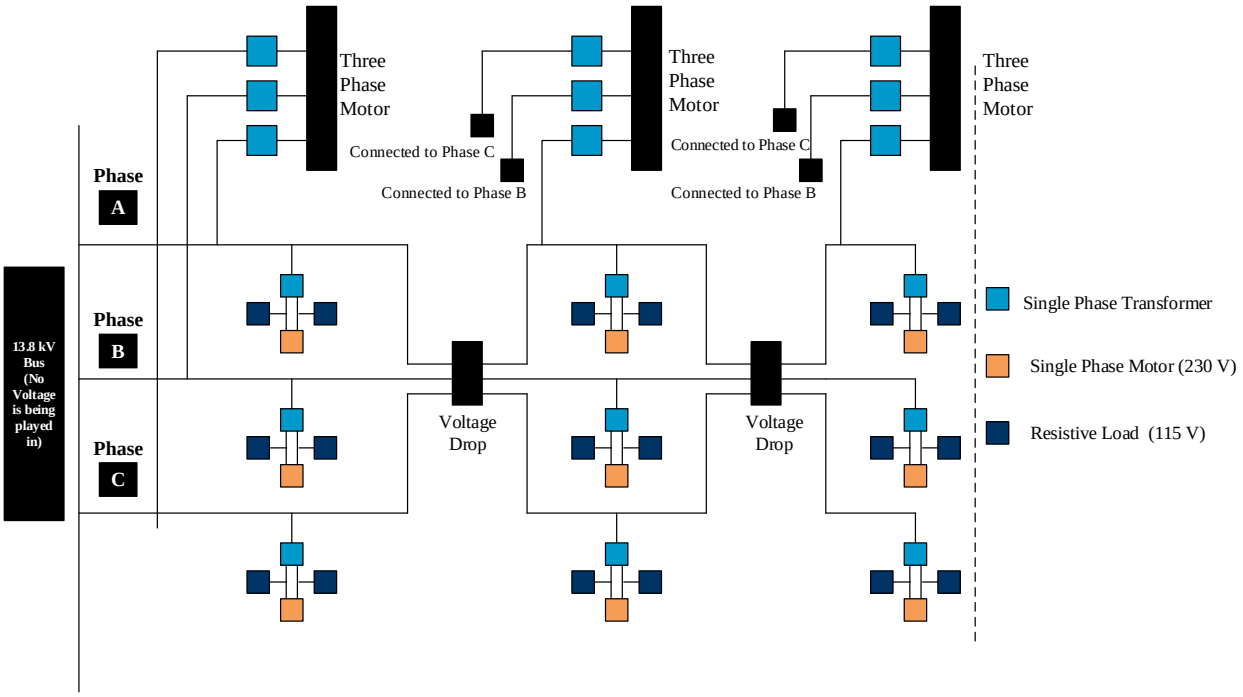

Fig. 39 Sub-Transmission feeder and load model at selected buses such as Bus19, Bus3, Bus14, Bus9, Bus11

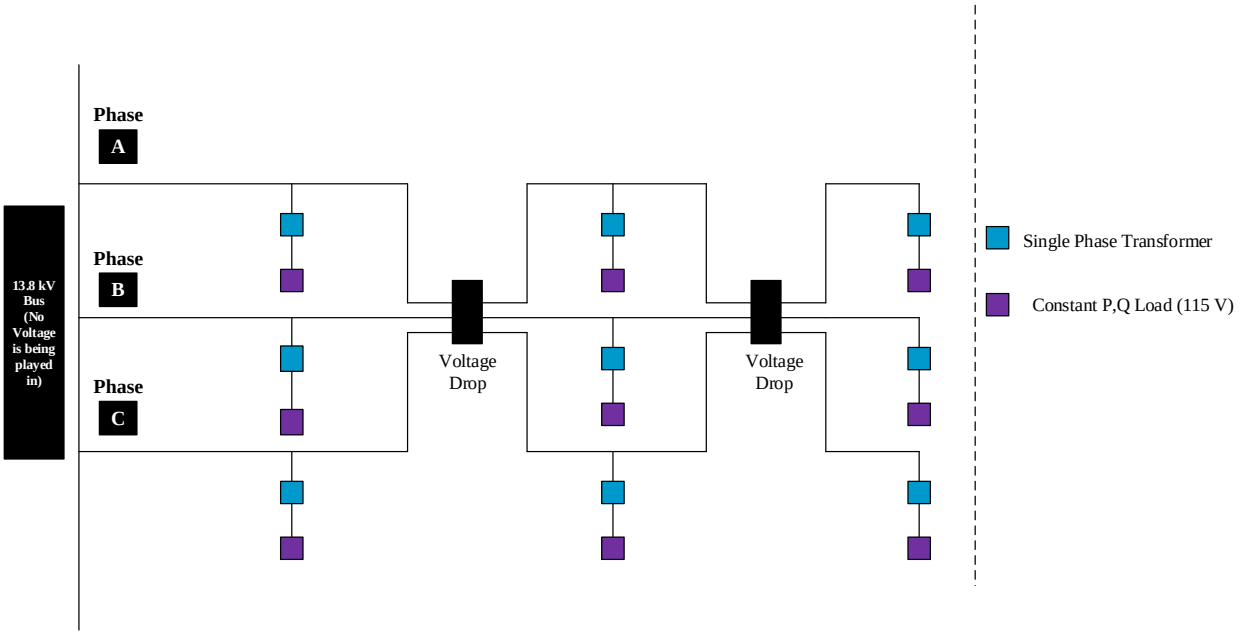

Fig. 40 Sub-transmission feeder and load model used at buses other than the ones mentioned in Fig. 39

5.4 Load Composition

As mentioned in Section 5.2, it should be noted that other than the substation B 69 kV bus, the load P, Q data for the other 69 kV buses is not available. Therefore, the 2016 summer case loading conditions (from the local utility planning case) has been assumed in this model for the buses other than substation B.

It should also be noted that, as mentioned in Section 5.3, two different types of feeder and load models (Fig. 39, Fig. 40) have been used depending on the bus location to make sure that the PSCAD simulation doesn't run too slowly. However, the total load composition across the three segments of these feeder and load models is distributed in the ratio of 1: 1.07: 1.07 (same as in feeder and load model in Chapter 4). The loads (three-phase load, single-phase load, impedance load) in this model are also distributed in the same ratio as mentioned in Chapter 4. Similarly, the constant P, Q loads used in this model are distributed in the ratio of 1: 1.07: 1.07 across the three segments of the feeder.

The load composition used across all the 69 kV buses in the Sub-transmission system near substation B is presented in Table 13, Table 14.

Table 13 Net Q (reactive power) load distribution across the three segments of the feeder at 69 kV buses

Number	Bus name	Q load (Segment1)	Q load (Segment 2)	Q load (Segment 3)	Net Q load in MVAR
1	Bus15	0.41	0.44	0.44	1.3
2	Bus21	0.16	0.17	0.17	0.5
3	Bus27	0.32	0.34	0.34	1
4	Bus29	0.07	0.08	0.08	0.23

Table 14 P (active power) load distribution across the three segments of the feeder at 69 kV buses

Number	Bus Name	P Load (Segment 1)	P Load (Segment 2)	P Load (Segment 3)	Total P load in MW
1	Bus3	2.03	2.18	2.18	6.4
2	Bus4	1.34	1.43	1.43	4.2
3	Bus6	2.1	2.25	2.25	6.6
4	Bus7	1.97	2.11	2.11	6.2
5	Bus13	3.56	3.81	3.81	11.2
6	Bus17	2.23	2.38	2.38	7
7	Bus9	2.16	2.32	2.32	6.8
8	Bus5	1.14	1.22	1.22	3.6
9	Bus12	3	3.2	3.2	9.4
10	Bus16	2.14	2.28	2.28	6.7
11	Bus22	1.6	1.7	1.7	5
12	Bus11	2.04	2.18	2.18	6.4
13	Bus15	0.96	1.02	1.02	3
14	Bus21	0.28	0.31	0.31	0.9
15	Bus24	2.56	2.72	2.72	8
16	Bus27	0.35	0.38	0.38	1.1
17	Bus28	0.06	0.07	0.07	0.2
18	Bus29	0.18	0.21	0.21	0.6
19	Bus14	1.27	1.36	1.36	4
20	Bus23	0.93	0.98	0.98	2.9
21	Bus26	1.18	1.26	1.26	3.7

Note7: It should be noted that in Table 13, the Q load distribution is the 'net' distribution across the feeder. This net distribution implies the value of Q seen from the head of the feeder after balancing the required amount of Q, from the total load across the feeder, by three-phase capacitor banks. It should also be noted that the buses whose net Q values are not presented in Table 13 have a net Q of 0 at the head of the feeder.

5.5 Results and Discussion

The simulated voltages and currents at the head of the substation B feeder are shown in Fig. 41, Fig. 42, Fig. 43, Fig. 44, Fig. 45, Fig. 46. From these results, it can be clearly observed that a good match between the simulated responses and the measured responses has been achieved in both voltage and current comparisons. It should also be noted that the simulated response of currents in this case (Fig. 44, Fig. 45, Fig. 46) are not as accurate as those observed in Case3 (Fig. 33, Fig. 34, Fig. 35). This is to be expected because in Case3, the voltages played into the feeder and load model are measured responses (which is as accurate as we can get) whereas in this case the voltages at substations are dependent on the assumptions made about the loadings of the 69kV system

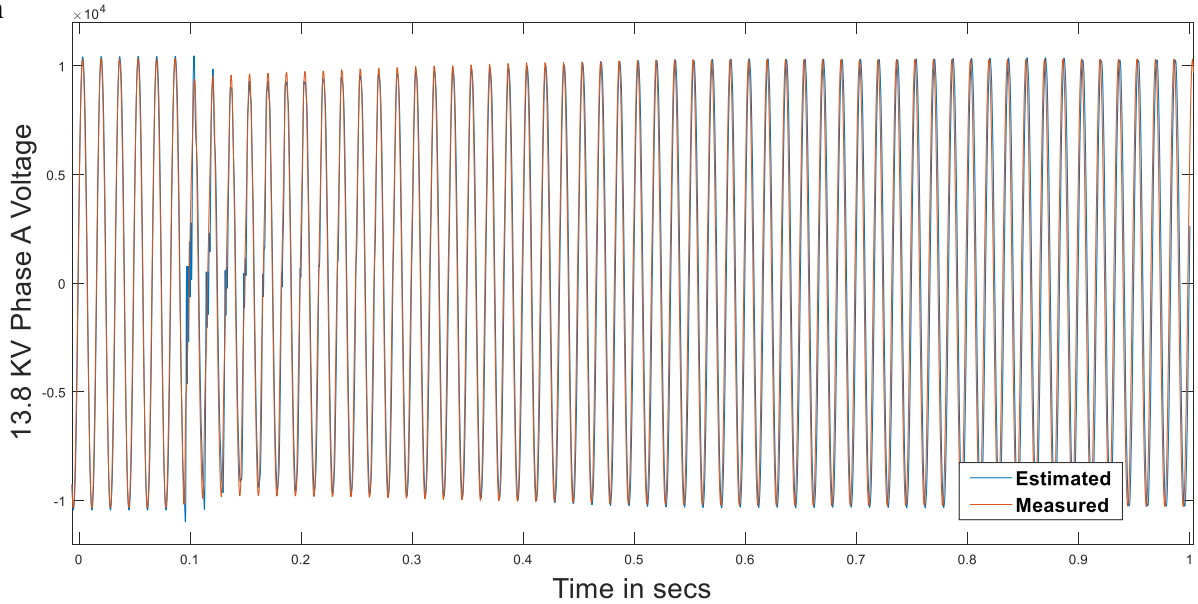

Fig. 41 Phase-A substation B voltage comparison

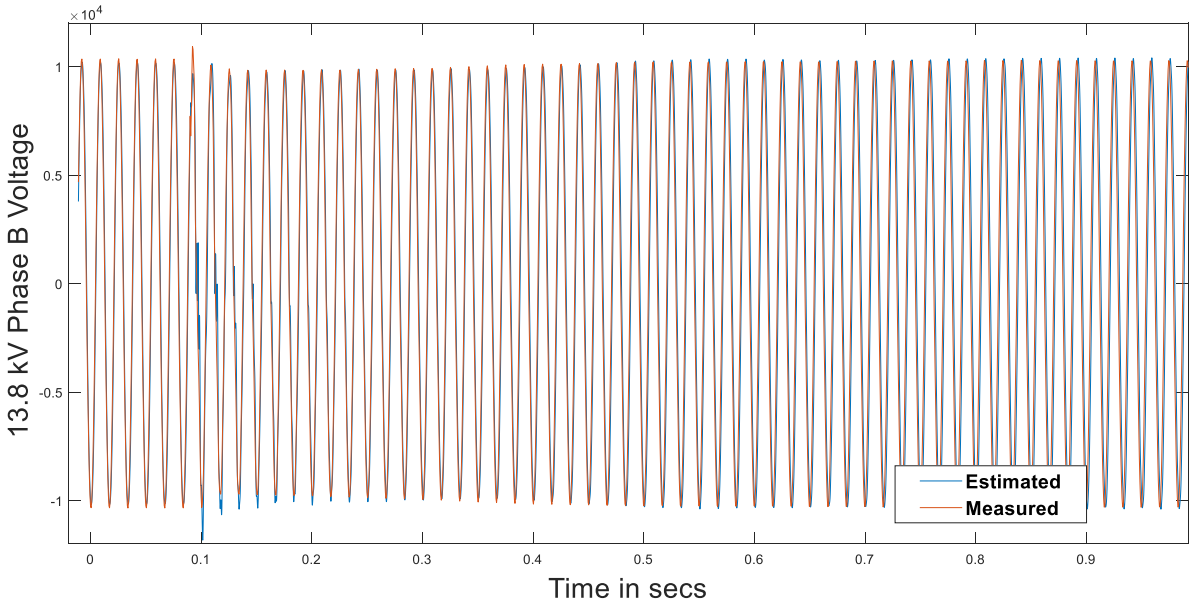

Fig. 42 Phase-B substation B voltage comparison

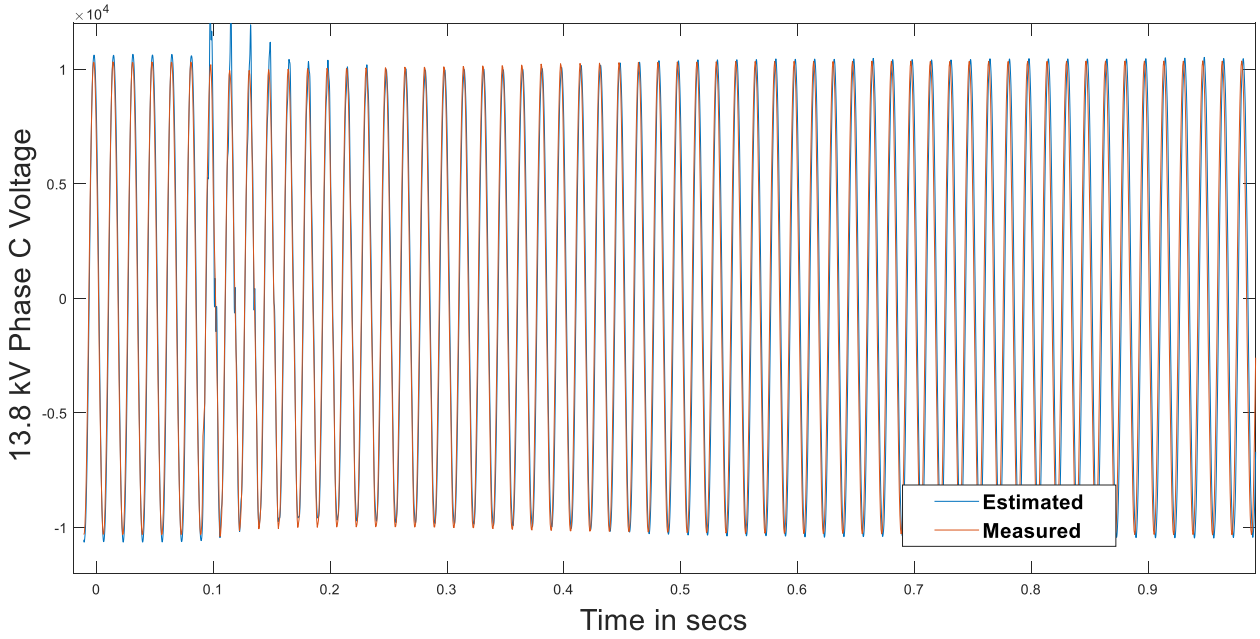

Fig. 43 Phase-C substation B voltage comparison

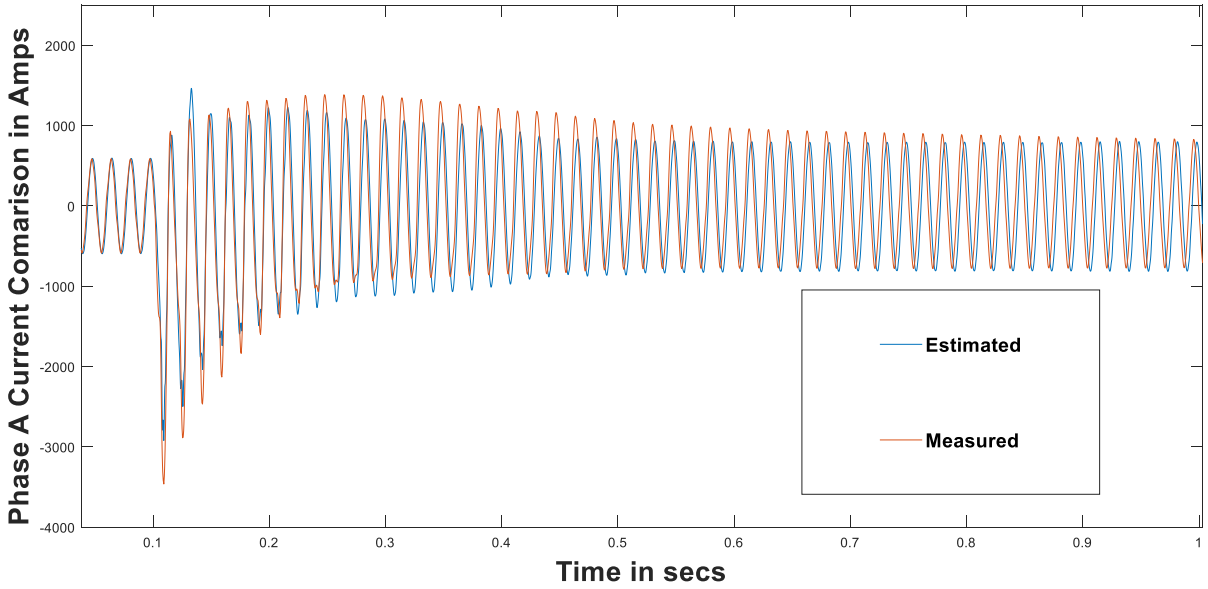

Fig. 44 Phase-A substation B current comparison

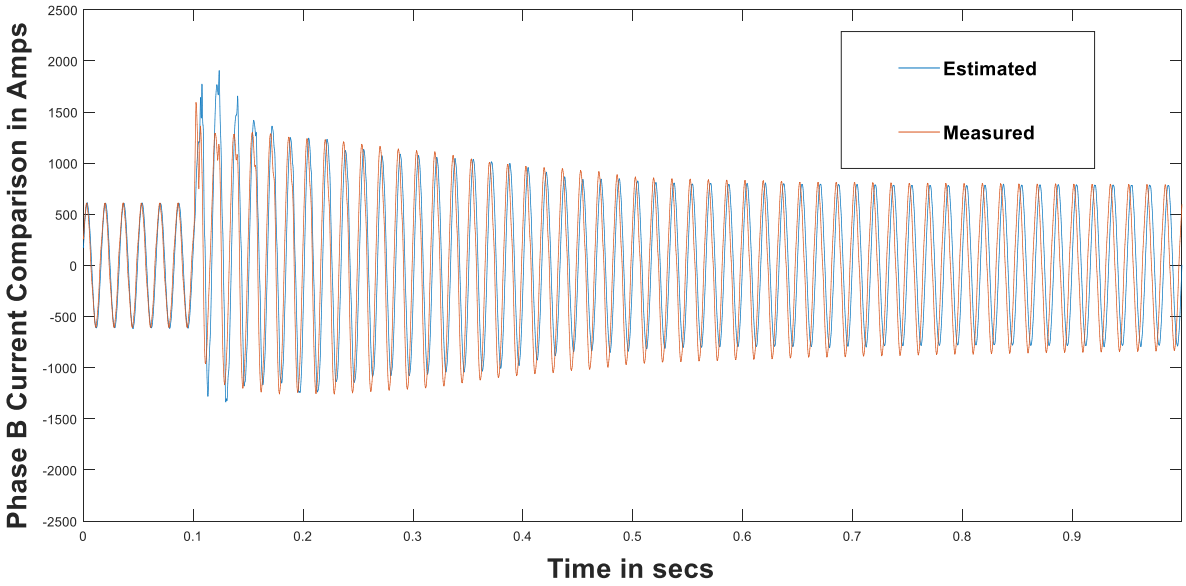

Fig. 45 Phase-B substation B current comparison

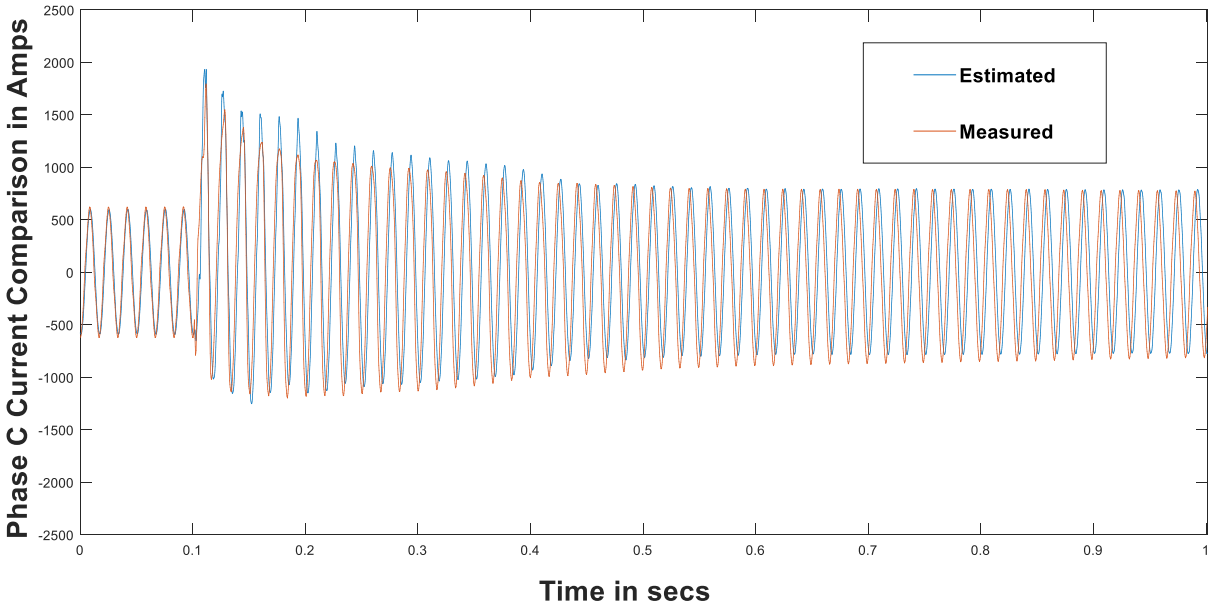

Fig. 46 Phase-C substation B current comparison

Fig. 47a shows the Phase-A voltage simulated response of the 69 kV substation B bus. Fig. 47a has been scaled to show the positive peaks in Fig. 47b. From Fig. 47b it can be clearly seen that there is a 2% voltage drop, at the 69-kV substation B bus, when the feeder pick-up transient occurs. This is clearly an important point to be noted because a 2% drop on a 69-kV bus is observed (which is a significant drop percentage) when a load of only 2.4 MVA has been added in the feeder pick-up event at substation B.

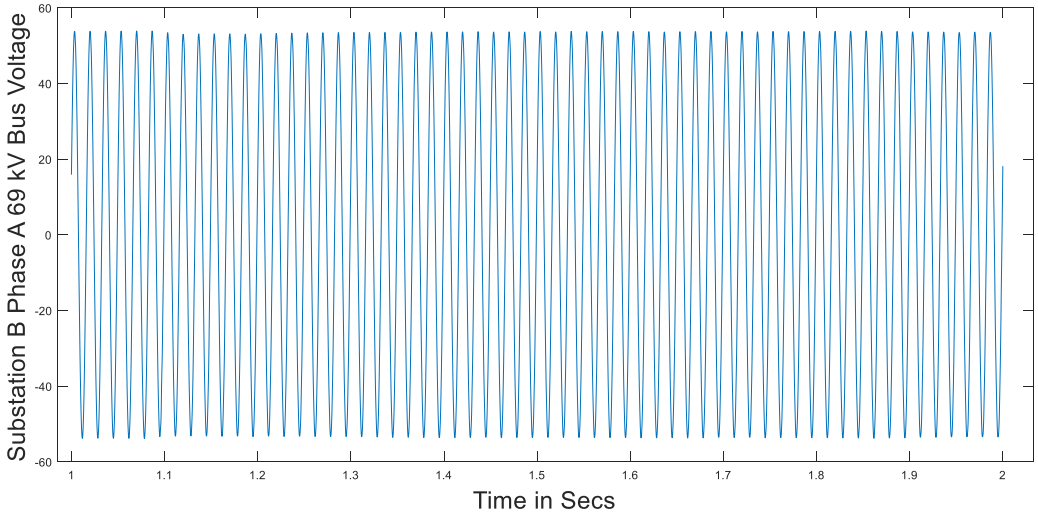

Fig. 47a Simulated Phase-A voltage response at substation B 69 kV bus

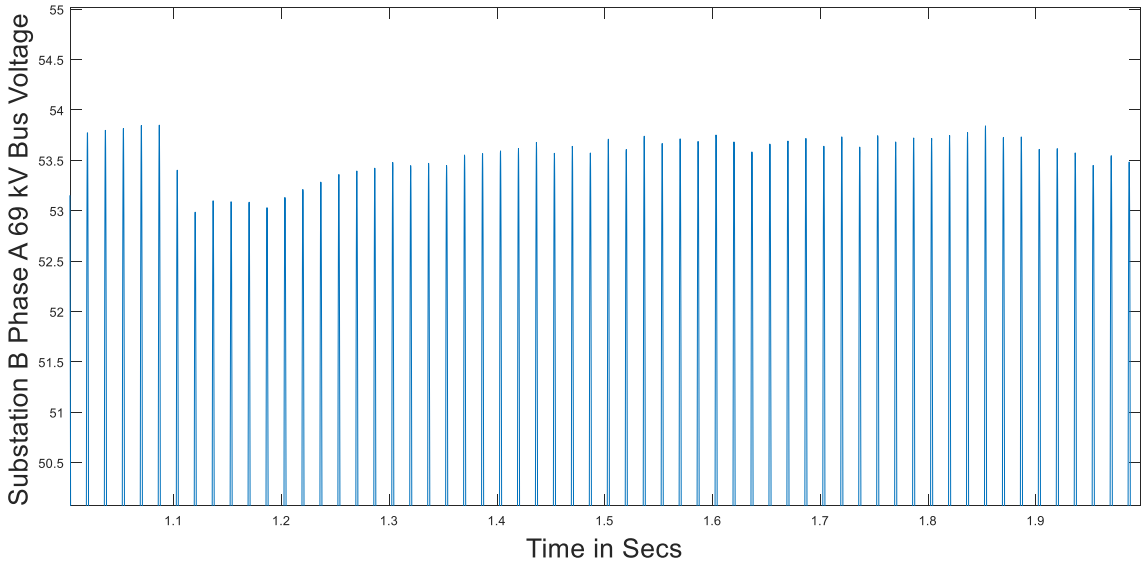

Fig. 47b Scaled positive peaks in Fig. 48a

Fig. 48a shows the simulated response of the 230 kV bus 1 voltage source. Fig. 48a has been scaled to show the positive peaks in Fig. 48b. From Fig. 48b, it can be inferred that only a drop of few hundred volts has been seen at the 230 kV bus 1 bus.

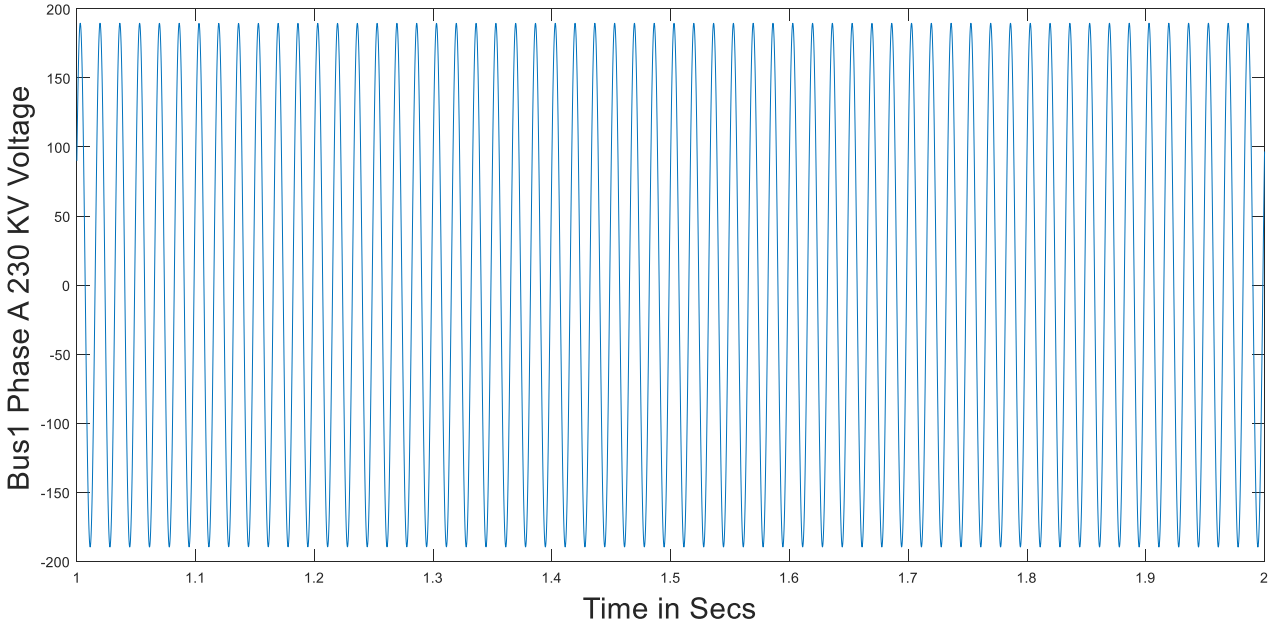

Fig. 48a Simulated Phase-A voltage response at bus 1 230 kV bus

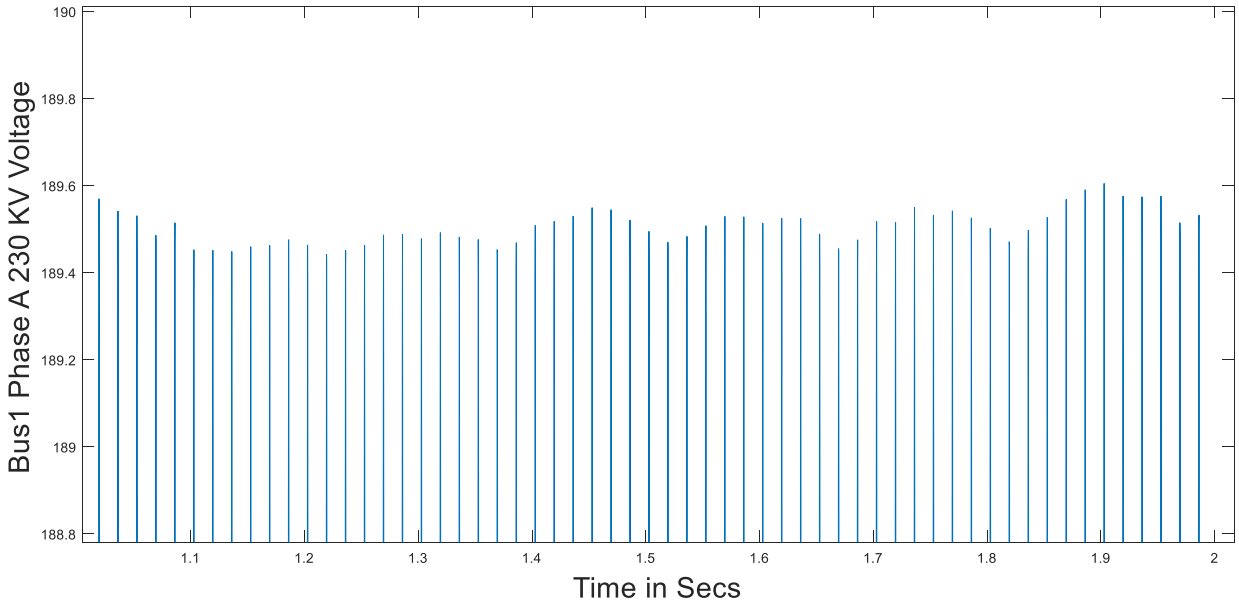

Fig. 48b Scaled positive peaks in Fig. 48a

Fig. 49a shows the simulated response of the 230 kV bus2 voltage source. Fig. 49a has been scaled to show the positive peaks in Fig. 49b. From Fig. 49b it can be observed that the voltage drop is even smaller than that was observed in Fig. 48b. This is to be expected because the bus2 voltage source is electrically farther from the substation B 69 kV bus compared to the bus1 voltage source. Therefore, it can be concluded that the 230 kV buses bus1and bus2 are not much affected by the feeder pick-up transient that occurred at the substation B.

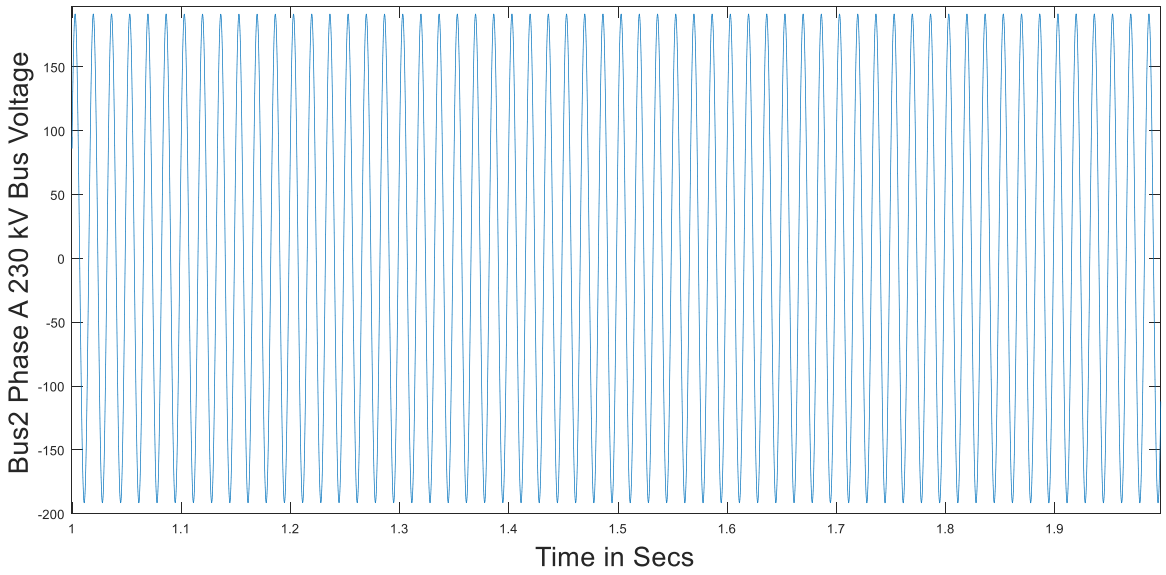

Fig. 49a Simulated Phase-A voltage response at bus 2 230 kV bus

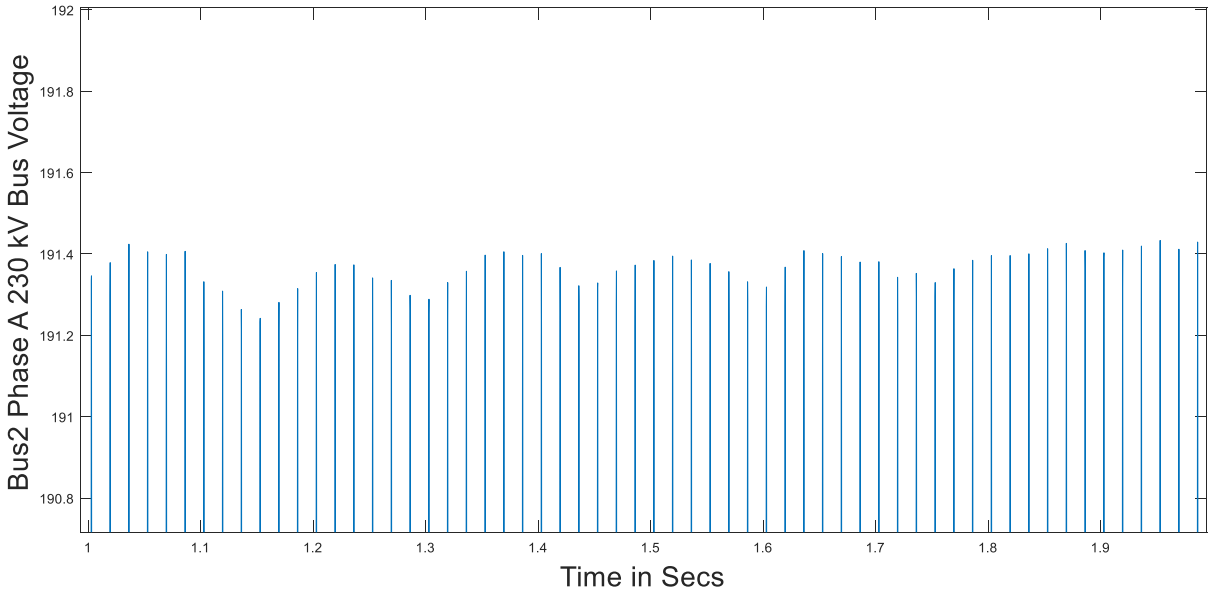

Fig. 49b Scaled positive peaks of Fig. 49a

6 CONCLUSIONS AND FUTURE WORK

6.1 Conclusions

Two standard feeder and load models with a same set of standard set of parameters have been successfully modeled in this work using PSCAD software. The load compositions for these models are modeled for two types of areas (residential and industrial/commercial). This set of parameters and load compositions were modeled by studying the effects of events such as FIDVR and feeder pickup events.

The following conclusions can be made from the work presented in Chapter 2, Chapter 3, Chapter 4, Chapter 5:

- **Conclusion1:** A standard feeder and load model (for a residential area – at substation A) comprising of single-phase motor load, three-phase motor load, impedance load is able to capture a good approximation of the measured current transient characteristics. This is validated by playing-in three-phase measured voltages (representing a fault at 69 kV level) into the model. It is also observed that this feeder and load model gives good approximate current responses for both summer and winter conditions. This model represents a load composition of single-phase motor load (72%), three-phase motor load (18%), impedance load (10%) at residential loading conditions.

- **Conclusion2:** Another standard feeder and load model (for an industrial/commercial area - at substation B) comprising of single-phase motor load, three-phase motor load, impedance load has been able to capture a good approximation of the measured current transient characteristics accurately. This is validated by playing-in three-phase measured voltages (representing a three-phase feeder pick-up event at substation B) into the model. This model represents a load composition of single-phase motor load (18%), three-phase

motor load (72%), impedance load (10%) at industrial/commercial loading conditions. The parameters for this standard feeder and load model is taken the same parameters from the standard feeder and load model at residential conditions.

- **Conclusion3:** The standard feeder and load model for industrial/commercial area has been validated by recreating the feeder closing event that occurred at substation B by building a 69-kV sub-transmission network near substation B in PSCAD software. It is observed that this model is able to capture a good approximation of both the measured voltages and currents when compared to their corresponding measured responses at the head of the substation B feeder. It is also observed that this pick-up event had a significant impact on the 69-kV substation B bus (a voltage drop of 2% is observed) during the pick-up transient. It is also observed that this pick-up event didn't have any impact on the 230-kV buses bus1 and bus 2.

6.2 Future Work

The standard feeder and load model developed in this work is obtained by simple manual tuning of the parameters of the load models and the distribution transformers so as to obtain a good match of the simulated current response when compared with the measured current response with the measured voltages played-in to the model. However, using an optimization technique, to obtain the load and transformer parameters, such as non-linear least square curve fitting method would be more efficient in obtaining more accurate simulated current response as compared to a manual tuning method.

The load model synthesis analysis in this work has been implemented in PSCAD simulation tool, which is typically not used for planning or operation studies in the power

industry. Positive sequence software tools such as PSLF, PSS®E, which are widely used in the industry, do not capture the point on wave transient characteristics of the model. Therefore, an equivalent positive sequence model for the three-phase feeder and load model, synthesized in this work, needs to be developed to integrate this model into the transmission planning studies.

BIBLIOGRAPHY

[1] Dong Han, Jin Ma, H. E. Renmu, Zhaoyang Dong and D. Hill, "Reducing identified parameters of measurement-based composite load model," *2008 IEEE Power and Energy Society General Meeting - Conversion and Delivery of Electrical Energy in the 21st Century*, Pittsburgh, PA, 2008, pp. 1-1.

[2] B. Choi and H. Chiang, "Multiple Solutions and Plateau Phenomenon in Measurement-Based Load Model Development: Issues and Suggestions," in *IEEE Transactions on Power Systems*, vol. 24, no. 2, pp. 824-831, May 2009.

[3] S. Son *et al*., "Improvement of Composite Load Modeling Based on Parameter Sensitivity and Dependency Analyses," in *IEEE Transactions on Power Systems*, vol. 29, no. 1, pp. 242-250, Jan. 2014.

[4] Jae-Kyeong Kim *et al*., "Fast and reliable estimation of composite load model parameters using analytical similarity of parameter sensitivity," *2016 IEEE Power and Energy Society General Meeting (PESGM)*, Boston, MA, 2016, pp. 1-1.

[5] Siming Guo and T. J. Overbye, "Parameter estimation of a complex load model using phasor measurements," *2012 IEEE Power and Energy Conference at Illinois*, Champaign, IL, 2012, pp. 1-6.

[6] B. Sapkota and V. Vittal, "Dynamic VAr Planning in a Large Power System Using Trajectory Sensitivities," in *IEEE Transactions on Power Systems*, vol. 25, no. 1, pp. 461-469, Feb. 2010.

[7] A. Gaikwad, P. Markham and P. Pourbeik, "Implementation of the WECC Composite Load Model for utilities using the component-based modeling approach," *2016 IEEE/PES Transmission and Distribution Conference and Exposition (T&D)*, Dallas, TX, 2016, pp. 1-5.

[8] R. Bravo, R. Yinger, D. Chassin, H. Huang, N. Lu, I. Hiskens, and G. Venkataramanan, Final Project Report Load Modeling Transmission Research, Lawrence Berkeley National Laboratory (LBNL), Mar. 2010.

[9] K. Tomiyama, J. P. Daniel and S. Ihara, "Modeling air conditioner load for power system studies," in *IEEE Transactions on Power Systems*, vol. 13, no. 2, pp. 414-421, May 1998.

[10] P. Pourbeik and B. Agrawal, "A hybrid model for representing air-conditioner compressor motor behavior in power system studies," *2008 IEEE Power and Energy Society General Meeting - Conversion and Delivery of Electrical Energy in the 21st Century*, Pittsburgh, PA, 2008, pp. 1-8.

[11] P. Shackshaft, O.C. Symons, and J.G. Hadwick: ’General-purpose model of power system loads’, *Proc. IEE*, Vol. 124, 1977, pp.715-723

[12] JA de Kock, FS van der Merwe, and HJ Vermeulen: 'Induction motor parameter estimation through an output error technique', *IEEE Trans*., Vol. EC-9, March 1994, pp.69-75

[13] D.Q. Ma, and P. Ju: 'A novel approach to dynamic load modelling', *IEEE Trans.*, Vol. PWRS-4, May 1989, pp.396-402

[14] Ma Jin, H. Renmu and D. J. Hill, "Load modeling by finding support vectors of load data from field measurements," in *IEEE Transactions on Power Systems*, vol. 21, no. 2, pp. 726-735, May 2006.

[15] H. Renmu, Ma Jin and D. J. Hill, "Composite load modeling via measurement approach," in *IEEE Transactions on Power Systems*, vol. 21, no. 2, pp. 663-672, May 2006.

[16] P. Ju *et al*., "Composite load models based on field measurements and their applications in dynamic analysis," in *IET Generation, Transmission & Distribution*, vol. 1, no. 5, pp. 724-730, September 2007.

[17] P. Mitra and V. Vittal, "Role of sensitivity analysis in load model parameter estimation," *2017 IEEE Power & Energy Society General Meeting*, Chicago, IL, 2017, pp. 1-5.

[18] Jingchao Zhang, Anhe Yan, Zhuoya Chen and Kun Gao, "Dynamic synthesis load modeling approach based on load survey and load curves analysis," *2008 Third International Conference on Electric Utility Deregulation and Restructuring and Power Technologies*, Nanjing, 2008, pp. 1067-1071.

[19] "WECC MVWG composite load model for dynamic simulations," WECC MVWG, 2012.

[20] Y. Liu, V. Vittal, J. Undrill and J. H. Eto, "Transient Model of Air-Conditioner Compressor Single Phase Induction Motor," in *IEEE Transactions on Power Systems*, vol. 28, no. 4, pp. 4528-4536, Nov. 2013.

[21] "Technical Reference Document: Dynamic Load Modelling". https://www.nerc.com/comm/PC/LoadModelingTaskForceDL/Dynamic%20Load%20Modeling%20Tech%20Ref%202016-11-14%20-%20FINAL.PDF

[22] Mike Holt, NEC Consultant. (2004). "Don't Let Voltage Drop Get Your System Down". *EC & M, 103*(6), 28-C31

[23] J. M. Undrill and R. E. Clayton, "Distribution line performance with imperfect grounding," *IEEE Transactions on Industry Applications*, vol. 24, no. 5, pp. 805-811, Sep/Oct 1988.

[24] PSCAD/EMTDC user manual, Manitoba HVDC, 2016.

[25] Claes Carrander, B 2017, ‘Magnetizing Currents in Power Transformers – Measurements, Simulations, and Diagnostic Methods', Doctoral thesis, KTH Electrical Engineering, Stockholm Sweden.

APPENDIX A

CODE FOR OPEN DSS POWER FLOW SOLUTION OF 69 KV NETWORK

```
New object=circuit.ieee37
!New Vsource.Vs1
Bus1=sourcebus basekv=230 pu=1.025 MVAsc3=14313.0 MVAsc1=21504

New Vsource.Vs
Bus1=Omre  basekv=230 pu=1.025 MVAsc3=10207.6 MVAsc1=10580

New Vsource.Vs2
Bus1=Omre1  basekv=230 pu=1.025 MVAsc3=10207.6 MVAsc1=10580

! Substation Transformer Whittank
New Transformer.SubXF Phases=3 Windings=3 XHL=6 XLT=6 XHT=6
~ wdg=1 bus=sourcebus conn=wye kv=230   Tap=1
~ wdg=2 bus=727.1.2.3       conn=wye kv=69   Tap=1.026
~ wdg=3 bus=740.1.2.3       conn=Delta kv=13.8  Tap=1

! Substation Transformer Whittank
New Transformer.SubXF1 Phases=3 Windings=3 XHL=6 XLT=10 XHT=4
~ wdg=1 bus=sourcebus conn=wye kv=230   Tap=1
~ wdg=2 bus=727       conn=wye kv=69   Tap=1.026
~ wdg=3 bus=741       conn=Delta kv=13.8  Tap=1

! Substation Transformer Omre 2 winding
New Transformer.SubXF2 Phases=3 Windings=2 XHL=6.5
~ wdg=1 bus=Omre conn=wye kv=230   Tap=1.025
~ wdg=2 bus=709       conn=wye kv=69   Tap=1.026

! Substation Transformer Omre 2 winding
New Transformer.SubXF3 Phases=3 Windings=2 XHL=6.5
~ wdg=1 bus=Omre conn=wye kv=230   Tap=1.025
~ wdg=2 bus=709       conn=wye kv=69   Tap=1.026

! Substation Transformer Omre 3 winding
New Transformer.SubXF4 Phases=3 Windings=3 XHL=6.1 XLT=13.6 XHT=5.3
~ wdg=1 bus=sourcebus conn=wye kv=230   Tap=1.025
~ wdg=2 bus=709       conn=wye kv=69   Tap=1.026
~ wdg=3 bus=742       conn=Delta kv=13.8  Tap=1

! Substation Transformer Omre
New Transformer.SubXF5 Phases=3 Windings=3 XHL=6.1 XLT=13.6 XHT=5.3
~ wdg=1 bus=sourcebus conn=wye kv=230   Tap=1.025
~ wdg=2 bus=709       conn=wye kv=69   Tap=1.026
~ wdg=3 bus=741       conn=Delta kv=13.8  Tap=1

! Substation Transformer distribution
New Transformer.XFM1  Phases=3 Windings=2 Xhl=2
~ wdg=1 bus=716       conn=wye kv=69  kva=100000
~ wdg=2 bus=775       conn=wye kv=13.8  kva=100000

! Substation Transformer distribution
New Transformer.XFM2  Phases=3 Windings=2 Xhl=0.02
~ wdg=1 bus=775       conn=wye kv=13.8  kva=1000
~ wdg=2 bus=776       conn=wye kv=0.23  kva=1000

!!!!
```

```
! Substation Transformer distribution
New Transformer.XFM3  Phases=3 Windings=2 Xhl=2
~ wdg=1 bus=701       conn=wye kv=69  kva=100000
~ wdg=2 bus=900       conn=wye kv=13.8  kva=100000

! Substation Transformer distribution
New Transformer.XFM4  Phases=3 Windings=2 Xhl=0.02
~ wdg=1 bus=900       conn=wye kv=13.8  kva=1000
~ wdg=2 bus=951       conn=wye kv=0.23  kva=1000

!!!!
! Substation Transformer distribution
New Transformer.XFM5  Phases=3 Windings=2 Xhl=2
~ wdg=1 bus=702       conn=wye kv=69  kva=100000
~ wdg=2 bus=901       conn=wye kv=13.8  kva=100000

! Substation Transformer distribution
New Transformer.XFM6  Phases=3 Windings=2 Xhl=0.02
~ wdg=1 bus=901       conn=wye kv=13.8  kva=1000
~ wdg=2 bus=952       conn=wye kv=0.23  kva=1000

!!!!

! Substation Transformer distribution
New Transformer.XFM7  Phases=3 Windings=2 Xhl=2
~ wdg=1 bus=703       conn=wye kv=69  kva=100000
~ wdg=2 bus=902       conn=wye kv=13.8  kva=100000

! Substation Transformer distribution
New Transformer.XFM8  Phases=3 Windings=2 Xhl=0.02
~ wdg=1 bus=902       conn=wye kv=13.8  kva=1000
~ wdg=2 bus=953       conn=wye kv=0.23  kva=1000

!!!!

! Substation Transformer distribution
New Transformer.XFM9  Phases=3 Windings=2 Xhl=2
~ wdg=1 bus=704       conn=wye kv=69  kva=100000
~ wdg=2 bus=903       conn=wye kv=13.8  kva=100000

! Substation Transformer distribution
New Transformer.XFM10  Phases=3 Windings=2 Xhl=0.02
~ wdg=1 bus=903       conn=wye kv=13.8  kva=1000
~ wdg=2 bus=954       conn=wye kv=0.23  kva=1000

!!!!

! Substation Transformer distribution
New Transformer.XFM11  Phases=3 Windings=2 Xhl=2
~ wdg=1 bus=705       conn=wye kv=69  kva=100000
~ wdg=2 bus=904       conn=wye kv=13.8  kva=100000

! Substation Transformer distribution
New Transformer.XFM12  Phases=3 Windings=2 Xhl=0.02
~ wdg=1 bus=904       conn=wye kv=13.8  kva=1000
~ wdg=2 bus=955       conn=wye kv=0.23  kva=1000
```

```
!!!!
! Substation Transformer distribution
New Transformer.XFM13  Phases=3 Windings=2 Xhl=2
~ wdg=1 bus=706       conn=wye kv=69  kva=100000
~ wdg=2 bus=905       conn=wye kv=13.8  kva=100000

! Substation Transformer distribution
New Transformer.XFM14  Phases=3 Windings=2 Xhl=0.02
~ wdg=1 bus=905       conn=wye kv=13.8  kva=1000
~ wdg=2 bus=956       conn=wye kv=0.23  kva=1000

!!!!
! Substation Transformer distribution
New Transformer.XFM15  Phases=3 Windings=2 Xhl=2
~ wdg=1 bus=707       conn=wye kv=69  kva=100000
~ wdg=2 bus=906       conn=wye kv=13.8  kva=100000

! Substation Transformer distribution
New Transformer.XFM16  Phases=3 Windings=2 Xhl=0.02
~ wdg=1 bus=906       conn=wye kv=13.8  kva=1000
~ wdg=2 bus=957       conn=wye kv=0.23  kva=1000

!!!!
! Substation Transformer distribution
New Transformer.XFM17  Phases=3 Windings=2 Xhl=2
~ wdg=1 bus=708       conn=wye kv=69  kva=100000
~ wdg=2 bus=907       conn=wye kv=13.8  kva=100000

! Substation Transformer distribution
New Transformer.XFM18  Phases=3 Windings=2 Xhl=0.02
~ wdg=1 bus=907       conn=wye kv=13.8  kva=1000
~ wdg=2 bus=958       conn=wye kv=0.23  kva=1000

!!!!
! Substation Transformer distribution
New Transformer.XFM19  Phases=3 Windings=2 Xhl=2
~ wdg=1 bus=723       conn=wye kv=69  kva=100000
~ wdg=2 bus=908       conn=wye kv=13.8  kva=100000

! Substation Transformer distribution
New Transformer.XFM20  Phases=3 Windings=2 Xhl=0.02
~ wdg=1 bus=908       conn=wye kv=13.8  kva=1000
~ wdg=2 bus=959       conn=wye kv=0.23  kva=1000

!!!!
! Substation Transformer distribution
New Transformer.XFM21  Phases=3 Windings=2 Xhl=2
~ wdg=1 bus=725       conn=wye kv=69  kva=100000
~ wdg=2 bus=909       conn=wye kv=13.8  kva=100000

! Substation Transformer distribution
New Transformer.XFM22  Phases=3 Windings=2 Xhl=0.02
~ wdg=1 bus=909       conn=wye kv=13.8  kva=1000
~ wdg=2 bus=960       conn=wye kv=0.23 kva=1000
```

```
!!!!
! Substation Transformer distribution
New Transformer.XFM23  Phases=3 Windings=2 Xhl=2
~ wdg=1 bus=726       conn=wye kv=69  kva=100000
~ wdg=2 bus=910       conn=wye kv=13.8  kva=100000

! Substation Transformer distribution
New Transformer.XFM24  Phases=3 Windings=2 Xhl=0.02
~ wdg=1 bus=910       conn=wye kv=13.8  kva=1000
~ wdg=2 bus=961       conn=wye kv=0.23  kva=1000

!!!!
! Substation Transformer distribution
New Transformer.XFM25  Phases=3 Windings=2 Xhl=2
~ wdg=1 bus=710       conn=wye kv=69  kva=100000
~ wdg=2 bus=911       conn=wye kv=13.8  kva=100000

! Substation Transformer distribution
New Transformer.XFM26  Phases=3 Windings=2 Xhl=0.02
~ wdg=1 bus=911       conn=wye kv=13.8  kva=1000
~ wdg=2 bus=962       conn=wye kv=0.23  kva=1000

!!!!
! Substation Transformer distribution
New Transformer.XFM27  Phases=3 Windings=2 Xhl=2
~ wdg=1 bus=711       conn=wye kv=69  kva=10000
~ wdg=2 bus=912       conn=wye kv=13.8  kva=100000

! Substation Transformer distribution
New Transformer.XFM28  Phases=3 Windings=2 Xhl=0.02
~ wdg=1 bus=912       conn=wye kv=13.8  kva=1000
~ wdg=2 bus=963       conn=wye kv=0.23  kva=1000

!!!!
! Substation Transformer distribution
New Transformer.XFM29  Phases=3 Windings=2 Xhl=2
~ wdg=1 bus=712       conn=wye kv=69  kva=100000
~ wdg=2 bus=913       conn=wye kv=13.8  kva=100000

! Substation Transformer distribution
New Transformer.XFM30  Phases=3 Windings=2 Xhl=0.02
~ wdg=1 bus=913       conn=wye kv=13.8  kva=1000
~ wdg=2 bus=964       conn=wye kv=0.23  kva=1000

!!!!
! Substation Transformer distribution
New Transformer.XFM31  Phases=3 Windings=2 Xhl=2
~ wdg=1 bus=713       conn=wye kv=69  kva=100000
~ wdg=2 bus=914       conn=wye kv=13.8  kva=100000

! Substation Transformer distribution
New Transformer.XFM32  Phases=3 Windings=2 Xhl=0.02
~ wdg=1 bus=914       conn=wye kv=13.8  kva=1000
~ wdg=2 bus=965       conn=wye kv=0.23  kva=1000

!!!!
```

```
! Substation Transformer distribution
New Transformer.XFM33  Phases=3 Windings=2 Xhl=2
~ wdg=1 bus=714       conn=wye kv=69  kva=100000
~ wdg=2 bus=915       conn=wye kv=13.8  kva=100000

! Substation Transformer distribution
New Transformer.XFM34  Phases=3 Windings=2 Xhl=0.02
~ wdg=1 bus=915       conn=wye kv=13.8  kva=1000
~ wdg=2 bus=966       conn=wye kv=0.23  kva=1000

!!!!
! Substation Transformer distribution
New Transformer.XFM35  Phases=3 Windings=2 Xhl=2
~ wdg=1 bus=715       conn=wye kv=69  kva=100000
~ wdg=2 bus=916       conn=wye kv=13.8  kva=100000

! Substation Transformer distribution
New Transformer.XFM36  Phases=3 Windings=2 Xhl=0.02
~ wdg=1 bus=916       conn=wye kv=13.8  kva=1000
~ wdg=2 bus=967       conn=wye kv=0.23  kva=1000

!!!!
! Substation Transformer distribution
New Transformer.XFM37  Phases=3 Windings=2 Xhl=2
~ wdg=1 bus=716       conn=wye kv=69  kva=100000
~ wdg=2 bus=917       conn=wye kv=13.8  kva=100000

! Substation Transformer distribution
New Transformer.XFM38  Phases=3 Windings=2 Xhl=0.02
~ wdg=1 bus=917       conn=wye kv=13.8  kva=1000
~ wdg=2 bus=968       conn=wye kv=0.23  kva=1000

!!!!
! Substation Transformer distribution
New Transformer.XFM39  Phases=3 Windings=2 Xhl=2
~ wdg=1 bus=728       conn=wye kv=69  kva=100000
~ wdg=2 bus=918       conn=wye kv=13.8  kva=100000

! Substation Transformer distribution
New Transformer.XFM40  Phases=3 Windings=2 Xhl=0.02
~ wdg=1 bus=918       conn=wye kv=13.8  kva=1000
~ wdg=2 bus=969       conn=wye kv=0.23  kva=1000

!!!!
! Substation Transformer distribution
New Transformer.XFM41  Phases=3 Windings=2 Xhl=2
~ wdg=1 bus=718       conn=wye kv=69  kva=100000
~ wdg=2 bus=919       conn=wye kv=13.8  kva=100000

! Substation Transformer distribution
New Transformer.XFM42  Phases=3 Windings=2 Xhl=0.02
~ wdg=1 bus=919       conn=wye kv=13.8  kva=1000
~ wdg=2 bus=970       conn=wye kv=0.23  kva=1000

!!!!
! Substation Transformer distribution
```

```
New Transformer.XFM43  Phases=3 Windings=2 Xhl=2
~ wdg=1 bus=719       conn=wye kv=69  kva=100000
~ wdg=2 bus=920       conn=wye kv=13.8  kva=100000

! Substation Transformer distribution
New Transformer.XFM44  Phases=3 Windings=2 Xhl=0.02
~ wdg=1 bus=920       conn=wye kv=13.8  kva=1000
~ wdg=2 bus=971       conn=wye kv=0.23  kva=1000

!!!!
! Substation Transformer distribution
New Transformer.XFM45  Phases=3 Windings=2 Xhl=2
~ wdg=1 bus=720       conn=wye kv=69  kva=100000
~ wdg=2 bus=921       conn=wye kv=13.8  kva=100000

! Substation Transformer distribution
New Transformer.XFM46  Phases=3 Windings=2 Xhl=0.02
~ wdg=1 bus=921       conn=wye kv=13.8  kva=1000
~ wdg=2 bus=972       conn=wye kv=0.23  kva=1000

!!!!
! Substation Transformer distribution
New Transformer.XFM47  Phases=3 Windings=2 Xhl=2
~ wdg=1 bus=721       conn=wye kv=69  kva=100000
~ wdg=2 bus=922       conn=wye kv=13.8  kva=100000

! Substation Transformer distribution
New Transformer.XFM48  Phases=3 Windings=2 Xhl=0.02
~ wdg=1 bus=922       conn=wye kv=13.8  kva=1000
~ wdg=2 bus=973       conn=wye kv=0.23  kva=1000

! import line codes with phase impedance matrices
!Redirect        IEEELineCodes.dss

! Lines
New Line.L1     Phases=3 Bus1=701.1.2.3  Bus2=702.1.2.3  R1=0.126 X1=0.633 R0=0.699 X0=2.036
B1=6.45E-006  B0=4.73E-006 Rg=0 Xg=0   Length=3.255 Units=mi
New Line.L2     Phases=3 Bus1=702.1.2.3  Bus2=703.1.2.3  R1=0.1255 X1=0.618 R0=0.61 X0=2.788
B1=6.75E-006  B0=4.95E-006 Rg=0 Xg=0 Length=1.616 Units=mi
New Line.L3     Phases=3 Bus1=703.1.2.3  Bus2=704.1.2.3  R1=0.147 X1=0.615 R0=0.553 X0=1.901
B1=7.01E-006  B0=5.12E-006 Rg=0 Xg=0 Length=1.377 Units=mi
New Line.L4     Phases=3 Bus1=704.1.2.3  Bus2=705.1.2.3  R1=0.127 X1=0.633 R0=0.664 X0=2.007
B1=6.7E-006  B0=4.91E-006 Rg=0 Xg=0 Length=2.35 Units=mi
New Line.L5     Phases=3 Bus1=705.1.2.3  Bus2=706.1.2.3  R1=0.165 X1=0.618 R0=0.623 X0=1.977
B1=6.64E-006  B0=4.87E-006 Rg=0 Xg=0 Length=0.695 Units=mi
New Line.L6     Phases=3 Bus1=706.1.2.3  Bus2=707.1.2.3  R1=0.165 X1=0.608 R0=0.648 X0=1.904
B1=6.77E-006  B0=4.96E-006 Rg=0 Xg=0 Length=0.93 Units=mi
New Line.L7     Phases=3 Bus1=707.1.2.3  Bus2=708.1.2.3  R1=0.164 X1=0.607 R0=0.633 X0=2.756
B1=6.98E-006  B0=5.11E-006 Rg=0 Xg=0 Length=3.91 Units=mi
New Line.L8     Phases=3 Bus1=708.1.2.3  Bus2=709.1.2.3  R1=0.077 X1=0.429 R0=0.516 X0=2.563
B1=9.49E-006  B0=6.95E-006 Rg=0 Xg=0 Length=2.876 Units=mi
New Line.L9     Phases=3 Bus1=710.1.2.3  Bus2=705.1.2.3  R1=0.077 X1=0.428 R0=0.629 X0=1.818
B1=9.39E-006  B0=6.88E-006 Rg=0 Xg=0  Length=3.353 Units=mi
New Line.L10    Phases=3 Bus1=710.1.2.3  Bus2=711.1.2.3  R1=0.125 X1=0.618 R0=0.592 X0=1.930
B1=6.94E-006  B0=5.08E-006 Rg=0 Xg=0 Length=2.309 Units=mi
```

```
New Line.L11    Phases=3 Bus1=711.1.2.3  Bus2=712.1.2.3  R1=0.149 X1=0.63 R0=0.624  X0=1.94
B1=6.44E-006  B0=4.72E-006 Rg=0 Xg=0 Length=2.286 Units=mi
New Line.L12    Phases=3 Bus1=712.1.2.3  Bus2=713.1.2.3  R1=0.125 X1=0.609 R0=0.605 X0=1.92
B1=6.93E-006  B0=5.07E-006 Rg=0 Xg=0 Length=1.938 Units=mi
New Line.L13    Phases=3 Bus1=713.1.2.3  Bus2=709.1.2.3  R1=0.122 X1=0.597 R0=0.601 X0=1.907
B1=7.00E-006  B0=5.11E-006 Rg=0 Xg=0 Length=2.369 Units=mi
New Line.L14    Phases=3 Bus1=714.1.2.3  Bus2=715.1.2.3  R1=0.132 X1=0.636 R0=0.562 X0=2.331
B1=6.66E-006  B0=4.88E-006 Rg=0 Xg=0 Length=1.673 Units=mi
New Line.L15    Phases=3 Bus1=715.1.2.3  Bus2=716.1.2.3  R1=0.138 X1=0.635 R0=0.626 X0=2.012
B1=6.69E-006  B0=4.90E-006 Rg=0 Xg=0 Length=1.13 Units=mi
New Line.L16    Phases=3 Bus1=716.1.2.3  Bus2=717.1.2.3  R1=0.13   X1=0.64   R0=0.59  X0=1.907
B1=7.09E-006  B0=5.198E-006 Rg=0 Xg=0 Length=1.007 Units=mi
New Line.L17    Phases=3 Bus1=717.1.2.3  Bus2=718.1.2.3  R1=0.125 X1=0.612 R0=0.595 X0=1.947
B1=6.7E-006  B0=4.91E-006 Rg=0 Xg=0 Length=1.444 Units=mi
New Line.L18    Phases=3 Bus1=718.1.2.3  Bus2=719.1.2.3  R1=0.154 X1=0.646 R0=0.565 X0=1.975
B1=6.75E-006  B0=4.95E-006 Rg=0 Xg=0 Length=2.306 Units=mi
New Line.L19    Phases=3 Bus1=719.1.2.3  Bus2=720.1.2.3  R1=0.129 X1=0.659 R0=0.612 X0=2.387
B1=6.75E-009  B0=4.95E-009 Rg=0 Xg=0 Length=0.07  Units=mi
New Line.L20    Phases=3 Bus1=720.1.2.3  Bus2=721.1.2.3  R1=0.126 X1=0.625 R0=0.677 X0=2.054
B1=7.17E-006  B0=5.25E-006 Rg=0 Xg=0 Length=0.644 Units=mi
New Line.L21    Phases=3 Bus1=721.1.2.3  Bus2=722.1.2.3  R1=0.153 X1=0.66 R0=0.603   X0=1.977
B1=9.27E-006  B0=6.79E-006 Rg=0 Xg=0 Length=0.453 Units=mi
New Line.L22    Phases=3 Bus1=723.1.2.3  Bus2=724.1.2.3  R1=0.126 X1=0.631 R0=0.575 X0=1.949
B1=6.61E-006  B0=4.85E-006 Rg=0 Xg=0 Length=2.929 Units=mi
New Line.L23    Phases=3 Bus1=724.1.2.3  Bus2=725.1.2.3  R1=0.126 X1=0.628 R0=0.575 X0=1.964
B1=6.75E-006  B0=4.95E-006 Rg=0 Xg=0 Length=3.105 Units=mi
New Line.L24    Phases=3 Bus1=725.1.2.3  Bus2=726.1.2.3  R1=0.126 X1=0.626 R0=0.584 X0=1.957
B1=6.78E-006  B0=4.93E-006 Rg=0 Xg=0 Length=2.415 Units=mi
New Line.L25    Phases=3 Bus1=726.1.2.3  Bus2=718.1.2.3  R1=0.126 X1=0.626 R0=0.571 X0=1.938
B1=4.55E-006  B0=3.34E-006 Rg=0 Xg=0 Length=4.616 Units=mi
New Line.L26    Phases=3 Bus1=727.1.2.3  Bus2=701.1.2.3  R1=0.118 X1=0.589 R0=0.683 X0=2.027
B1=7.17E-006  B0=5.25E-006 Rg=0 Xg=0 Length=3.228 Units=mi
New Line.L27    Phases=3 Bus1=727.1.2.3  Bus2=710.1.2.3  R1=0.126 X1=0.618 R0=0.593 X0=1.924
B1=6.96E-006  B0=5.1E-006 Rg=0 Xg=0 Length=5.131 Units=mi
New Line.L28    Phases=3 Bus1=727.1.2.3  Bus2=714.1.2.3  R1=0.126 X1=0.776 R0=0.572 X0=1.994
B1=7.06E-006  B0=5.18E-006 Rg=0 Xg=0 Length=1.545 Units=mi
New Line.L29    Phases=3 Bus1=727.1.2.3  Bus2=723.1.2.3  R1=0.166 X1=0.636 R0=0.572 X0=1.959
B1=36.5E-006  B0=26.7E-006 Rg=0 Xg=0 Length=1.322 Units=mi
New Line.L30    Phases=3 Bus1=722.1.2.3  Bus2=709.1.2.3  R1=0.128 X1=0.616 R0=0.679 X0=2.179
B1=7.12E-006  B0=5.226E-006 Rg=0 Xg=0 Length=5.008 Units=mi
New Line.L31    Phases=3 Bus1=717.1.2.3  Bus2=728.1.2.3  R1=0.161 X1=0.663 R0=0.442 X0=2.763
B1=6.75E-009  B0=4.95E-009 Rg=0 Xg=0 Length=0.056 Units=mi

!New Load.S776a      Bus1=776.1 Phases=1 Conn=delta Model=1 kV=  0.23 kW= 740 kVAR=  200
!New Load.S776b      Bus1=776.2 Phases=1 Conn=delta Model=1 kV=  0.23 kW= 740 kVAR=  200
!New Load.S776c      Bus1=776.3 Phases=1 Conn=delta Model=1 kV=  0.23 kW= 740 kVAR= 200

!New Load.S701      Bus1=701 Phases=3 Conn=delta Model=1 kV=  69 kW= 5500 kVAR= 0
New Load.S951a      Bus1=951.1 Phases=1 Conn=delta Model=1 kV=  0.23 kW= 1833 kVAR= 0
New Load.S951b      Bus1=951.2 Phases=1 Conn=delta Model=1 kV=  0.23 kW= 1833 kVAR= 0
New Load.S951c      Bus1=951.3 Phases=1 Conn=delta Model=1 kV=  0.23 kW= 1833 kVAR= 0
!New Generator.G1    Bus1=951 Phases=3 kV =0.23 kW= 900 Pf=0.92 Model =3 Status = Fixed Maxkvar
= 500 Minkvar = 0 Pvfactor =1 MVA=50
New Capacitor.C1    Bus1=951 Phases=3 Kv =0.23 Kvar= 500

!New Load.S702      Bus1=702 Phases=3 Conn=delta Model=1 kV=  69 kW= 3600 kVAR= 0
```

```
New Load.S952.a      Bus1=952.1 Phases=1 Conn=delta Model=1 kV=  0.23 kW= 1200 kVAR= 0
New Load.S952.b      Bus1=952.2 Phases=1 Conn=delta Model=1 kV=  0.23 kW= 1200 kVAR= 0
New Load.S952.c      Bus1=952.3 Phases=1 Conn=delta Model=1 kV=  0.23 kW= 1200 kVAR= 0
!New Generator.G2    Bus1=952 Phases=3 kV =0.23 kW= 600 Pf=0.92 Model =3 Status = Fixed Maxkvar
= 500 Minkvar = 0 Pvfactor =1 MVA=50
New Capacitor.C2    Bus1=952 Phases=3 Kv =0.23 Kvar= 500

!New Load.S703      Bus1=703 Phases=3 Conn=delta Model=1 kV=  69 kW= 3600 kVAR= 0
New Load.S953.a      Bus1=953.1 Phases=1 Conn=delta Model=1 kV=  0.23 kW= 1200 kVAR= 0
New Load.S953.b      Bus1=953.2 Phases=1 Conn=delta Model=1 kV=  0.23 kW= 1200 kVAR= 0
New Load.S953.c      Bus1=953.3 Phases=1 Conn=delta Model=1 kV=  0.23 kW= 1200 kVAR= 0
!New Generator.G3    Bus1=953 Phases=3 kV =0.23 kW= 500 Pf=0.92 Model =3 Status = Fixed Maxkvar
= 500 Minkvar = 0 Pvfactor =1 MVA=50
New Capacitor.C3    Bus1=953 Phases=3 Kv =0.23 Kvar= 500

!New Load.S704      Bus1=704 Phases=3 Conn=delta Model=1 kV=  69 kW= 5700 kVAR= 0
New Load.S954.a      Bus1=954.1 Phases=1 Conn=delta Model=1 kV=  0.23 kW= 1900 kVAR= 0
New Load.S954.b      Bus1=954.2 Phases=1 Conn=delta Model=1 kV=  0.23 kW= 1900 kVAR= 0
New Load.S954.c      Bus1=954.3 Phases=1 Conn=delta Model=1 kV=  0.23 kW= 1900 kVAR= 0
!New Generator.G4    Bus1=954 Phases=3 kV =0.23 kW= 900 Pf=0.92 Model =3 Status = Fixed Maxkvar
= 500 Minkvar = 0 Pvfactor =1 MVA=50
New Capacitor.C4    Bus1=954 Phases=3 Kv =0.23 Kvar= 500

!New Load.S705      Bus1=705 Phases=3 Conn=delta Model=1 kV=  69 kW= 5300 kVAR= 0
New Load.S955.a      Bus1=955.1 Phases=1 Conn=delta Model=1 kV=  0.23 kW= 1766 kVAR= 0
New Load.S955.b      Bus1=955.2 Phases=1 Conn=delta Model=1 kV=  0.23 kW= 1766 kVAR= 0
New Load.S955.c      Bus1=955.3 Phases=1 Conn=delta Model=1 kV=  0.23 kW= 1766 kVAR= 0
!New Generator.G5    Bus1=955 Phases=3 kV =0.23 kW= 900 Pf=0.92 Model =3 Status = Fixed Maxkvar
= 500 Minkvar = 0 Pvfactor =1 MVA=50
New Capacitor.C5    Bus1=955 Phases=3 Kv =0.23 Kvar= 500

!New Load.S706      Bus1=706 Phases=3 Conn=delta Model=1 kV=  69 kW= 0 kVAR= 0
New Load.S956.a      Bus1=956.1 Phases=1 Conn=delta Model=1 kV=  0.23 kW= 0 kVAR= 0
New Load.S956.b      Bus1=956.2 Phases=1 Conn=delta Model=1 kV=  0.23 kW= 0 kVAR= 0
New Load.S956.c      Bus1=956.3 Phases=1 Conn=delta Model=1 kV=  0.23 kW= 0 kVAR= 0

!New Load.S707      Bus1=707 Phases=3 Conn=delta Model=1 kV=  69 kW= 9700 kVAR=0
New Load.S957.a      Bus1=957.1 Phases=1 Conn=delta Model=1 kV=  0.23 kW= 3233 kVAR= 0
New Load.S957.b      Bus1=957.2 Phases=1 Conn=delta Model=1 kV=  0.23 kW=3233 kVAR= 0
New Load.S957.c      Bus1=957.3 Phases=1 Conn=delta Model=1 kV=  0.23 kW= 3233 kVAR= 0
!New Generator.G7    Bus1=957 Phases=3 kV =0.23 kW= 1500 Pf=0.92 Model =3 Status = Fixed
Maxkvar = 500 Minkvar = 0 Pvfactor =1 MVA=50
New Capacitor.C7    Bus1=957 Phases=3 Kv =0.23 Kvar= 500

!New Load.S708      Bus1=708 Phases=3 Conn=delta Model=1 kV=  69 kW= 6000 kVAR= 0
New Load.S958.a      Bus1=958.1 Phases=1 Conn=delta Model=1 kV=  0.23 kW= 2000 kVAR= 0
New Load.S958.b      Bus1=958.2 Phases=1 Conn=delta Model=1 kV=  0.23 kW= 2000 kVAR= 0
New Load.S958.c      Bus1=958.3 Phases=1 Conn=delta Model=1 kV=  0.23 kW= 2000 kVAR= 0
!New Generator.G8    Bus1=958 Phases=3 kV =0.23 kW= 1000 Pf=0.92 Model =3 Status = Fixed
Maxkvar = 500 Minkvar = 0 Pvfactor =1 MVA=50
New Capacitor.C8    Bus1=958 Phases=3 Kv =0.23 Kvar= 500

!New Load.S723      Bus1=723 Phases=3 Conn=delta Model=1 kV=  69 kW= 3460 kVAR= 0
New Load.S959.a      Bus1=959.1 Phases=1 Conn=delta Model=1 kV=  0.23 kW= 1153 kVAR= 0
New Load.S959.b      Bus1=959.2 Phases=1 Conn=delta Model=1 kV=  0.23 kW= 1153 kVAR= 0
New Load.S959.c      Bus1=959.3 Phases=1 Conn=delta Model=1 kV=  0.23 kW= 1153 kVAR= 0
```

```
!New Generator.G23    Bus1=959 Phases=3 kV =0.23 kW= 540 Pf=0.92 Model =3 Status = Fixed
Maxkvar = 500 Minkvar = 0 Pvfactor =1 MVA=50
New Capacitor.C23    Bus1=959 Phases=3 Kv =0.23 Kvar= 500

!New Load.S725      Bus1=725 Phases=3 Conn=delta Model=1 kV=  69 kW= 2500 kVAR= 0
New Load.S960.a      Bus1=960.1 Phases=1 Conn=delta Model=1 kV=  0.23 kW= 833 kVAR= 0
New Load.S960.b      Bus1=960.2 Phases=1 Conn=delta Model=1 kV=  0.23 kW= 833 kVAR= 0
New Load.S960.c      Bus1=960.3 Phases=1 Conn=delta Model=1 kV=  0.23 kW= 833 kVAR= 0
!New Generator.G25    Bus1=960 Phases=3 kV =0.23 kW= 400 Pf=0.92 Model =3 Status = Fixed
Maxkvar = 500 Minkvar = 0 Pvfactor =1 MVA=50
New Capacitor.C25    Bus1=960 Phases=3 Kv =0.23 Kvar= 500

!New Load.S726      Bus1=726 Phases=3 Conn=delta Model=1 kV=  69 kW= 3200 kVAR= 0
New Load.S961.a      Bus1=961.1 Phases=1 Conn=delta Model=1 kV=  0.23 kW= 1066 kVAR= 0
New Load.S961.b      Bus1=961.2 Phases=1 Conn=delta Model=1 kV=  0.23 kW= 1066 kVAR= 0
New Load.S961.c      Bus1=961.3 Phases=1 Conn=delta Model=1 kV=  0.23 kW= 1066 kVAR= 0
!New Generator.G26    Bus1=961 Phases=3 kV =0.23 kW= 500 Pf=0.92 Model =3 Status = Fixed
Maxkvar = 500 Minkvar = 0 Pvfactor =1 MVA=50
New Capacitor.C26    Bus1=961 Phases=3 Kv =0.23 Kvar= 500

!New Load.S710      Bus1=710 Phases=3 Conn=delta Model=1 kV=  69 kW= 5900 kVAR= 0
New Load.S962.a      Bus1=962.1 Phases=1 Conn=delta Model=1 kV=  0.23 kW= 1966 kVAR= 0
New Load.S962.b      Bus1=962.2 Phases=1 Conn=delta Model=1 kV=  0.23 kW= 1966 kVAR= 0
New Load.S962.c      Bus1=962.3 Phases=1 Conn=delta Model=1 kV=  0.23 kW= 1966 kVAR= 0
!New Generator.G10    Bus1=962 Phases=3 kV =0.23 kW= 900 Pf=0.92 Model =3 Status = Fixed
Maxkvar = 500 Minkvar = 0 Pvfactor =1 MVA=50
New Capacitor.C10    Bus1=962 Phases=3 Kv =0.23 Kvar= 500

!New Load.S711      Bus1=711 Phases=3 Conn=delta Model=1 kV=  69 kW= 8100 kVAR= 0
New Load.S963.a      Bus1=963.1 Phases=1 Conn=delta Model=1 kV=  0.23 kW= 2700 kVAR= 0
New Load.S963.b      Bus1=963.2 Phases=1 Conn=delta Model=1 kV=  0.23 kW= 2700 kVAR= 0
New Load.S963.c      Bus1=963.3 Phases=1 Conn=delta Model=1 kV=  0.23 kW= 2700 kVAR= 0
!New Generator.G11    Bus1=963 Phases=3 kV =0.23 kW= 1300 Pf=0.92 Model =3 Status = Fixed
Maxkvar = 500 Minkvar = 0 Pvfactor =1 MVA=50
New Capacitor.C11    Bus1=963 Phases=3 Kv =0.23 Kvar= 500

!New Load.S712      Bus1=712 Phases=3 Conn=delta Model=1 kV=  69 kW= 5800 kVAR= 0
New Load.S964.a      Bus1=964.1 Phases=1 Conn=delta Model=1 kV=  0.23 kW= 1933 kVAR= 0
New Load.S964.b      Bus1=964.2 Phases=1 Conn=delta Model=1 kV=  0.23 kW= 1933 kVAR= 0
New Load.S964.c      Bus1=964.3 Phases=1 Conn=delta Model=1 kV=  0.23 kW= 1933 kVAR= 0
!New Generator.G12    Bus1=964 Phases=3 kV =0.23 kW= 900 Pf=0.92 Model =3 Status = Fixed
Maxkvar = 500 Minkvar = 0 Pvfactor =1 MVA=50
New Capacitor.C12    Bus1=964 Phases=3 Kv =0.23 Kvar= 500

!New Load.S713      Bus1=713 Phases=3 Conn=delta Model=1 kV=  69 kW=4300 kVAR= 0
New Load.S965.a      Bus1=965.1 Phases=1 Conn=delta Model=1 kV=  0.23 kW= 1433 kVAR= 0
New Load.S965.b      Bus1=965.2 Phases=1 Conn=delta Model=1 kV=  0.23 kW= 1433 kVAR= 0
New Load.S965.c      Bus1=965.3 Phases=1 Conn=delta Model=1 kV=  0.23 kW= 1433 kVAR= 0
!New Generator.G13    Bus1=965 Phases=3 kV =0.23 kW= 700 Pf=0.92 Model =3 Status = Fixed
Maxkvar = 500 Minkvar = 0 Pvfactor =1 MVA=50
New Capacitor.C13    Bus1=965 Phases=3 Kv =0.23 Kvar= 500

!New Load.S714      Bus1=714 Phases=3 Conn=delta Model=1 kV=  69 kW= 5500 kVAR= 0
New Load.S966.a      Bus1=966.1 Phases=1 Conn=delta Model=1 kV=  0.23 kW= 1833 kVAR= 0
New Load.S966.b      Bus1=966.2 Phases=1 Conn=delta Model=1 kV=  0.23 kW= 1833 kVAR= 0
New Load.S966.c      Bus1=966.3 Phases=1 Conn=delta Model=1 kV=  0.23 kW= 1833 kVAR= 0
```

```
!New Generator.G14    Bus1=966 Phases=3 kV =0.23 kW= 900 Pf=0.92 Model =3 Status = Fixed
Maxkvar = 500 Minkvar = 0 Pvfactor =1 MVA=50
New Capacitor.C14    Bus1=966 Phases=3 Kv =0.23 Kvar= 500

!New Load.S715      Bus1=715 Phases=3 Conn=delta Model=1 kV=  69 kW= 3000 kVAR= 1300
New Load.S967.a      Bus1=967.1 Phases=1 Conn=delta Model=1 kV=  0.23 kW= 1000 kVAR= 433
New Load.S967.b      Bus1=967.2 Phases=1 Conn=delta Model=1 kV=  0.23 kW= 1000 kVAR= 433
New Load.S967.c      Bus1=967.3 Phases=1 Conn=delta Model=1 kV=  0.23 kW= 1000 kVAR= 433

!New Load.S716      Bus1=716 Phases=3 Conn=delta Model=1 kV=  69 kW= 5300 kVAR= 0
New Load.S968.a      Bus1=968.1 Phases=1 Conn=delta Model=1 kV=  0.23 kW= 2766 kVAR= 300
New Load.S968.b      Bus1=968.2 Phases=1 Conn=delta Model=1 kV=  0.23 kW= 2766 kVAR= 300
New Load.S968.c      Bus1=968.3 Phases=1 Conn=delta Model=1 kV=  0.23 kW= 2766 kVAR= 300
!New Generator.G16    Bus1=968 Phases=3 kV =0.23 kW= 7900 Pf=0.92 Model =3 Status = Fixed
Maxkvar = 500 Minkvar = 0 Pvfactor =1 MVA=50
New Capacitor.C16    Bus1=968 Phases=3 Kv =0.23 Kvar= 500

!New Load.S728      Bus1=728 Phases=3 Conn=delta Model=1 kV=  69 kW= 900 kVAR= 500
New Load.S969.a      Bus1=969.1 Phases=1 Conn=delta Model=1 kV=  0.23 kW= 300 kVAR= 166
New Load.S969.b      Bus1=969.2 Phases=1 Conn=delta Model=1 kV=  0.23 kW= 300 kVAR= 166
New Load.S969.c      Bus1=969.3 Phases=1 Conn=delta Model=1 kV=  0.23 kW= 300 kVAR= 166

!New Load.S718      Bus1=718 Phases=3 Conn=delta Model=1 kV=  69 kW= 6900 kVAR= 0
New Load.S970.a      Bus1=970.1 Phases=1 Conn=delta Model=1 kV=  0.23 kW= 2300 kVAR= 0
New Load.S970.b      Bus1=970.2 Phases=1 Conn=delta Model=1 kV=  0.23 kW= 2300 kVAR= 0
New Load.S970.c      Bus1=970.3 Phases=1 Conn=delta Model=1 kV=  0.23 kW= 2300 kVAR= 0
!New Generator.G18    Bus1=970 Phases=3 kV =0.23 kW= 1100  Pf=0.92 Model =3 Status = Fixed
Maxkvar = 500 Minkvar = 0 Pvfactor =1 MVA=50
New Capacitor.C18    Bus1=970 Phases=3 Kv =0.23 Kvar= 500

!New Load.S719       Bus1=719 Phases=3 Conn=delta Model=1 kV=  69      kW= 1100 kVAR= 1000
New Load.S971.a      Bus1=971.1 Phases=1 Conn=delta Model=1 kV=  0.23 kW= 366 kVAR= 333
New Load.S971.b      Bus1=971.2 Phases=1 Conn=delta Model=1 kV=  0.23 kW= 366 kVAR= 333
New Load.S971.c      Bus1=971.3 Phases=1 Conn=delta Model=1 kV=  0.23 kW= 366 kVAR= 333

!New Load.S720      Bus1=720 Phases=3 Conn=delta Model=1 kV=  69 kW= 180 kVAR= 0
New Load.S972.a      Bus1=972.1 Phases=1 Conn=delta Model=1 kV=  0.23 kW= 60 kVAR= 0
New Load.S972.b      Bus1=972.2 Phases=1 Conn=delta Model=1 kV=  0.23 kW= 60 kVAR= 0
New Load.S972.c      Bus1=972.3 Phases=1 Conn=delta Model=1 kV=  0.23 kW= 60 kVAR= 0
!New Generator.G20    Bus1=972 Phases=3 kV =0.23 kW= 200 Pf=0.92 Model =3 Status = Fixed
Maxkvar = 100 Minkvar = 0 Pvfactor =1 MVA=50
New Capacitor.C20    Bus1=972 Phases=3 Kv =0.23 Kvar= 500

!New Load.S721      Bus1=721 Phases=3 Conn=delta Model=1 kV=  69 kW= 600 kVAR= 220
New Load.S973.a      Bus1=973.1 Phases=1 Conn=delta Model=1 kV=  0.23 kW= 200 kVAR= 73
New Load.S973.b      Bus1=973.2 Phases=1 Conn=delta Model=1 kV=  0.23 kW= 200 kVAR= 73
New Load.S973.c      Bus1=973.3 Phases=1 Conn=delta Model=1 kV=  0.23 kW= 200 kVAR= 73

Set VoltageBases = "230,69,13.8,0.23"
CalcVoltageBases
!BusCoords IEEE37_BusXY.csv

! solve mode=direct
!set maxiterations=1000
solve
```

```
show voltages LL Nodes
! show currents residual=y elements
show powers kva elements
show taps
```